Advanced System Monitoring with Phasor Measurements

Ming Zhou

Dissertation Submitted to the Faculty of
Virginia Polytechnic Institute and State University
In partial fulfillment of the requirements for the degree of:

Doctor of Philosophy

In

Electrical Engineering

Dr. Virgilio Centeno, Chairman
Dr. Arun G. Phadke
Dr. James S. Thorp
Dr. Yilu Liu
Dr. Daniel Stilwell
Dr. Tao Lin

May 19, 2008

Blacksburg, Virginia

Keywords: Phasor Measurements, PMU, State Estimation, Calibration

Advanced System Monitoring with Phasor Measurements

by
Ming Zhou

Abstract

Phasor Measurement Units (PMUs) are widely acknowledged as one of the most promising developments in the field of real-time monitoring of power systems. By aligning the time stamps of voltage and current phasor measurements that are consistent with Coordinated Universal Time (UTC), a coherent picture of the power system state can be achieved through either direct measurements or simple linear calculations. With the growing number of PMUs planned for installation in the near future, both utilities and research institutions are looking for the best solutions to the placement of units as well as to the applications that make the most of phasor measurements.

This dissertation explores a method for optimal PMU placement as well as two applications of synchronized phasor measurements in state estimation. The pre-processing PMU placement method prepares the system data for placement optimization and reduces the size of the optimization problem. It is adaptive to most of the optimal placement methods and can save a large amount of computational effort. Depth of un-observability is one of the criteria to allow the most benefit out of a staged placement of the units. PMUs installed in the system provide synchronized phasor measurements that are highly beneficial to power system state estimations. Two related applications are proposed in the dissertation. First, a post-processing inclusion of phasor measurements in state estimators is introduced. This method avoids the revision of the existing estimators and is able to realize similar results as mixing phasor data with traditional SCADA with a linear afterwards step. The second application is a method to

calibrate instrument transformers remotely using phasor measurements. Several scans of phasor measurements are used to accomplish estimating system states in conjunction with complex instrument transformer correction factors. Numerical simulation results are provided for evaluation of the calibration performance with respect to the number of scans and load conditions.

Conducting theoretical and numerical analysis, the methods and algorithms developed in this dissertation are aimed to strategically place PMUs and to incorporate phasor measurements into state estimators effectively and extensively for better system state monitoring. Simulation results show that the proposed placement method facilitates approaching the exact optimal placement while keep the computational effort low. Simulation also shows that the use of phasor measurement with the proposed instrument transformer correction factors and proposed state estimation enhancement largely improves the quality of state estimations.

Acknowledgements

I am greatly indebted to my academic advisor, Dr. Virgilio Centeno, for his guidance, support, suggestions, and encouragement, without which this dissertation would not have been possible. I also wish to express my most sincere gratitude to Dr. Arun G. Phadke and Dr. James S. Thorp, for their participation on my committee and for their valuable guidance, enlightenments and constructive criticism. Thanks are also extended to committee member Dr. Yilu Liu, for her consistent encouragement, suggestions, and advices. I also thank Dr. Tao Lin and Dr. Daniel Stilwell for serving in the committee and for their valuable guidance and helpful comments.

Special thanks go to Dr. Damir Novosol and Dr. Yi Hu of Quanta Technology and Mr. Hector Volskis of Brazilian Independent System Operator for supervising the PMU placement research and providing the data.

I would like to express my deepest appreciation to my husband, Hao Wang, my parents, Baoyuan Zhou and Ying Huang, and my parents-in-law, Wuming Wang and Hongmei Yu. Their endless love, support and encouragement are emotionally critical, without which my pursuit of a doctorate would not have been possible.

Table of Contents

List of Figures

List of Tables

Chapter 1. Introduction

1.1. Background

In the mid 1980s, the first Phasor Measurement Unit (PMU) prototype was developed in the Power System Research Laboratory at Virginia Tech. The PMUs' ability to accurately and instantaneously calculate synchronized phasors of voltages and currents has promoted their persistent propagation in power systems throughout the world. More and more applications are being researched, studied, and implemented to meet measurement, protection, and control requirements in the increasingly stressed market-deregulated power systems.

1.1.1. Phasor Measurement Units

"Time synchronizing techniques, coupled with the computer-based measurement techniques, provide a novel opportunity to measure phasors and phase angle differences in real time." [1]

PMUs are designed to measure in real time the positive, negative, and zero sequence phasors of voltages and currents, in addition to the system frequency and the rate of change of frequency, through numerical algorithms implemented in the unit. This device enables the long-term desire of performing local computations in real time [2-4] and solves the problem of measurement time skews through sampling clock synchronization.

1.1.1.1. Features

- **Real-time System State Calculation**

Conventionally, the state of the power system is estimated using system models and traditional measurements of power flows, current magnitudes, and voltage magnitudes. At least several seconds are required for the estimator to process the raw measurements

before the result of system state is available. Dissimilarly, PMUs are able to provide immediate state of the buses they are installed and, if the system parameters are accurately known, calculate in real time the state of neighboring buses through one simple linear step.

The PMUs' ability of real-time system state measurement can be attributed to the algorithms for phasor calculation from sampled data implemented in the unit. Discrete Fourier Transform (DFT) is the most commonly known methods for phasor calculation [1]. A simplified phasor calculation can be obtained from the following equation:

$$X = \frac{\sqrt{2}}{N}\sum_{k=1}^{N} X_k \varepsilon^{-j2k\pi/N} \tag{1.1}$$

where,

X is the calculated phasor;

N is the total number of samples in one cycle;

and X_k is the k^{th} sample of waveform.

A computationally more efficient method to calculate phasors is to recursively compute phasors by adding the new sample to, and discarding the oldest sample from, the data set. With the recursive procedure, only two multiplications need to be executed with each new sample point [3]. This simpler algorithm allows implementation with most digital devices currently used in power system as long as time synchronization is performed. This increased availability of synchronized data with little additional cost has a great potential to simplify and improve real-time analysis programs, such as power system state estimation and adaptive relaying.

- **Synchronization**

The ability to synchronize measurements system-wide is an innovative feature that sets PMUs apart from traditional measurement devices. Traditional measurements (real

and reactive powers, voltage magnitudes, and current magnitudes) have very limited time synchronization and the time skews among measurements vary according to devices, distances, and communication channel conditions between substations and data centers. In the past, various communication systems, like leased lines, optical fibers, microwave, or AM radio broadcasts, have been considered for synchronization of measurement devices. However, most of them failed to provide high enough precision signals or to be reasonably economical.

In the early 1980s, the US government began the deployment of a Global Positioning System (GPS) navigation system. By the mid-90's the system was fully deployed and was being used around the world. A by-product of the GPS navigation signals is a high precision synchronized one second pulse available worldwide. The GPS timing pulse keeps accuracy better than 250 nanoseconds and allows, in the case of PMUs, for the synchronization of local sampling pulses to precisions better than one microsecond. One microsecond in a 60 Hz system corresponds to an angle error in the measured phasor of less than 0.02 degrees [3], which is more precise than what is required by most advanced power system applications.

The invention of integrating GPS into measurement devices is a pioneering work in the elimination of the time skew problem in traditional measurement data collected from different substations. With the further development of system interconnection, the wide area measurement system (WAMS) that takes advantage of synchronized measurements, is able to supervise the grid from a system-wide perspective instead of a local one [3]. Therefore, it can provide attractive options for improving system monitoring, control, operation, and protection on modern power systems.

1.1.1.2. PMU Spreading and Placement

As a new class of measurement, synchronized phasor measurements greatly elevate the availability as well as the quality of data and information useful to improve system monitoring, protection, control, and operation of the increasingly stressed power systems. Though currently, the number of PMUs installed in the system is not large enough to

make significant differences, the power industry has acknowledged the importance of rapidly propagating the use of PMUs into systems threatened by more frequent blackouts. Many utilities and consultants are endeavoring with research institutions to search for the practical PMU installation strategies.

PMU placement strategies have been studied in the past to meet the requirements of specific applications. L. Mili and T. Baldwin investigated PMU placement for voltage stability analysis in the early 1990s [5]. In this study, power systems were decomposed into coherent regions, and in each of the regions a PMU is placed on the bus used as a pilot point for the secondary voltage control of that system. Optimal PMU placement for improving the accuracy of power flow calculation was explored by G. Mueller, P. Komarnicki etc. [6]. This algorithm encourages placing PMUs at those points that react most noticeably and most sensitively to angle variation judged from the results of sensitivity analysis and decoupled Newton-Raphson power flow analysis.

PMU placement algorithms developed for specific applications are no optimal for other applications. Ultimately, only a PMU placement algorithm for full observability of the system would be beneficial to most monitoring and control applications. Though widely deploying PMUs on every bus will allow any possible application to be implemented, this installation strategy will require a major economic undertaking. Baldwin and Mili [7] showed that PMUs need to be installed on at least 1/4 to 1/3 of the system buses to completely observe the grid with pure phasor measurements. A larger number may be required, if there are devices already installed in the system.

The intention for accelerating the PMU proliferation also stimulates the research of the applications that make the most of the synchronized phasor measurements, among which, state estimation is the ones that may achieve the greatest positive impact from PMUs.

1.1.2. State Estimation

The concept of state estimation is to produce the best possible estimate of the true

state of the system using the available imperfect information. After being proposed and introduced by Fred Schweppe in the late 1960's, state estimation broadened the capabilities of Supervisory Control and Data Acquisition (SCADA) systems by taking advantage of the measurement redundancy. Now, all Energy Management Systems (EMS) are equipped with a State Estimator (SE) [8] to provide the latest information on the operating state of the power system .

Most state estimators in practical use are formulated as a group of non-linear equations in an over-determined system and are solved through the weighted least squares (WLS) method. Non-linear equations are linearized with first-order Taylor expansion and updated with the estimate of system state iteratively to minimize the objective function [9-11],

$$J = (z - Hx)^T W^{-1} (z - Hx) \tag{1.2}$$

and in each iteration, x is updated as equation (1.3)

$$x = (H^T W^{-1} H)^{-1} H^T W^{-1} z \tag{1.3}$$

where, H is the linearized measurement matrix, called Jacobian matrix; J is the optimal estimate objective; z is the raw noisy measurements; and W is the noise covariance matrix, whose inversion is used as weight matrix [12, 13].

The state estimator functions as a data-processing scheme that computes the state of a system from the information of measurements of system variables (real powers, reactive powers, voltage magnitudes, and current magnitudes), the mathematical model of the system, and the distribution functions of various measurements. The output of the estimator approaches the exact true state of the system although it is affected by the noise and spurious errors in the instruments and telemetry channels, the time skews within a scan of measurements, and inaccurate grid parameters [12]. Consequently, the PMUs' high accuracy measurements and their ability to calculate time-synchronized phasors make them very attractive for state estimators.

1.1.2.1. Applications of Synchronized Phasor Measurements in State Estimations

As a supplement of existing measurements, phasor measurements can extend measurement redundancy of the estimator. Former research showed that PMUs provide important measurements for state estimators and greatly enhance the estimation accuracy when 10% or more buses are installed with PMUs [14].

When state estimation is reformulated in terms of pure direct measurements of phasor voltages and currents, the resulting estimation problem would be a directly solvable problem, with the gain matrix constant, sparse, and in most cases real. This will lead to a linear state estimator that converges in one step requiring just the same amount of computation as one iteration of traditional estimators [15]. Calculation complexities can be reduced and system states can be measured and calculated in real time. In the future, most devices will be time synchronized with the same accuracy of a PMU, and the direct state measurement will be a sound choice to supplement state estimator aimed to implementing multi-level security monitoring for the operators' situational awareness.

1.2. Motivation

As electricity deregulation grows and the demand for electric energy increases, power markets become extremely competitive. As expected, deregulated power markets increase system efficiency and reduce costs by relying less on public enterprise and regulated monopoly, and by depending more upon market mechanisms like private ownership and competition [16]. But at the same time, competitive wholesale and retail markets have been driving transmission systems into much more intensive and stressed state. Systems tend to be operated at their limits for longer time, which largely increases the probability of blackouts.

D. Kirschen and G. Strbac point out that upgrading monitoring, control, and computational tools would enhance the situational awareness for operators in case of contingencies. Hence, responses with improved speed and quality could be achieved to decrease the possibility, size and duration of blackouts [17]. PMUs are just one of the

most promising devices that can provide the accurate measurements required to promote better system observability and monitoring accuracy.

Due to the conflict between the demand and trend of rapid PMU propagation throughout the system and the high installation cost of a wide area system, the optimal placement of PMUs for better system monitoring are in great need of research.

1.3. Objective

The major objective of this dissertation is to enhance the available knowledge and tools that will promote a better system-wide monitoring accuracy through the applications of synchronized phasor measurements. This requires that the system is properly equipped with PMUs and the phasor measurements are extensively and appropriately utilized in applications for enhancing system state supervision. Therefore, explanations and theoretical solutions for four closely related topics were explored in this dissertation:

1. Improving optimal placement of PMUs to achieve wide area measurement with pure phasors.

2. Strategically installing PMUs to progressively reach the optimal placement while maximizing the benefits for the entire system at each stage.

3. Efficiently including synchronized phasor measurements into estimators for better system state estimation.

4. Calibrating instrument transformers with synchronized phasor measurements to upgrade the system monitoring accuracy.

The direct phasor measurements and their wide integration in state estimations are expected to greatly improve the system monitoring accuracy, which serves as the goal of this work.

1.4. Organizations of the Dissertation

This dissertation is organized as follows:

Chapter 1: General introduction.

This chapter introduces the general background of PMU and state estimation, presents the motivation and objective of this dissertation and briefly describes the contents of each chapter.

Chapter 2: The development of a pre-processing PMU placement technique of reducing system scale to decrease the computational efforts needed for optimal PMU placement problem.

This chapter is concerned with modifying system models by eliminating virtual buses that are not practically valid locations for PMU installation, and decreasing the problem scale beforehand by identifying "known status" buses with a Matrix Reduction Algorithm. Five sample systems have been studied to show how much this method can save on the computational effort. In order to prove the performance guarantee of the proposed algorithm, Lagrangian Relaxation is applied to calculate the low bound of the exact minimum number of PMUs necessary for full observability.

Chapter 3: The development of a staged PMU installation methodology.

A staged PMU installation method has been explored through incremental PMU installation for minimal "depth of un-observability". Binary integer programming was used to optimize the installation of PMUs at each stage. The staged placement strategy follows a bottom-to-top style to assure the optimization of the final objective, using minimum number of PMUs to achieve full observability.

Chapter 4: The development of an alternative method for including phasor measurements in state estimators [18].

A straightforward application of state estimation theory that treats phasor

measurements of currents and voltages as additional measurements to be appended to traditional measurements is now being used in most energy management system (EMS) state estimators. The resulting state estimator is once again non-linear and requires significant modifications to existing EMS software. An alternative approach, which leaves the traditional state estimation software in place is introduced in chapter 3. This novel method incorporates the phasor measurements and the results of the traditional state estimator in a post-processing linear estimator. The underlying theory and verification through simulations of the two alternative strategies is presented. It is shown that the new technique practically provides the same results as the non-linear state estimator and does not require modification of the existing EMS software.

Chapter 5: The development of a method of remotely calibrating instrument transformers with phasor measurements.

The proposed method makes use of several scans of phasor measurements to incorporate Ratio Correction Factors (RCFs) and Phase Angle Correction Factors (PACFs) of instrument transformers as appended unknown parameters. Through the combination of state estimation with instrument transformer calibration, this method does not require the inclusion of accurate instrument transformer models. And as an off-line application, it could be run several times a day to keep calibration up to date. Simulation results on the IEEE 14 bus system are presented after theory analysis to prove the feasibility and validity of the proposed method.

Chapter 6: Conclusion and future work.

This chapter summarizes the research work of this dissertation and recommends future work worthy of further explorations.

Chapter 2. A Pre-processing Method for Optimal PMU Placement

2.1. Introduction

Methods for determining a minimum number of PMU installations to achieve a full observability of an electric power system have been actively investigated in recent years. The ability of the PMU to measure line currents makes all buses adjacent to a PMU observable as long as the line parameters are accurately known. If sufficient numbers of PMUs are installed, it is possible to implement a State Measurement System or State Calculator, by which the system state can be either measured or calculated instead of estimated. In order to determine an optimal PMU placement to minimize the cost of a fully observable Wide Area Measurement System, several algorithms have been introduced to determine the minimum number of PMUs necessary for achieving full system observability. In 1993, Baldwin & Mili proposed a dual search algorithm that uses a modified bisecting search and a Simulated Annealing based method to find the placement of a minimal set of PMUs to make the system measurement model observable. They concluded that when the system parameters are known accurately, PMUs are required only in 1/4 to 1/3 of the network buses to ensure a full observability [7]. In addition to Simulated Annealing, Genetic Algorithm, Tabu Search, and other meta-heuristic approaches have also been applied to accomplish the objective of determining minimum number of PMUs for full observability [19]. Nuqui & Phadke made use of spanning trees of the power system graph to find the optimal location of PMUs by generating and searching a large number of those trees. They then extended the application of simulated annealing for the communication facility restrictions [20]. Xu & Abur employed Integer Programming to solve optimized PMU placement problem. In order to properly take advantage of zero injection buses, topology transformation and non-linear Integer Programming were tested as well [21].

In Graph Theory, the PMU placement problem is a “set covering problem”, that is a

typical Non-deterministic Polynomial-time hard (NP-hard) problem for which the exact solution, for an input of size n, cannot be achieved in polynomial time of $O(n^c)$ for a certain constant c. Presently, known algorithms for this type of problems tend to search through all possible solutions for a given system model to find the exact optimal solution. As the size of the system model increases, the required computational efforts increase exponentially. In this chapter a pre-processing methodology is introduced to reduce the scale of a PMU placement study beforehand to significantly reduce the computational effort.

2.2. Virtual Buses Reduction Rules

For system study and modeling purposes, the system models used by utilities typically include virtual buses that either do not exist or are not practical locations to install PMUs, such as tapped line buses and series capacitor nodes. If these virtual buses are included in the system model of the placement study, it is quite possible that some PMUs will be assigned to these non-existent and non-practical virtual buses. Eliminating virtual buses afterwards will change the system topology, the distribution of the assigned PMUs, and the desired system observability. This problem is solved by developing methods to eliminate virtual buses beforehand from the system data model. Eliminating these buses reduces the size of the system and the dimension of the optimization problem.

In the PMU placement study for large real systems, virtual buses can be categorized into five different types with the assumption that all local line currents originated from one bus are monitored by a PMU placed on that bus. The categories and the corresponding bus reduction rules applied to each type are listed below:

2.2.1. Tapped Line

A tapped line creates a bus in the middle of a line where there are no physical measurement facilities to monitor the signals at the tap, Bus 2 in Figure 2-1. Since there are no metering CTs and PTs, no proper signal input is available for PMU at the tapped line bus.

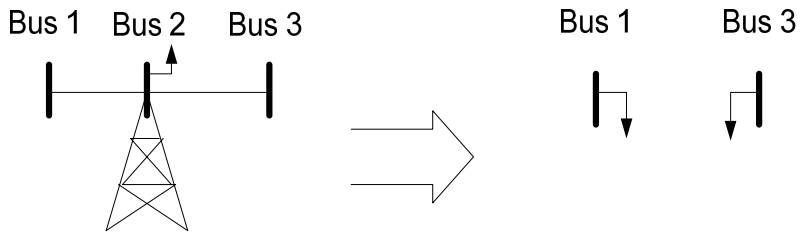

Figure 2-1 Tapped Line

Tapped Line Elimination Rule:

For a virtual bus at a tapped line, the bus representing the tapped line and the lines connecting the tapped line to the system are removed and equivalent injections are added to the adjoining buses.

2.2.2. Virtual Generator

In order to simplify the system model, generators located in close proximity may be grouped together in an equivalent larger generator connected to the system by a virtual (non-existent) bus, bus 1 in Figure 2-2.

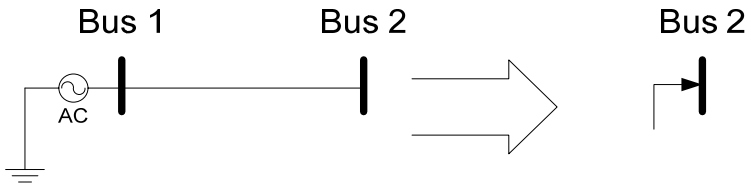

Figure 2-2 Virtual Generator

Virtual Generator and its Bus Elimination Rule:

Virtual buses connecting equivalent generators to the system are removed and replaced by an equivalent injection on the actual bus, bus 2 in Figure 2-2.

2.2.3. Shunt Elements

For the convenience of analysis, a shunt circuit is modeled with its own virtual bus, bus 1 in Figure 2-3, which physically is the same as the connecting bus, bus 2 in Figure 2-3.

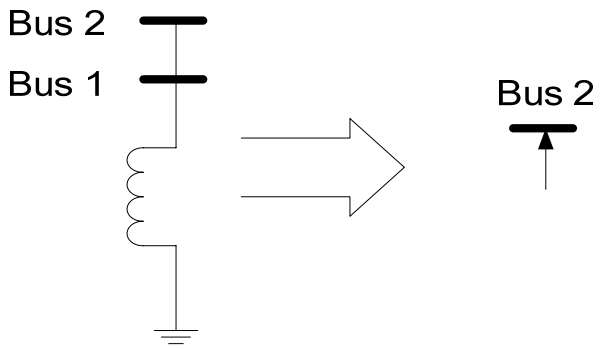

Figure 2-3 Shunt Elements

Shunt Element Bus Elimination Rule:

If a virtual bus connects to a shunt device, the virtual bus and the shunt element are removed and replaced by a corresponding injection.

2.2.4. Series Capacitor

Series capacitors are modeled with a virtual bus that connects them to the transmission line, bus 2 in Figure 2-4. This bus represents the coupling point but it lacks metering PTs and CTs.

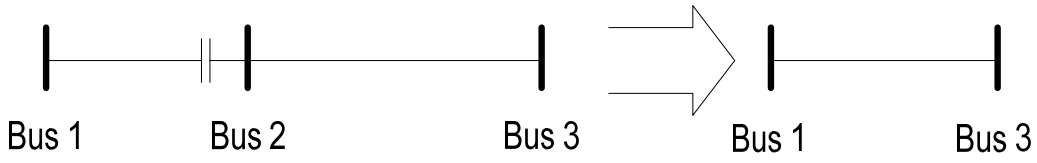

Figure 2-4 Series Capacitor

Series Capacitor Bus Elimination Rule:

If a virtual bus connects to a series capacitor (regardless of the capacitor bus location), the bus and the two connecting lines are removed and replaced by an equivalent line.

2.2.5. Three Winding Transformers

Three winding transformers are modeled as three 2-winding transformers with one side in common. In per unit, the three buses represent the same voltage and if needed, can be monitored by a single PMU.

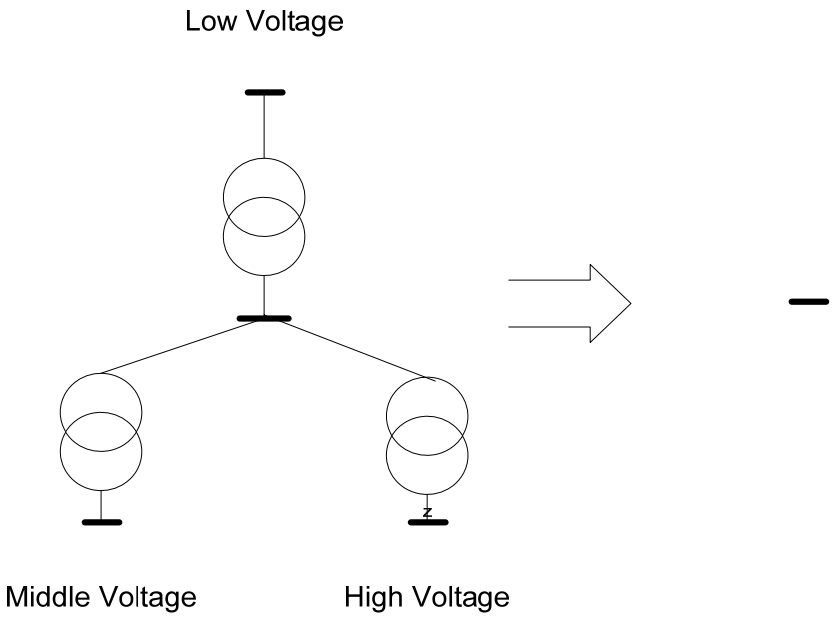

Figure 2-5 Three Winding Transformer

Three Winding Transformer Bus Elimination Rule:

The three winding buses and the middle point of the transformers are replaced by a single bus. This bus is connected to the buses originally connecting the middle and high voltage windings. The low voltage winding is usually connected to distribution system that is not part of the transmission system.

2.2.6. Reduced System Results

The reduction rules listed in the previous sections were applied to a real system model, and it was reduced from 2234 buses with 3641 lines to 1457 buses with 1932 lines. The result on this real system showed that about 1/3 of the system buses were identified as either not practical locations to install PMUs or non-existing physical locations. The remaining buses were identified as candidates for PMU installation.

The reduced system serves as the basis for the studies of placement problems. Optimization results from the studies on the reduced system will be practical in the sense that no PMU will be placed on a virtual bus. The derived rules ensure that the observability of the reduced system accurately represents the observability of the original system since virtual buses reduction only reduces the scale of optimization problem and keeps the system topology intact. As the result shows, the reduction of system size is substantial for a large system. It is then both beneficial and necessary to apply the proposed reduction rules ahead of an optimization process to reduce the computational effort and at the same time to assure the validity of the optimization results.

2.3. Matrix Reduction Algorithm

2.3.1. Coverage Matrix Introduction

For every placement problem, there exists a coverage matrix that indicates the coverage ranges when facilities are installed at different locations. For example, the incidence matrix with diagonal elements as ones is a coverage matrix for power systems. The IEEE 14 bus system, Figure 2-6, is used as an example to illuminate the structure of coverage matrix and its scale. Table 2-1 displays the coverage matrix for this system.

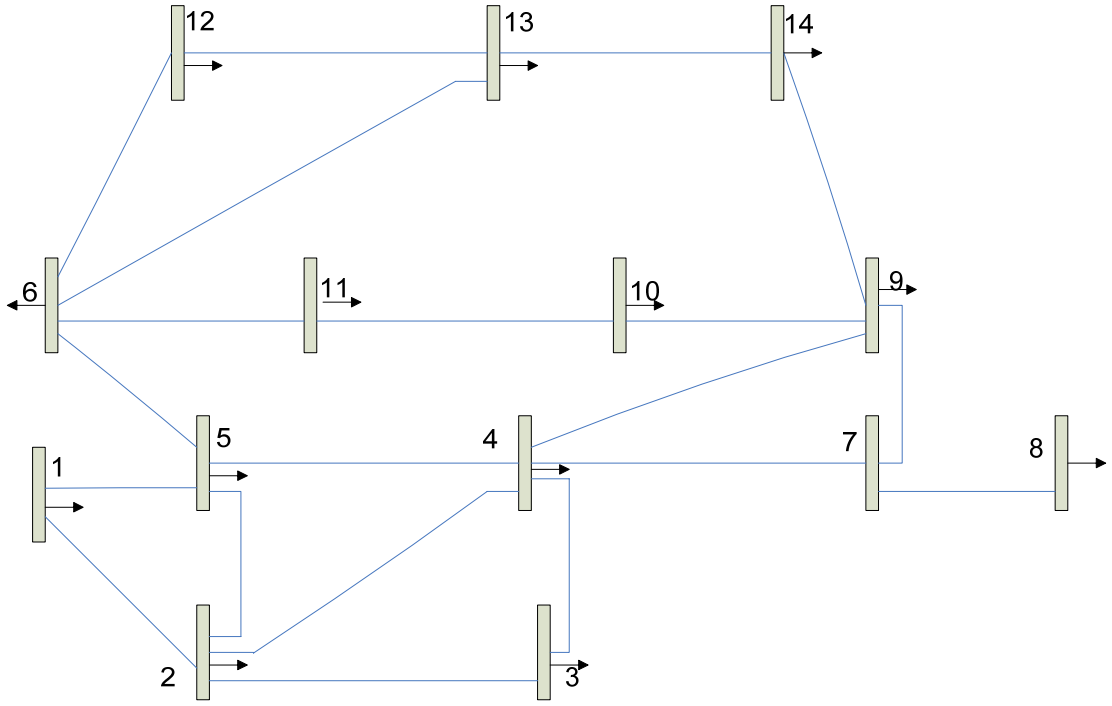

Figure 2-6 IEEE 14 Bus System

Each row of an incidence matrix represents a candidate for PMU installation and each column represents a bus whose state needs to be measured or calculated by phasor measurements. If a PMU is installed on bus i and the voltage and current phasor measurements are able to extend the observability to buses j and k, the corresponding elements of (i, i), (i, j) and (i, k) are entered as ones in the incident matrix and any others are entered as zeros. Since a PMU installed on one bus measures the voltage phasor of this bus and all current phasors in the lines originated from this bus, the bus itself and immediate neighbors could be observed with one PMU deployed on this bus. Therefore, the coverage matrix for PMU placement problem in power system is the same as the incidence matrix. The dimension of the coverage matrix indicates the scale of the problem. With the reduction of this matrix, the computational effort decreases significantly.

Table 2-1 Coverage Matrix (Incidence Matrix) of IEEE 14 Bus System

	1	2	3	4	5	6	7	8	9	10	11	12	13	14
1	1	1	0	0	1	0	0	0	0	0	0	0	0	0
2	1	1	1	1	1	0	0	0	0	0	0	0	0	0
3	0	1	1	1	0	0	0	0	0	0	0	0	0	0
4	0	1	1	1	1	0	1	0	1	0	0	0	0	0
5	1	1	0	1	1	1	0	0	0	0	0	0	0	0
6	0	0	0	0	1	1	0	0	0	0	1	1	1	0
7	0	0	0	1	0	0	1	1	1	0	0	0	0	0
8	0	0	0	0	0	0	1	1	0	0	0	0	0	0
9	0	0	0	1	0	0	1	0	1	1	0	0	0	1
10	0	0	0	0	0	0	0	0	1	1	1	0	0	0
11	0	0	0	0	0	1	0	0	0	1	1	0	0	0
12	0	0	0	0	0	1	0	0	0	0	0	1	1	0
13	0	0	0	0	0	1	0	0	0	0	0	1	1	1
14	0	0	0	0	0	0	0	0	1	0	0	0	1	1

2.3.2. Observability of Zero Injection Buses and their Immediate Neighbors

Zero injection buses and their immediate neighbors are special nodes in PMU placement studies. If all the buses incident to an observed zero injection bus are observable, except one, Kirchhoff's current law allows direct inference of the current going through the lines connecting the zero injection bus to the un-observable one. (Kirchhoff's current law: the current entering any node is equal to the current leaving that node.) Therefore, the state of this un-observable bus can be calculated, thus completing the observation of all the buses in the set of zero injection bus and its immediate neighbors. Assume that a 4 bus system consists of one zero injection bus 0 (shown in red in Figure 2-7) and its 3 immediate neighbor buses with injections. As long as there is no

more than one un-observable bus (shown in yellow), the system state on every single bus can be determined either by direct phasor measuring or by calculation through ohm's law or Kirchhoff's current law.

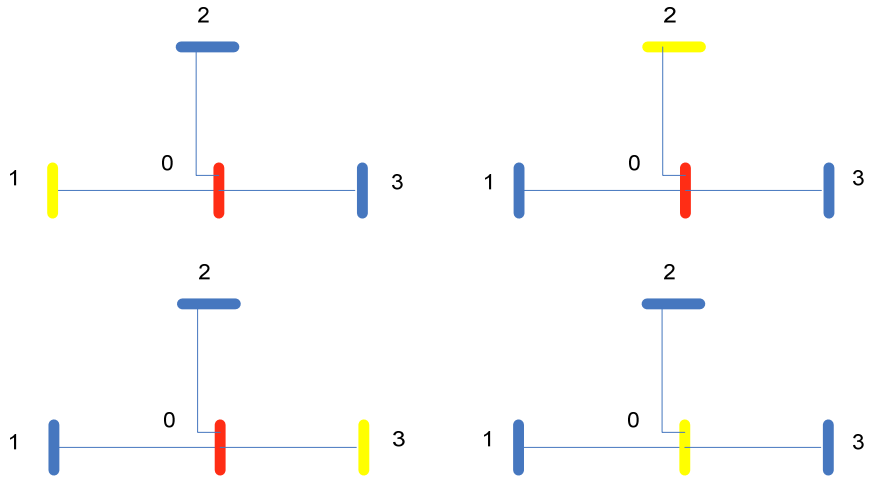

Figure 2-7 Buses Observed through Kirchhoff's Law

When there are more than one interconnected zero injection buses constituted in a pure zero injection island, the island could be considered as a single zero injection bus. The rules applicable to a single zero injection bus hold true to the zero injection island.

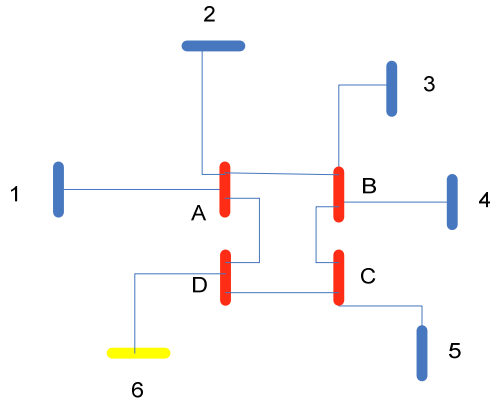

Figure 2-8 Connected Zero Injection Buses

Take Figure 2-8 as an example. Bus A, B, C, and D are zero injection buses (shown in red) interconnected with each other, composing a zero-injection island of the system.

Suppose that all those buses that are adjacent to the zero-injection island are observable, then for every zero injection bus, the sum of currents injected into the bus is zero, according to Kirchhoff's current law. For instance, in Figure 2-8, if buses 1 to 6 are all observable, then Kirchhoff's equations are as follows,

$$\begin{aligned}
&\frac{V_1 - V_A}{Z_{1A}} + \frac{V_2 - V_A}{Z_{2A}} + \frac{V_B - V_A}{Z_{AB}} + \frac{V_D - V_A}{Z_{AD}} = \frac{V_A}{Z_A} \\
&\frac{V_3 - V_B}{Z_{3B}} + \frac{V_4 - V_B}{Z_{4B}} + \frac{V_A - V_B}{Z_{AB}} + \frac{V_C - V_B}{Z_{BC}} = \frac{V_B}{Z_B} \\
&\frac{V_5 - V_C}{Z_{5C}} + \frac{V_B - V_C}{Z_{BC}} + \frac{V_D - V_C}{Z_{CD}} = \frac{V_C}{Z_C} \\
&\frac{V_6 - V_D}{Z_{6D}} + \frac{V_A - V_D}{Z_{AD}} + \frac{V_C - V_D}{Z_{CD}} = \frac{V_D}{Z_D}
\end{aligned} \tag{2.1}$$

where, V_x represents the voltage of bus x; Z_{xy} represents the line impedance; and Z_x represents the summation of shunting impedance of connecting lines.

The equation could be simplified as (2.2), where Y is the node admittance matrix for the zero-injection island.

Since Y is determined by the system structure and parameters, the impedance matrix $Z = Y^{-1}$ can be used to calculate the state of bus A through bus D. As described in [22], the admittance matrix is generally invertible for a normal transmission network, and for a sub network with the inclusion of pure zero injection buses, the non-singularity of Y matrix is usual, if not universal.

$$Y\times\begin{bmatrix}Z_A\\Z_B\\Z_C\\Z_D\end{bmatrix}=\begin{bmatrix}\frac{V_1}{Z_{1A}}+\frac{V_2}{Z_{2A}}\\\frac{V_3}{Z_{3B}}+\frac{V_4}{Z_{4B}}\\\frac{V_5}{Z_{5C}}\\\frac{V_6}{Z_{6D}}\end{bmatrix}\longrightarrow\begin{bmatrix}Z_A\\Z_B\\Z_C\\Z_D\end{bmatrix}=Z\times\begin{bmatrix}\frac{V_1}{Z_{1A}}+\frac{V_2}{Z_{2A}}\\\frac{V_3}{Z_{3B}}+\frac{V_4}{Z_{4B}}\\\frac{V_5}{Z_{5C}}\\\frac{V_6}{Z_{6D}}\end{bmatrix} \tag{2.2}$$

The same rule could be applied to any group of zero injection buses by considering each of them as a zero injection island. With Kirchhoff's law, the observability is enhanced by iteratively calculating states of those special buses although they are not directly connected with the one installed with a PMU.

In conclusion, when a bus is zero injection bus, or it is an immediate neighbor of a zero injection bus, the state of this bus may be calculated with the knowledge of the states of other buses in the set. The requirement for observability of a PMU installed on the bus itself or one of the neighboring buses is not as strict at the presence of a zero injection bus around.

2.3.3. Steps for Implementing the Matrix Reduction Algorithm

The Matrix reduction algorithm considers the special features of zero injection buses and reduces the dimension of the coverage matrix by iteratively eliminating rows and columns of the matrix according to the topology and distribution of zero injection buses in the system.

Different power systems have different topologies, thus different incidence matrices. To a specific PMU placement problem, the optimal placement problem can be defined as that given a finite set X and a family $F=S_1,S_2,\cdots,S_n$ composed of sets

$S_j \subseteq X, j = 1, \cdots, n$, find a minimum cardinality $J \subseteq \{1, \cdots, n\}$ such that $\bigcup_{j \in J} S_j = X$, where the set X includes candidates to be covered and $S_j \subseteq X, j = 1, \cdots, n$ correspond to sets of covered buses by n candidate buses to be installed with PMUs. $|J|$ is the minimum number of PMUs necessary for full observability.

For a practical power system, some buses may have installed PMUs from existing applications; this correlates the optimal PMU placement to these existing locations. By repeatedly attempting to eliminate rows and columns of the incidence matrix, the 'Matrix Reduction Algorithm' introduced in this chapter reduces the scale of the matrix iteratively according to the properties of each PMU installation candidate. During this process, an optimal set $M \subseteq \{1, \cdots, n\}$ and a reduced instance are constructed. As long as the optimal set $M' \subseteq \{1, \cdots, n\}$ of the reduced instance could be achieved, the final optimal solution of the original instance is $M \cup M'$, and the computational effort is restricted by identifying M'. All the optimization methods, like Genetic Algorithm, Integer Programming, and Simulated Annealing, etc. can be applied to the reduced system model to achieve M', the optimization set for a smaller sized system.

The steps of Matrix Reduction Algorithm for PMU placement are:

1. Generate a coverage matrix {p(i,j)}, which equals the incidence matrix with diagonal elements as ones. Each row represents a candidate bus for PMU installation, and each column is a member of X, representing a bus in the system to be observed with phasor measurements.

2. Eliminate the rows in the coverage matrix corresponding to the buses with PMUs already installed. Then eliminate the columns corresponding to the buses which can be covered by these existing PMUs. All the remaining rows in the coverage matrix are the available candidates for PMU installation. Once a certain bus is identified a PMU or non-PMU bus, the corresponding row is eliminated from the coverage matrix. Similarly, once a certain bus is identified as covered, the corresponding column is eliminated from the

coverage matrix.

3. Determine if there is any column that has only one non-zero element. Assuming that the non-zero element is in the row i. If this column does not represent a bus within 1 step distance from zero injection buses, a PMU must be deployed at the bus that corresponds to row i. Add this bus to the list of PMU locations. Eliminate row i and all columns observable by current PMU set. Here, 1 step distance from zero injection buses means zero injection buses and the immediate neighbor buses connected through transmission lines.

4. Eliminate columns that are observable by the current PMU set. Different from traditional 'set covering' problems, PMU placement also deals with special placement and coverage candidates, the zero injection buses. Zero injection buses provide a positive effect in optimal PMU placement by enabling state calculation using Kirchhoff's law. Therefore, when zero injection buses are taken into consideration, the coverage candidate set can be further reduced.

5. Eliminate row i'' if all its elements are less than or equal to the corresponding elements of another row i' ($p(i'',j)<=p(i',j)$ for $\forall j$). The assumption behind this operation is that the performance of a PMU installed on the bus corresponding to row i' is superior to the one of row i''. One would rather install a PMU on the bus related to row i', since a PMU at i' will cover the same or more buses than a PMU at the bus corresponding to bus i''.

6. Eliminate column j'' if all its elements are greater than or equal to the corresponding elements of another column j' ($p(i,j')<=p(i,j'')$ for $\forall i$). The assumption behind the operation is that if the bus corresponding to column j' is observable, then the one corresponding to column j'' will be observable as well.

7. Repeat steps 3 to 6 until: (a) the coverage matrix becomes completely empty;

or (b) no more rows and columns can be eliminated.

The expected ideal situation is for the coverage matrix to be completely empty. Under this situation, the final optimal number of needed PMUs and their locations are determined. However, if the iteration stops because no more rows and columns can be eliminated, it is necessary to apply some other algorithms like the Greedy Algorithm, Genetic Algorithm, etc. to achieve the optimization of the reduced system model.

2.3.4. Simulation Results

The Matrix Reduction Algorithm has been applied to 5 systems, including 4 IEEE systems and the reduced 1457 bus real system. The results, shown in Table 2-2, demonstrate the effectiveness of the proposed method to reduce the scale of the problem:

Table 2-2 Problem Scales Before and After Reduction

System	Number of Lines	Problem Scale	
		Before Reduction	After Reduction
IEEE 14 bus	20	14×14	5×5
IEEE 30 bus	41	30×30	1×1
IEEE 57 bus	78	57×57	29×30
IEEE 118 bus	179	118×118	45×46
1457 bus	1932	1457×1457	139×137

Compare the problem scales before and after the application of Matrix Reduction Algorithm, it is clear that the reduced problem is much smaller in dimension. Different types of optimization algorithms can then be applied to the reduced systems. The Greedy Algorithm has been used in this research and is introduced in the next section.

2.4. Combine Matrix Reduction Algorithm with Greedy Algorithm for Optimal PMU Placement

In this section, the Greedy Algorithm is employed to find the optimal PMU placement set on the smaller systems generated by Matrix Reduction Algorithm. This

algorithm makes decisions according to one rule: at each stage, choose to install a PMU at the bus that covers the largest number of uncovered buses.

Assume that there is a set of n buses $K = P_1, P_2, \cdots, P_n$ in the system, serving as a finite PMU placement candidate set, of which, m buses $U = P_{j1}, P_{j2}, \cdots, P_{jm}$ with PMUs already installed. The set of uncovered buses by the current PMUs is represented as $X = P_{i1}, P_{i2}, \cdots, P_{ik}$. While X is not empty, choose a P_* from $K - U$, such that maximum number of P_{i*} from X will be covered.

As mentioned before, the PMU placement problem is a Nondeterministic Polynomial-time hard problem. In order to balance the computational efforts and feasibility of optimization performance, an approximated optimum will be achieved instead of the exact one. In reference [23], a theorem is presented to show that the Greedy Algorithm is a performance guaranteed method for the placement problem. If one assumes an instance of the set covering problem given by $F = S_1, S_2, \cdots, S_n$, where each $S_m \subseteq X$, and $\bigcup_{m \in M} S_m = X$. If J_{opt} is the exact optimal solution, and J_{greedy} is a solution found by the greedy algorithm. Then

$$| J_{greedy} | \leq H(\max_{m=1,\cdots,n} | S_m |) \cdot | J_{opt} | \tag{2.3}$$

where $H(d) = \log_e(d)$ (2.4)

The equality is held true if and only if $| S_k | = \max_{m=1,\cdots,n} | S_m |$, for $k = 1, \cdots, n$, which means every single bus throughout the system connects with the same number of neighbor buses. Generally, this is not the case for a large real system, so, "<" is always established.

An approximate optimal PMU placement set can be achieved by using the combination of Matrix Reduction Algorithm and Greedy Algorithm. The workflow is shown in Figure 2-9.

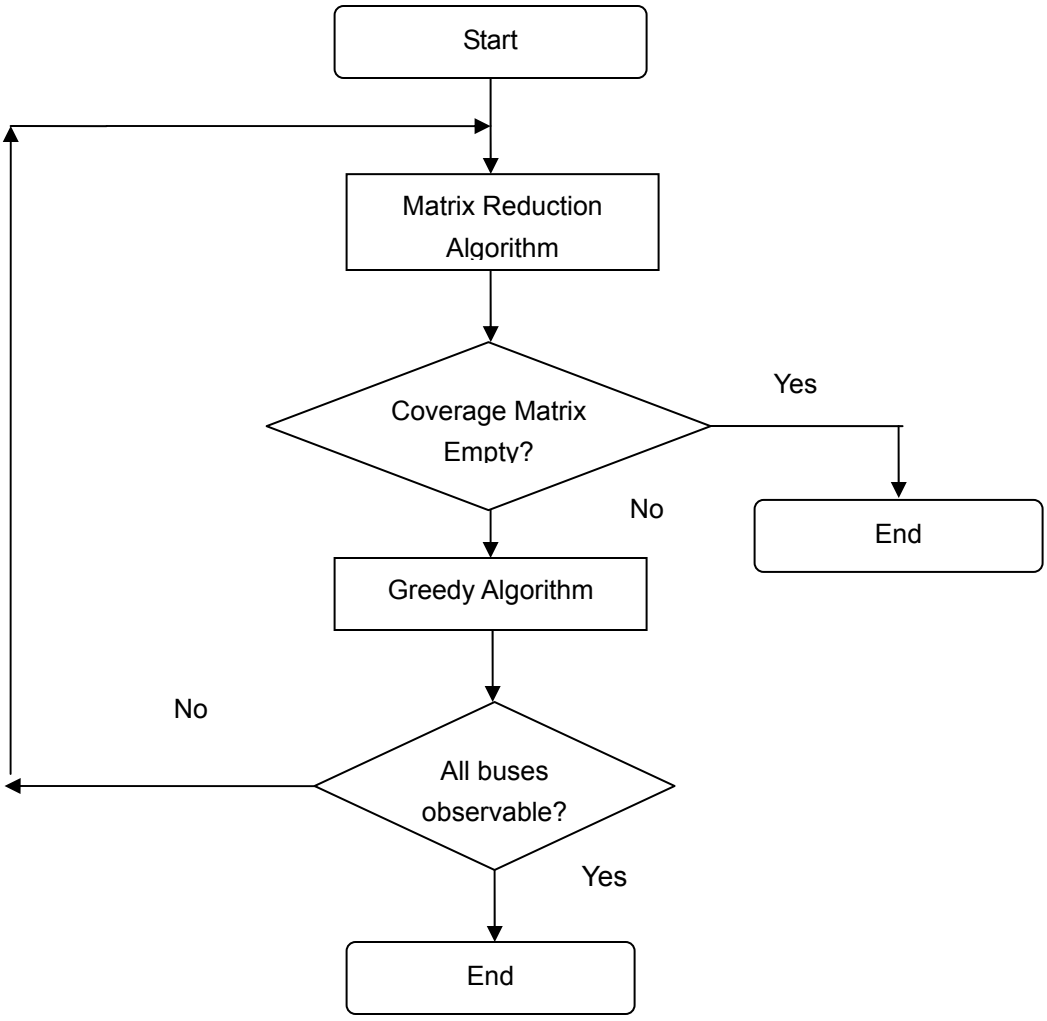

Figure 2-9 Workflow of the Combination of Matrix Reduction Algorithm and Greedy Algorithm

Five systems were tested with the placement method proposed. Approximate optimal PMU placement sets are tabulated below.

Table 2-3 Approximate Optimal PMU Placement Set

System	Number of Zero Injection Buses	PMUs Required by Different Methods		
		Non-linear Constraints	Topology Transformation	Proposed
IEEE 14 bus	1	3	3	3
IEEE 30 bus	5	7	8	8
IEEE 57 bus	15	13	12	12
IEEE 118 bus	10	29	28	29
1457 bus	228	N/A	N/A	389

It is not very difficult to verify the performance feasibility for the IEEE test bed systems, for they have been used as the standard systems to deploy minimal set of PMUs by several researchers through several methods. Like the binary integer programming method with non-linear constraints and the binary integer programming method with topology transformation [21] tabulated in Table 2-10. However, no verified optimal placement set is available as comparison for the 1457 bus system, a real-world bulk system. Therefore, Lagrangian Relaxation is introduced in the next section to verify the performance feasibility on the 1457 bus system.

2.5. Performance Feasibility Verification by Lagrangian Relaxation

Lagrangian relaxation [24] is a technique which works by moving hard constraints into the objective and punishing the objective if they are not satisfied.

Consider an Integer Programming (IP) problem in the following form:

$$\begin{aligned} &\text{Min} \quad f = \sum_{j=1}^{n} x_j \\ &c_k(x_j) \geq 1, \quad x_j = 0 \quad \text{or} \quad 1, \quad j = 1, \cdots, n \quad k = 1, \cdots, m \end{aligned} \tag{2.5}$$

If the constraints are introduced into the objective:

$$\text{Min} \quad f = \sum_{j=1}^{n} x_j + \sum_{k=1}^{m} \sum_{j=1}^{n} \lambda_k \left(1 - c_k\left(x_j\right)\right) \tag{2.6}$$

$$\lambda_k \geq 0, \quad k = 1, \cdots, m; \qquad x_j = 0 \quad \text{or} \quad 1$$

λ_k are non-negative weights. The optimal solution to this problem is a relaxation of the original problem for any value of $\lambda_k \geq 0$. For any feasible solution to the original problem, the objective of the relaxed one is definitely no greater, since a negative value is added. Therefore, the maximum is certainly less than or equal to the true optimal value.

If the positive effect of zero injection buses is not considered, the placement optimization can be relaxed by adding hard constraints constructed according to incidence matrix only. However, the number of required PMUs will be more than its need by an extent determined by the number and locations of zero injection buses. In order to include as much as possible the positive effect of zero injection buses, Xu and Abur introduced a method of modifying the constraints associated with the neighboring buses of zero injection buses and forming a set of non-linear constraints [21]. Therefore, the problem is not a 0-1 linear program any more. Instead, it is a 0-1 polynomial programming one.

Glover discussed a standard approach for transforming the 0-1 polynomial programming problem into a 0-1 linear programming with the following steps [25].

1. Substitute each x_j^k by x_j(Multiplication of x_j and itself, no matter how many times, equals to itself).
2. Substitute each cross product $\prod_{j \in Q} x_j$ by the new variable x_Q that is to satisfy the constraints

$$\begin{aligned} &\textstyle\sum_{j \in Q} x_j - x_Q \leq q - 1, \\ &-\textstyle\sum_{j \in Q} x_j + q x_Q \leq 0, \\ &x_Q = 0 \text{or} 1. \end{aligned} \tag{2.7}$$

where q represents the number of elements in Q.

Finding λ_k k=1,…,m that maximize the result of the relaxed problem is the Lagrangian dual problem; the approach is shown in Figure 2-14 [24] :

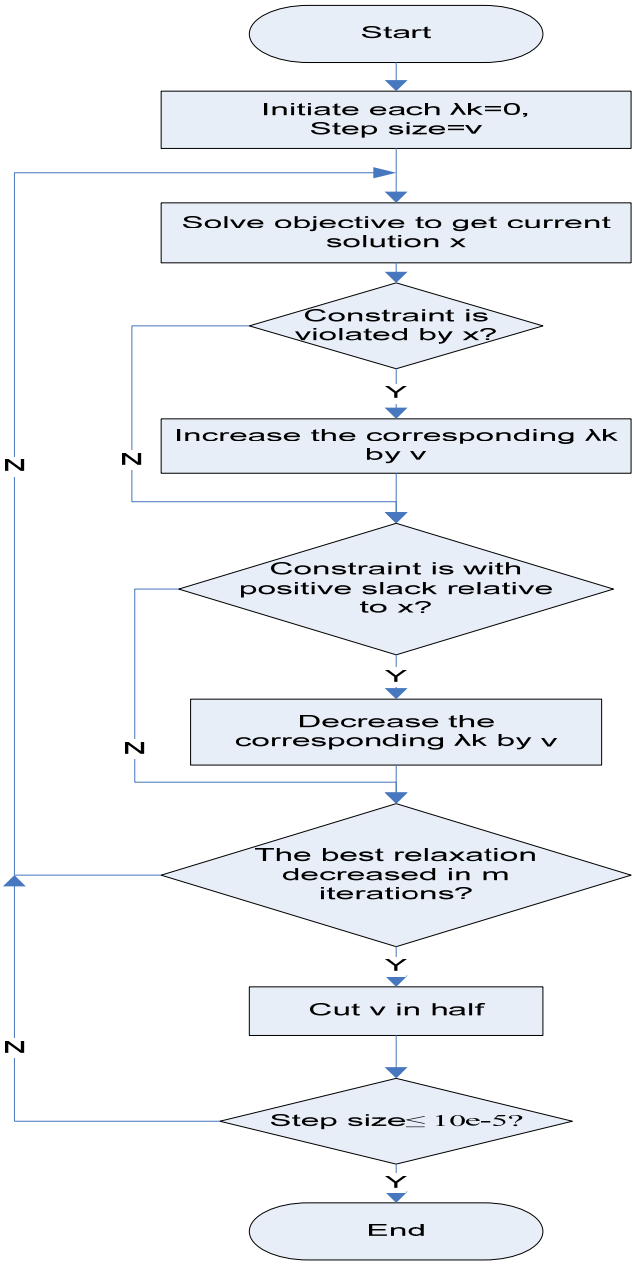

Figure 2-10 Approach of Finding the Low Bound of the Optimal Solution by Lagrangian Relaxation

The solution could be used as a low bound of the number of elements in exact optimal set. If the solution by Greedy Algorithm is close enough to the low bound, say, 3%, it could be claimed, with good quality, that the solution is a feasible one.

The low bound of the real world system model with 1457 buses is 387, which is 2 less than 389, the optimal solution achieved by the combination of matrix reduction algorithm and greedy algorithm. Since $2 \div 387 = 0.51\% << 3\%$, it is safe to conclude that the difference between the low bound and the optimal solution is small enough that the algorithm combination applied is able to achieve a feasible solution close enough to the exact optimal one. This proves that the pre-processing does not significantly degrade the performance guarantee, if it does. The pre-processing is an efficient way to reduce the size of the system under research beforehand, while keeps the feasibility of the optimization.

2.6. Conclusion

In this chapter, a pre-processing virtual bus elimination method and a matrix reduction algorithm were used to reduce the size of the placement model and thus significantly decrease the computational effort for the determination of the optimal PMU placement set. The proposed methodology has been applied to four IEEE systems and a real-world 1457 bus system model. The reduction in the sizes of these systems is considerable and exponentially decreases the required computational effort. To prove the performance guarantee of the proposed algorithm, Lagrangian Relaxation was used to show that the minimum set obtained with the proposed method is very close to the exact optimal set. Therefore, data processing of the system model helps simplify the PMU placement problem, and it is applicable to all optimal placement methods that have been proposed in the past. And it can be performed beforehand independently of the algorithm or method used to obtain the optimal placement set.

Chapter 3. Staged PMU Installation

3.1. Introduction

It is clear that to achieve a high level of performance improvement and to meet the system redundancy requirement, a large number of PMUs and communication links are needed. As procuring and installing such a large number of PMUs and communication channels at once would require a huge capital investment from utilities, it is conceivable to take a staged approach to implement a phasor measurement system with a large number of PMUs.

Dua explored the optimal multistage scheduling problem of PMU placement in 2003 [26]. He proposed an integer linear programming approach to maximize the number of observed buses as an objective at each stage. Since buses connecting with more lines are likely to cover more buses, they tend to have higher priority. Therefore, the first few PMUs are most likely installed on the hub-like buses originating many lines. If these buses are close to each other rather than scattered in the system, portions of the system away from these hubs may benefit little from the PMU installations. Nuqui and Phadke introduced the concept of depth of un-observability in paper [20]. The concept is derived from the generated tree of the real network. A new definition of depth of un-observability from the network point of view is introduced in this chapter. Based on this criterion, a staged PMU installation that guarantees the final optimal PMU placement solution using Binary Integer Programming approach is proposed.

3.2. Depth of Un-observability and Corresponding Matrix

Depth of un-observability for one bus is defined as one less than the number of lines between the given bus and the nearest bus with a PMU installed. The reason of -1 in the definition is to emphasize that the buses directly connected with PMU buses are always

observable by ohm's law. The maximum depth of un-observability among all buses is defined as the depth of un-observability for the system.

$$\text{depth} = \max_{j}\left(\min_{i}\left(d(i,j)\right)\right) - 1 \qquad j:\text{no\_PMU\_buses} \quad i:\text{PMU\_buses}$$

$$d(i,j):\text{dist\_between\_i\&j}$$

Obviously, the larger the depth the further a bus is from a PMU and consequently, the smaller the benefits obtained from the PMUs. The state calculation or estimation for the buses with larger depth has a larger probability of encountering mis-estimation propagations due to errors or uncertainties in system model and conventional measurements. For an extreme example, if all the PMUs are centralized in a certain area of the system, buses far from this area will barely benefit from the accuracy of phasor measurements. Therefore, generally, the depth of un-observability is a control mechanism that leads to the even distribution of the limited PMUs in the system, so as to take the utmost advantages of available PMUs.

Problems related to depth are conceptive topology problems depicted by the incidence matrices. Assume a small system is topologically constructed as shown in Figure 3-1.

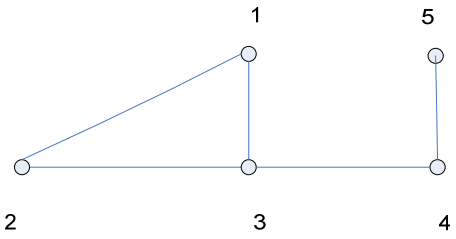

Figure 3-1 4 Bus System

The incidence matrix is a 4×4 symmetrical matrix, shown in Table 3-1:

Table 3-1 Incidence Matrix of 4 Bus System

	1	2	3	4	5
1	1	1	1	0	0
2	1	1	1	0	0
3	1	1	1	1	0
4	0	0	1	1	1
5	0	0	0	1	1

If this incidence matrix is squared, the resulting matrix contains non-zero elements denoting the existence of at least one path between two buses composed of two lines or less [27].

Table 3-2 Square of Incidence Matrix

	1	2	3	4	5
1	3	3	3	1	0
2	3	3	3	1	0
3	3	3	4	2	1
4	1	1	2	3	2
5	0	0	1	2	2

After substituting the non-zero elements in the square matrix with 1s, a new incidence matrix representing the relationship of buses of "depth 1" or less is obtained in Table 3-3. The equivalent topology for Table 3-3 is shown in Figure 3-2.

Table 3-3 Incidence Matrix of "Depth 1" of Un-observability

	1	2	3	4	5
1	1	1	1	1	0
2	1	1	1	1	0
3	1	1	1	1	1
4	1	1	1	1	1
5	0	0	1	1	1

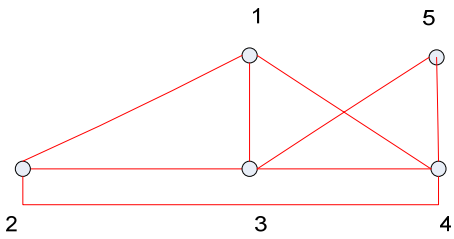

Figure 3-2 "Depth 1" of Un-observability of 4 Bus System

The same procedure can be applied repeatedly to an incidence matrix to obtain any desired depth of un-observability. For instance, incidence matrix of "depth d" of un-observability could be presented as $\text{sign}(A^{d+1})$, where A is the original incidence matrix of the system. The new incidence matrix represents a new system topology with each line denoting the existence of a path of length d or less [27]. Therefore, if a set of PMUs are able to satisfy the observability of the system with topology of "depth d", then every bus in the system is guaranteed to be d+1 or fewer lines away from a PMU in the set, that is, the system fulfills the requirements of "depth d" of un-observability.

3.3. Staged Installation

In the situation where there are enough conventional measurements to meet the observability requirement without leaving any un-observable islands, which is often the case in the real world, phasor measurements are beneficial to state estimators mainly by enhancing the measurement redundancy and thus estimation accuracy. However, if phasor measurements are used to cover the parts of the system un-observable by conventional measurements, those PMUs that augment the area of observability would be assigned a higher installation priority.

For those PMUs used to promote estimator accuracy, the installation at each stage is expected to be evenly distributed over the system to achieve the optimal depth possible

with minimum number of PMUs. Binary integer programming can be used to determine the minimum set of PMUs out of the optimal set for full observability to satisfy a “depth d” of un-observability.

It is clear that the final optimization objective for full observability is that a minimal set of PMUs provides the necessary phasor measurements to cover the entire system, making the system state available through measuring and calculating. Consequently, when deliberating “depth 1” of un-observability, one needs to keep the final objective in mind and confine the “depth 1” set inside the one for full observability. Namely, candidate buses for “depth 1” of un-observability must be members of the full observability set. This pattern is inherited as taking the “depth d” set into account while searching for the “depth d+1” set.

In accordance with the depth of un-observability, the PMU installation could be staged in the following steps:

1) PMUs with special priorities, such as those supplementing conventional measurements for observability purposes, constitute the first batch S.

2) Generate an incidence matrix {P(i,j)} for the system with n buses. Determine the optimal set W for full observability. Assume that the incidence matrix of “depth d” of un-observability is {Q(i,j)} and the optimal set of “depth d” is M(d). Initialize d=1 and M(0)=W-S, Q=sign(Q*P).

3) Solve binary integer programming problem in:

$$\text{Min} \quad f = \sum_{j=1}^{n} x_j$$

$$c_k(x_j) \geq 1, \quad x_j = 0 \quad \text{or} \quad 1, \quad j = 1, \cdots, n \quad k \in \{\{1 \cdots n\} - S\} \qquad (2.8)$$

$$x_t = 1, \quad t \in S; \quad x_r = 0, \quad r \in \{\{1 \cdots n\} - S - M(d-1)\}$$

where, x_j denotes the status of bus j; If a PMU is installed on bus j, x_j=1; otherwise, x_j=0; and c_k stands for the inner product of the selected row vector in "depth d" incidence matrix Q and binary decision variable vector of $\{x_1, x_2, \cdots x_n\}$.

This binary integer programming intends to determine the minimal set, M(d), of buses to be installed with PMUs for "depth d" of un-observability, while satisfying two constraints:

a). PMU installation candidates are restricted to those inside the optimal set M(d-1) of "depth d-1" of un-observability, and

b). Buses with special priorities have PMUs already deployed and therefore have 1s in the corresponding positions of the decision variable vector.

M(d) will make every bus in the "depth d" incidence matrix Q observable with the minimal number of PMUs.

4) Update d = d + 1, Q = sign(Q*P) and iterate step 3 until no more PMUs could be eliminated from the optimal set for "depth d", that is |M(d)| = 1.

3.4. Simulation Results

Five sample systems including four IEEE systems and one real large system model with 1457 buses have been tested. The final optimization results are obtained using the method introduced in the previous chapter. And the simulation results of staged installation for different depths are shown in Table 3-4:

Table 3-4 Numbers of PMUs Necessary for Different Depths of Un-observability

	System Tested				
	IEEE 14 Bus System	IEEE 30 Bus System	IEEE 57 Bus System	IEEE 118 Bus System	1457 Bus System
Fully Observed	3	8	12	29	389
Depth 1	2	4	11	29	389
Depth 2	1	3	7	9	122
Depth 3		1	4	6	87
Depth 4			3	3	59
Depth 5			2	3	42
Depth 6			1	2	30
Depth 7				2	23
Depth 8				2	13
Depth 9				2	10
Depth 10				1	9
Depth 11-12					7
Depth 13					6
Depth 14-15					4
Depth 16-18					3
Depth 19-31					2
Depth 32					1

With the increase of depth of un-observability, the number of PMUs necessary to satisfy that depth is decreasing. The set of PMUs required for “depth d” is always a subset of the one of “depth d-1”. If PMUs are installed in a staged manner, those in the set of greater depth are going to be installed first, followed by those in the set of smaller depth. Take the example of the IEEE 57 bus system, 12 PMUs are required for full

observability, out of which, 11 can make the "depth 1" of un-observability, out of which, 7 can make the "depth 2" of un-observability… The lists of PMUs necessary for "depth d" of un-observability are given in Table 3-5.

Table 3-5 PMU Installation Strategy for IEEE 57 Bus System

Full Obs.		Dep. 1		Dep. 2		Dep. 3		Dep. 4		Dep. 5		Dep. 6
PMUs	Full - Dep. 1	PMUs	Dep. 1-2	PMUs	Dep. 2-3	PMUs	Dep. 3-4	PMUs	Dep. 4-5	PMUs	Dep. 5-6	PMUs
1	**9**	**1**	**1**	**14**	**19**	**14**	**14**	**28**	**32**	**28**	**28**	**38**
6		**6**	**6**	**19**	**41**	**28**		**32**		**38**		
9		**14**	**25**	**28**	**53**	**32**		**38**				
14		**19**	**51**	**32**		**38**						
19		**25**		**38**								
25		**28**		**41**								
28		**32**		**53**								
32		**38**										
38		**41**										
41		**51**										
51		**53**										
53												

According to the depth of un-observability and the corresponding set of required PMUs, the installation for this system can start with bus 38. The largest distance between bus 38 and any other buses in the system -1, the depth of un-observability of the system, is equal to 6. It needs to be recognized that for synchronized measurement, at least two PMUs are needed to calculate the relative phasor angles between them. Therefore, bus 28 is preferred to be deployed with a PMU at the same time as bus 38 to reach "depth 5". After that, the order of installation is:

32-14-{19, 41, 53}-{1, 6, 25, 51}-9

For large systems, it takes a considerable number of PMUs to reach one less depth of

un-observability; other criteria can be used to determine the installation sequence, like taking the voltage level of buses as the sub-key, considering the augment of observable buses, the measurement redundancy increase, etc..

3.5. Conclusion

A staged PMU placement strategy is introduced in this chapter. This staged installation strategy based on the minimum depth of un-observability adopted binary integer programming to facilitate evenly installation of PMUs progressively throughout the system, achieving the desired least distances of every bus to those with PMUs with the minimum number of PMUs. The depth of un-observability is a control mechanism that leads to the even distribution of the limited PMUs in the system. It reflects the least advantage any bus in the system can take from the accurate phasor measurements. Since the final objective is to realize the full observability of the entire system, a staged placement method from bottom to top has been adopted. The candidates for “depth d+1” placement set are those buses in the set of “depth d”. This progressive installation minimizes the number of PMUs for each stage and assures the satisfaction of ultimate objective of full observability.

The pre-processing method of reduction of system dimension introduced in the previous chapter and staged PMU placement provide a sound tool to perform optimal PMU placement study and the best deployment procedures.

Chapter 4. An Alternative for Including Phasor Measurements in State Estimators

Synchronized phasor measurement units were developed in mid-1980s. These instruments use GPS signals to synchronize measurements of positive sequence voltage phasors at network buses and positive sequence current phasors in the lines connected to those buses. The accuracy of synchronization is better than one micro-second, and the set of measurements provide a real-time snapshot of the state of the power system. Since positive sequence voltages at all network buses constitute the state vector of a power system, it is obvious that there is a paradigm shift in the manner in which the state estimation problem can be solved by using phasor measurements exclusively [2, 28]. With these measurements one is led to a process which measures the system state, rather than estimating it using measurements which are non-linear functions of the state.

Although a phasor based state vector measurement system is a preferable technique to traditional state estimators, it is recognized that in many cases one is not able to provide PMU measurements in sufficient numbers to accomplish this goal. It has been shown that when phasor measurements are added to the other measurements in sufficient numbers the accuracy of the state estimate is much improved [15, 29, 30].

It should be emphasized that this chapter addresses one specific aspect of PMU applications in state estimation: viz. the inclusion of PMU data in the state estimation process. The traditional state estimator is assumed to be functioning normally in the absence of PMU data, i.e. it is implicitly assumed that the existing SCADA system provides traditional measurements in sufficient numbers with proper placement so that the state estimate based on those measurements is able to handle bad data and provide complete observability. An alternative approach of including PMU data in the state estimation process which is efficient and avoids the necessity of changing the state estimation software in the existing EMS system will be proposed in this chapter.

It is recognized that state estimation is but one application in a modern EMS system

[31, 32]. The approach proposed in this chapter is such that it should be possible to continue with all other application functions exactly as before. The output of the traditional state estimator is processed by the proposed algorithm to incorporate PMU data and is then put back in the same format as that produced by the traditional state estimator so that the application functions such as user visualization, contingency analysis, optimal power flows, corrective actions required, alarms, etc. do not require any changes. The common data format also allows the application of existing bad data detection algorithms to check for bad PMU data.

In this chapter, first, in Section 4.1 a brief overview is given of the traditional non-linear state estimator based upon non-synchronized measurements of active and reactive power flows, voltage magnitudes, injections, ect. It is assumed that bad data has been eliminated in the normal fashion, and that the measurements are distributed throughout the network with uniform level of redundancy. The resulting state estimate is labeled $[E^{(1)}]$. Section 4.2 provides the modification necessary to the traditional procedure when synchronized positive sequence voltage and current phasors are added to the measurement set. The result of this estimator is labeled $[E^{(2)}]$. This is the process generally used when phasor measurements are added to the traditional measurement set. As mentioned before, this process requires very significant modifications to the existing EMS software. Section 4.3 proposes an alternative strategy of using $[E^{(1)}]$ and the phasor measurements to provide a new estimate $[E^{(3)}]$. This process is linear, and requires as inputs the estimate $[E^{(1)}]$, its error covariance matrix, the phasor measurements, and their error covariance matrix. If, as an approximation, one assumes that the state estimator problem is close to being linear, Section 4.4 shows that the estimate $[E^{(3)}]$ is identical to $[E^{(2)}]$. Section 4.5 provides results of simulations carried out on a test system, which confirm that $[E^{(2)}]$ and $[E^{(3)}]$ are identical within the bounds of computational errors. This chapter concludes with a summary of the results obtained in Section 4.6.

4.1. Traditional State Estimator

Consider a set of measurements $[z_1]$ consisting of non-synchronized (scanned) data of active and reactive power flows in network elements, bus injections, and voltage magnitudes at buses. It is assumed that bad data has been eliminated from this measurement set by the usual methods. The measurements are non-linear functions of the state vector $[E]$ (a set of positive sequence voltages at all the buses of the network):

$$[z_1] = [h_1(E)] + [\varepsilon_1] \tag{4.1}$$

where, $[h_1]$ are the non-linear functions of the state vector $[E]$ expressed in polar coordinates; and $[\varepsilon_1]$ is the measurement error vector with a covariance matrix $[W_1]$.

The Jacobian matrix $[H_1]$ is obtained by taking partial derivatives of $[h_1]$ with respect to $[E]$

$$[H_1(E)] = \left[\frac{\partial h_1(E)}{\partial (E)}\right] \tag{4.2}$$

Assuming a starting value for $[E]$, one proceeds with iterations to obtain the weighted least squares solution for state vector. For example, if $[E_k]$ is the state vector at the start of an iteration, the next iterate $[E_{k+1}]$ is given by

$$[E_{k+1}] = [E_k] + [G_1(E_k)][H_1^T(E_k)W_1^{-1}][z_1 - h_1(E_k)] \tag{4.3}$$

where $[G_1(E_k)]$ is the gain matrix given by

$$[G_1(E_k)] = [H_1{}^T(E_k)W_1^{-1}H_1(E_k)]^{-1} \tag{4.4}$$

The estimator is considered to have converged when $[E_{k+1}] - [E_k]$ has reached some prescribed low value. Let the converged estimate of this process be denoted by $[E^{(1)}]$.

The error covariance matrix of the estimate $[E^{(1)}]$ is given by

$$\mathrm{Cov}\left(\left[E^{(1)}\right]\right) = \left[H_1^T W_1^{-1} H_1\right]^{-1} \tag{4.5}$$

4.2. Estimator with Phasor Measurements Mixed with Traditional Measurements

Now consider the measurement set consisting of the vector $[z_1]$ of previous section, and a set of positive sequence voltage and current phasors $[z_2]$. The measurement error covariance matrix of the phasor measurements is assumed to be $[W_2]$. The voltage and current phasor measurements are obtained in rectangular coordinates, while the state vector is in polar coordinates. The error covariance matrix $[W_2]$ corresponds to errors in polar coordinates, and hence, it must be transformed according to the transformation rule for converting from polar to rectangular coordinates.

The relationship between incremental representation in polar and rectangular coordinates is a rotation:

$$\begin{bmatrix} \Delta E_{(1)r} \\ \Delta E_{(2)r} \\ \vdots \\ \Delta E_{(1)i} \\ \Delta E_{(2)i} \\ \vdots \end{bmatrix} = \begin{bmatrix} \cos\theta_1 & 0 & 0 & -|E_1|\sin\theta_1 & 0 & 0 \\ 0 & \cos\theta_2 & 0 & 0 & -|E_2|\sin\theta_2 & 0 \\ 0 & 0 & \vdots & 0 & 0 & \vdots \\ \sin\theta_1 & 0 & 0 & |E_1|\cos\theta_1 & 0 & 0 \\ 0 & \sin\theta_2 & 0 & 0 & |E_2|\cos\theta_2 & 0 \\ 0 & 0 & \vdots & 0 & 0 & \vdots \end{bmatrix} \times \begin{bmatrix} \Delta|E_{(1)}| \\ \Delta|E_{(2)}| \\ \vdots \\ \Delta\theta_{(1)} \\ \Delta\theta_{(2)} \\ \vdots \end{bmatrix} \tag{4.6}$$

A similar formula holds for the current phasor transformation as well. Note that all voltages are approximately of one per unit magnitude, and hence, as an approximation the voltage transformation given above may disregard the voltage magnitude multipliers. In terms of a general rotation matrix $[R]$

$$\begin{bmatrix} \Delta E_{rect} \\ \Delta I_{rect} \end{bmatrix} = [R] \begin{bmatrix} \Delta E_{polar} \\ \Delta I_{polar} \end{bmatrix} \tag{4.7}$$

The error covariance matrix of the phasor measurements corresponding to polar coordinates $[W_2]$ is thereby transformed by the rotation matrix into $[W_2']$ corresponding to measurements in rectangular coordinate

$$[W_2'] = [R][W_2][R^T] \tag{4.8}$$

The appended measurement vector $[z]$ is obtained by adding the current and voltage phasors to the previous measurement vector $[z_1]$:

$$[z] = \begin{bmatrix} z_1 \\ z_2 \end{bmatrix} \equiv \begin{bmatrix} z_1 \\ E_r \\ E_i \\ I_r \\ I_i \end{bmatrix} \tag{4.9}$$

the subscripts ‘r’ and ‘i’ representing the real and imaginary parts of the phasor measurements. The voltage and current phasors are non-linear functions of the state vector. For example, the voltage phasor $E_{(p)}$ at bus ‘p’ and the current phasor $I_{(pq)}$ in line ‘pq’ are related to the bus voltages $E_{(p)}$ and $E_{(q)}$ by the relationship

$$\begin{bmatrix} E_{(p)r} \\ E_{(p)i} \\ I_{(pq)r} \\ \\ \\ I_{pq(i)} \\ \\ \end{bmatrix} = \begin{bmatrix} |E_{(p)}|\cos\theta_p \\ |E_{(p)}|\sin\theta_p \\ \{(|E_{(p)}|\cos\theta_p - |E_{(q)}|\cos\theta_q)g_{(pq)} - \\ \quad (|E_{(p)}|\sin\theta_p - |E_{(q)}|\sin\theta_q)b_{(pq)} \\ \quad - b_{(p0)}|E_{(p)}|\sin\theta_p\} \\ \{(|E_{(p)}|\cos\theta_p - |E_{(q)}|\cos\theta_q)b_{(pq)} + \\ \quad (|E_{(p)}|\sin\theta_p - |E_{(q)}|\sin\theta_q)g_{(pq)} \\ \quad + b_{(p0)}|E_{(p)}|\cos\theta_p\} \end{bmatrix} \tag{4.10}$$

where the series admittance of the line connecting buses ‘p’ and ‘q’ is

$$y_{(pq)} = (g_{(pq)} + jb_{(pq)}) \tag{4.11}$$

and the shunt admittance at bus ‘p’ is

$$y_{(p0)} = jb_{(p0)} \tag{4.12}$$

These non-linear relations are added to the new measurement equation set:

$$\begin{bmatrix} z_1 \\ z_2 \end{bmatrix} = \begin{bmatrix} h_1(E) \\ h_2(E) \end{bmatrix} + \begin{bmatrix} \varepsilon_1 \\ \varepsilon_2 \end{bmatrix} \tag{4.13}$$

where $[h_2]$ being the non-linear equations of the type shown in equation (4.10). The corresponding Jacobian matrix is also partitioned in a similar way.

$$[H(E)] = \begin{bmatrix} H_1(E) \\ \\ H_2(E) \\ \\ \end{bmatrix} = \begin{bmatrix} \dfrac{\partial h_1(E)}{\partial (E)} \\ \dfrac{\partial h_2(E)}{\partial (E)} \end{bmatrix} \tag{4.14}$$

Let the converged value of the state vector be $[E^{(2)}]$. The covariance matrix of the errors of $[E^{(2)}]$ is

$$\mathrm{Cov}([E^{(2)}]) = [H(E^{(2)})^T W^{-1} H(E^{(2)})]^{-1} \tag{4.15}$$

where $[W]$ is the block diagonal matrix of the two error covariances:

$$[W] = \begin{bmatrix} W_1 & 0 \\ 0 & W_2' \end{bmatrix} \tag{4.16}$$

Substituting for $[H(E)]$ from equation (4.14) in equation (4.15), and using equation (4.16), one gets

$$\mathrm{Cov}([E^{(2)}]) = [H_1(E)^T W_1^{-1} H_1(E) + H_2(E)^T W'^{-1}_2 H_2(E)]^{-1} \quad (4.17)$$

The weighted least squares solution proceeds as before, and is given by

$$[E_{k+1}] = [E_k] + [G(E_k)][H_1^T W_1^{-1}][z_1 - h_1(E_k)] + [G(E_k)][H_2^T W_2'^{-1}][z_2 - h_2(E_k)] \quad (4.18)$$

where the gain matrix $[G(E_k)]$ is given by

$$[G(E_k)] = [H_1{}^T(E_k) W_1^{-1} H_1(E_k) + H_2{}^T(E_k) W_2'^{-1} H_2(E_k)]^{-1} \quad (4.19)$$

4.2.1. Inapplicability of Fast PQ Decoupled Formulation at the Presence of Current Phasor Measurements

It needs to be clarified that in the previous section, the conventional estimator is assumed not applying fast PQ decouple to the Jacobian matrix, although it is generally used in estimators to reduce the computational effort associated with the calculation and triangular decomposition of the gain matrix.

Decoupled formulation partitions measurement equations into two parts [32]:

1. Real power related measurements, including real power bus injections and real power flows in lines.
2. Reactive power related measurements, including reactive power bus injections, reactive power flows in lines and bus voltage magnitude measurements.

This partition is feasible thanks to both the low sensitivity of real power equations to changes in bus voltage magnitudes, and the low sensitivity of reactive power equations to changes in the bus voltage phase angles.

For high voltage transmission systems, $B_{ij} >> G_{ij}$, $\theta_{ij} \approx 0$. Therefore,

$$\frac{\partial P}{\partial \theta} >> \frac{\partial P}{\partial |E|}$$
$$\frac{\partial Q}{\partial |E|} >> \frac{\partial Q}{\partial \theta} \tag{4.20}$$

The approximation of eliminating off diagonal blocks in the Jacobian matrix facilitates the decomposition of gain matrix into real and reactive parts.

$$H = \begin{bmatrix} \frac{\partial P}{\partial \theta} & \frac{\partial P}{\partial |E|} \\ \frac{\partial Q}{\partial \theta} & \frac{\partial Q}{\partial |E|} \end{bmatrix} \approx \begin{bmatrix} \frac{\partial P}{\partial \theta} & 0 \\ 0 & \frac{\partial Q}{\partial |E|} \end{bmatrix} \tag{4.21}$$

$$G = \begin{bmatrix} \frac{\partial P}{\partial \theta}^T W_P^{-1} \frac{\partial P}{\partial \theta} & 0 \\ 0 & \frac{\partial Q}{\partial |E|}^T W_Q^{-1} \frac{\partial Q}{\partial |E|} \end{bmatrix} \tag{4.22}$$

However, both bus voltage angles and bus voltage magnitudes are closely related with current phasor measurements, especially when the current is not low. Thereby, current phasor measurements can not be decoupled into real and reactive parts [33]. If the fast PQ decoupled formulation is adopted by the estimator, there will be difficult to incorporate current phasors directly into the decoupled estimator.

4.3. Adding Phasor Measurements through a Post-processing Step

In order to formulate the post-processing step as a linear problem, the state vector and the measurement vector are expressed in rectangular coordinates. The new measurement set $[z']$ is made up of the result of the traditional state estimator $[E^{(1)}]$ and the positive sequence voltage and current phasor measurements, all expressed in rectangular coordinates. All angles are referred to the swing bus, whose angle is assumed to be zero. The error covariance matrix of $[E^{(1)}]$ is $Cov(E^{(1)})$ given by equation (4.5)

as found in the traditional estimation step, and is modified to reflect the transformation of the state variables to rectangular coordinates.

$$\mathrm{Cov}([E])_{\mathrm{rect}} = [R'][\mathrm{Cov}([E])][R']^{T} \equiv [W_1'] \tag{4.22}$$

The rotation matrix $[R']$ used here is only for state vector rotation, and it is different from $[R]$ used in equation (4.8) which was responsible for rotating the voltage and current phasor measurements. The two rotation matrices are similar in form although different in detail and size.

The phasor measurement error covariance matrix is the same as that used in section 4.2, $[W_2']$. The combined measurement equation now becomes

$$\begin{bmatrix} E_r^1 \\ E_i^1 \\ E_r \\ E_i \\ I_r \\ I_i \end{bmatrix} = \begin{bmatrix} 1 & 0 \\ 0 & 1 \\ 1' & 0 \\ 0 & 1' \\ C_1 & C_2 \\ C_3 & C_4 \end{bmatrix} \begin{bmatrix} E_r \\ E_i \end{bmatrix} \equiv [A] \begin{bmatrix} E_r \\ E_i \end{bmatrix} \tag{4.23}$$

The '1' in the above equation represents a unit matrix, whereas the '1′' represents a unit matrix with zeros on the diagonal where no voltage phasors have been measured. The matrices C_1 through C_4 are composed of line conductances and susceptances for those lines where current phasor measurements are available. For example, consider the current measurement I_{pq} in line 'pq'. Using the line admittance data given in section 4.2,

$$\begin{bmatrix} I_{(pq)r} \\ I_{(pq)i} \end{bmatrix} = \begin{bmatrix} g_{(pq)} & -g_{(pq)} & \{-b_{(pq)} - b_{(p0)}\} & b_{(pq)} \\ \{b_{(pq)} + b_{(p0)}\} & -b_{(pq)} & g_{(pq)} & -g_{(pq)} \end{bmatrix} \begin{bmatrix} E_{(p)r} \\ E_{(q)r} \\ E_{(p)i} \\ E_{(q)i} \end{bmatrix} \tag{4.24}$$

The 'C' matrices of equation (4.23) are similar to the bus admittance matrix, with

only those non-zero entries that correspond to lines where current phasors are measured.

Equation (4.23) is linear, and leads to a weighted least squares solution for the system state

$$\left[E^{(3)}\right] = \left[A^T W^{-1} A\right]^{-1} \left[A^T W^{-1}\right] \left[z'\right] \tag{4.25}$$

Where $[A]$ is defined in equation (4.23), and $[W]$ is the covariance matrix

$$[W] = \begin{bmatrix} W_1' & 0 \\ 0 & W_2' \end{bmatrix} \tag{4.26}$$

where both error covariance sub-matrices have been transformed through rotation to account for the use of rectangular coordinates.

It is obvious that equation (4.25) as a linear post-processing step is far more convenient to use instead of the estimator in section 4.2, which requires major revision of existing EMS software.

It is shown through simulations in Section 4.4 that the results of the post-processing technique, viz. $[E^{(3)}]$ are practically the same as those obtained with modified EMS software, viz. $[E^{(3)}]$.

4.4. Equivalence of the Two Solution Techniques for a Linear Estimator

Power system state estimation is not a linear problem; however, as the iterations of the non-linear estimator approach the converged solution, the problem becomes almost linear. It is instructive to show that if the problem was linear, the two approaches of adding phasor measurements to the state estimator, the traditional and the proposed method, are identical.

4.4.1. Solution of Technique 1: Mix Phasor Measurements with Traditional Measurements

The estimator based upon traditional measurements leads to the state vector as given by equation (4.3):

$$[E^{(1)}] = [H_1^T W_1'^{-1} H_1]^{-1} [H_1^T W_1'^{-1}][S_1] \tag{4.27}$$

where for simplicity, the measurement mismatch is denoted by the measurement vector $[S_1]$. The covariance matrix of the errors of estimation is given by equation (4.5)

$$\text{Cov}([E^{(1)}]) = [H_1^T W_1'^{-1} H_1]^{-1} \tag{4.28}$$

As the phasor measurements are added to the traditional measurement set, the resulting estimate is given by

$$[E^{(2)}] = \{[H_1^T W_1'^{-1} H_1 + H_2^T W_2'^{-1} H_2]^{-1}\} \{[H_1^T W_1'^{-1}][S_1] + [H_2^T W_2'^{-1}][S_2]\} \tag{4.29}$$

where the measurement mismatch is once again denoted by $[S]$.

4.4.2. Solution of Technique 2: Add Phasor Measurements as a Post-processing Step

Now consider the addition of the phasor measurements to the result obtained in equation (4.28), using its error covariance matrix given by equation (4.29). The resulting equation for the vector $[E^{(3)}]$ is given by (with measurements and state vector both expressed in rectangular coordinates)

$$\begin{bmatrix} E^{(1)} \\ S_2 \end{bmatrix} = \begin{bmatrix} 1 \\ H_2 \end{bmatrix} \begin{bmatrix} E^{(3)} \end{bmatrix} \tag{4.30}$$

with the measurement error covariance matrix given by

$$\mathrm{Cov}\begin{bmatrix} E^{(1)} \\ S_2 \end{bmatrix} = \begin{bmatrix} [H_1^T W'^{-1}_1 H_1]^{-1} & 0 \\ 0 & W'_2 \end{bmatrix} \tag{4.31}$$

where $[W'_2]$ is the error covariance matrix of the phasor measurements. The weighted least squares solution of equation (4.28) with the error covariance matrix given by equation (4.31) is

$$[E^{(3)}] = \{[H_1^T W'^{-1}_1 H_1 + H_2^T W'^{-1}_2 H_2]^{-1}\}\{[H_1^T W'^{-1}_1][S_1] + [H_2^T W'^{-1}_2][S_2]\} \tag{4.32}$$

which is identical to the result given in equation (4.29).

Although this is not a proof of equivalence of the two approaches for the non-linear problem, it does provide a plausible explanation as to why the results are identical in practical state estimation cases, as will be shown through simulations in the next section.

4.5. Simulation Results

The simulations have been carried out on a 300 bus system [34]. The base case load flow was taken as a starting point, and it was assumed that the load flow solution is the basis for generating measurements with appropriate measurement errors.

4.5.1. Error Models

The conventional measurements are assumed to have errors with Gaussian distribution with a standard deviation which consists of two components:

1. one component proportional to the full scale of the meter being used, and
2. the other component being proportional to the actual measurement [35].

In this study it is assumed that the measurement errors have a standard deviation

equal to 3% of the actual measured value. Thus, the term proportional to the full scale of the meter is omitted, and is of no significance in this discussion.

The phasor magnitude errors are assumed to have a standard deviation of 3% of the actual measurement in keeping with the errors of the traditional measurement system. The phase angles are assumed to have an error due only to time synchronization errors. With GPS synchronization accuracy of the order of 1 microsecond, the phase angle error is assumed to have a standard deviation of 0.02°.

The power system chosen for the study has 300 buses and 411 lines. Measurements for traditional state estimation consist of P and Q measured at 411 line terminals, P and Q injections at 60 buses, and voltage magnitudes at 300 buses. The measurements are distributed evenly across the system. The load flow solution is assumed to provide the true value of the state vector. A normal random number generator is used to add errors to the measured quantities with appropriate standard deviation as described above. The Gaussian normal distribution is truncated at $\pm 3\sigma$ in order to eliminate gross errors, which should have been eliminated by the bad data detection procedure.

It is assumed that 30, 100, and 250 phasor measurement units are placed on the network and that they are evenly distributed for uniform coverage. Each PMU is assumed to measure the bus voltage, and all line currents that originate on that bus. The phasor angles are adjusted so that they conform with the convention that the swing bus angle is 0°.

4.5.2. Simulation Results

The results of the simulation are presented as follows.

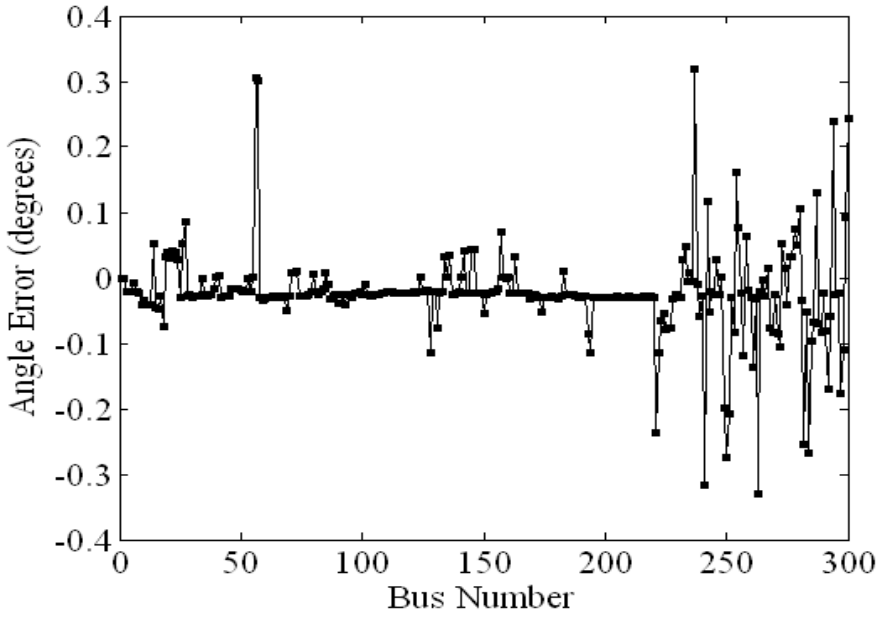

Figure 4-1 Error in Voltage Angle Estimation Using Traditional State Estimation Data

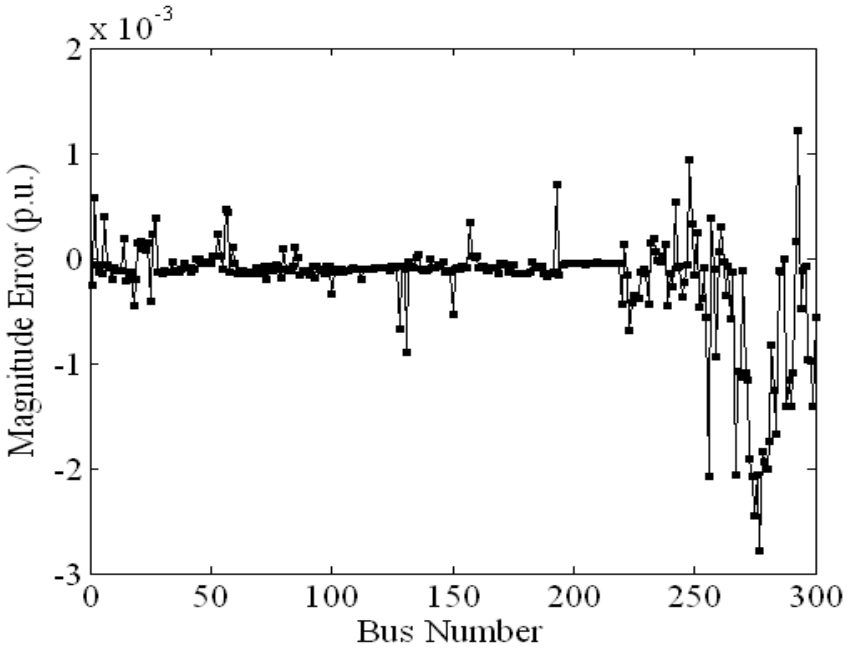

Figure 4-2 Error in Voltage Magnitude Estimation Using Traditional State Estimation Data

Figures 4-1 and 4-2 present the result of the traditional state estimator without any phasor measurements. The errors in estimated bus voltages at all the buses are presented as differences from the nominal values for both magnitudes and angles.

Figures 4-3 through 4-8 are results of the cases where 100 PMUs are added to the network and their voltage and current measurements are included in the state estimation in the two described techniques.

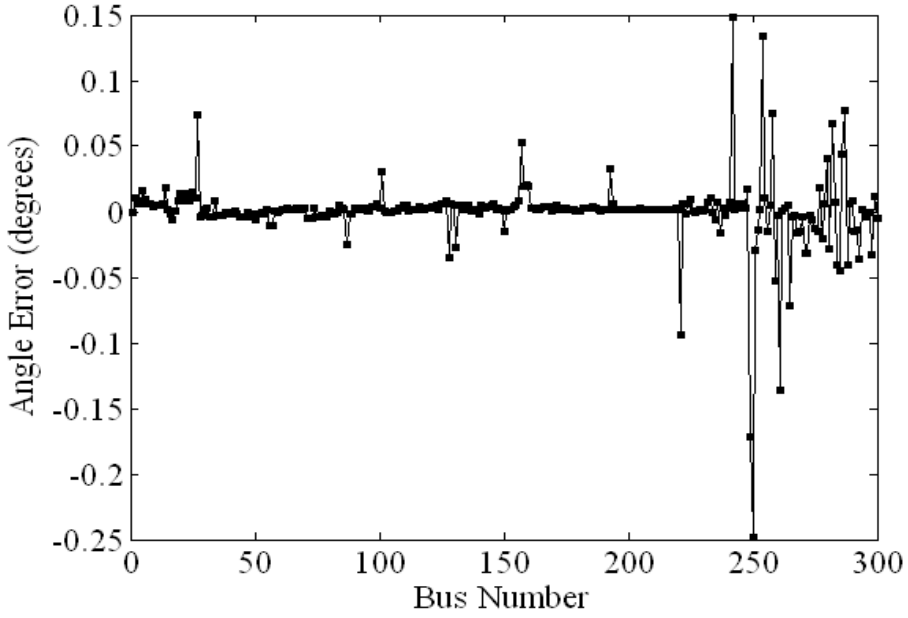

Figure 4-3 Error in Voltage Angle Estimation Using Traditional State Estimation Algorithm with Phasor Data Added

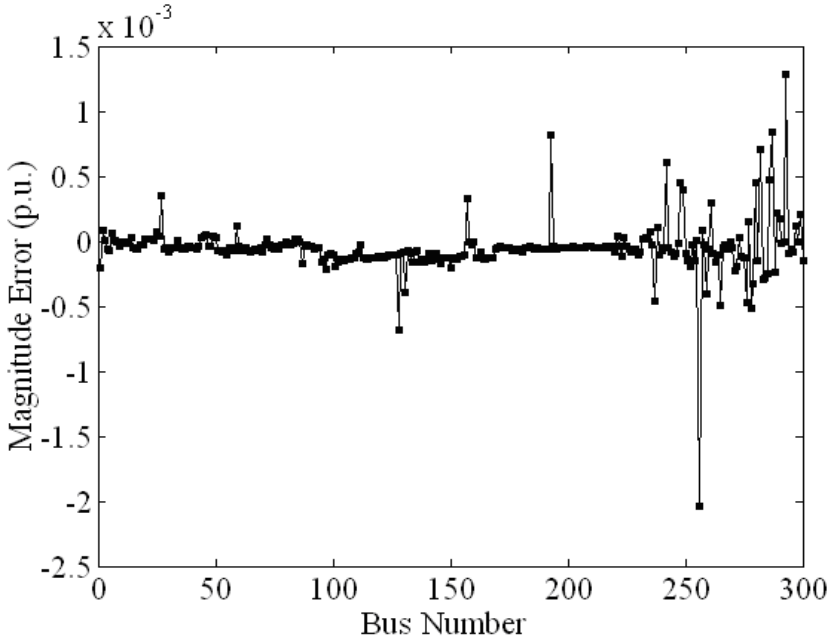

Figure 4-4 Error in Voltage Magnitude Estimation Using Traditional State Estimation Algorithm with Phasor Data Added

Figures 4-3 and 4-4 show the effect of adding the phasor measurements to the traditional measurement set, and computing the state vector through a non-linear iterative process as per Section 4.2. Once again the errors in estimated voltage magnitudes and angles are plotted for all the buses.

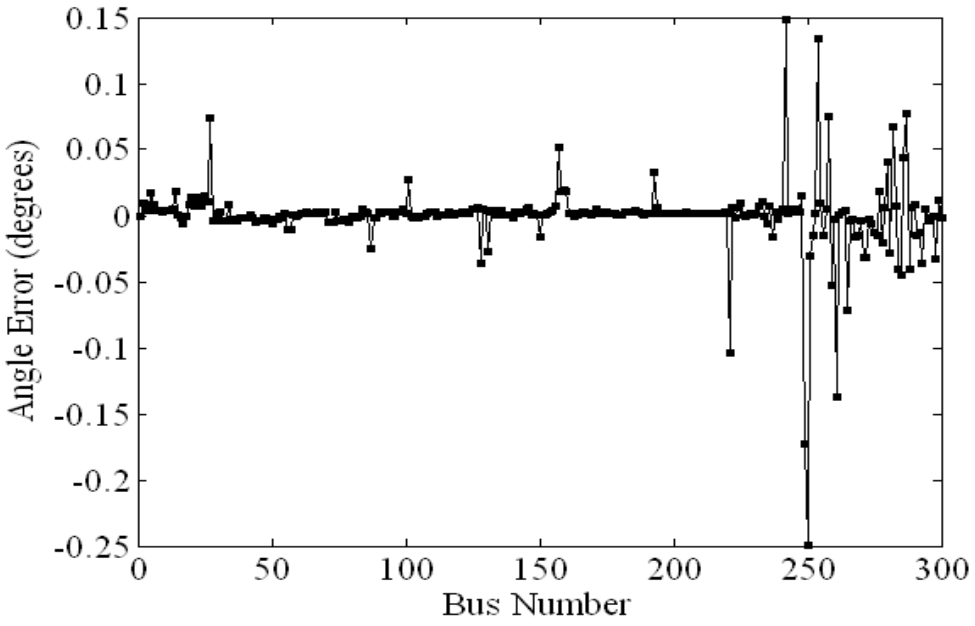

Figure 4-5 Error in Voltage Angle Estimation Using Phasor Data in A Post-processing Step

Figures 4-5 and 4-6 show similar results for the case of adding phasor measurements in a post-processing mode as explained in Section 4.3. The differences between Figure 4-3 and 4-5, Figure 4-4 and 4-6 can not be determined through eyeball comparison.

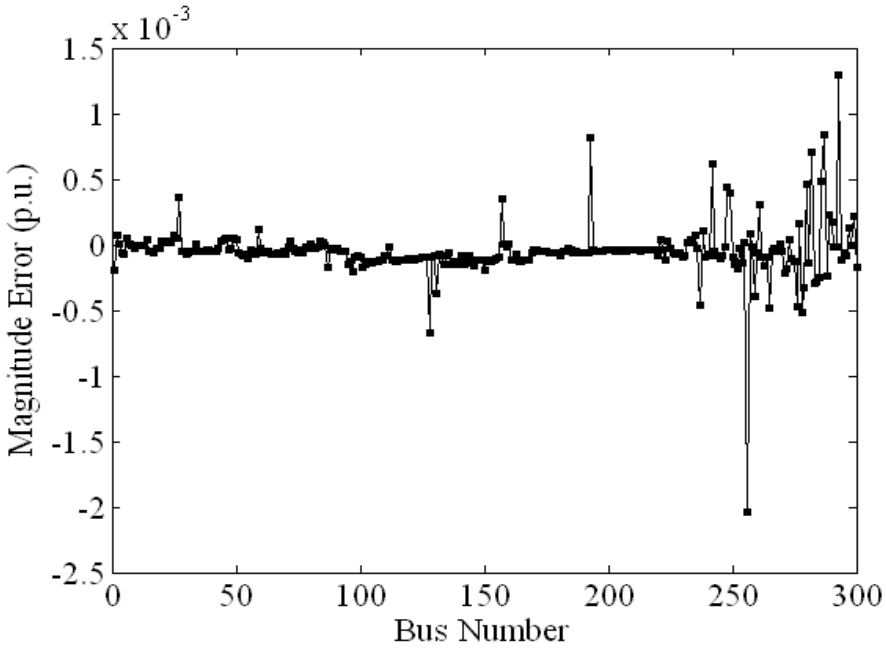

Figure 4-6 Error in Voltage Magnitude Estimation Using Phasor Data in A Post-processing Step

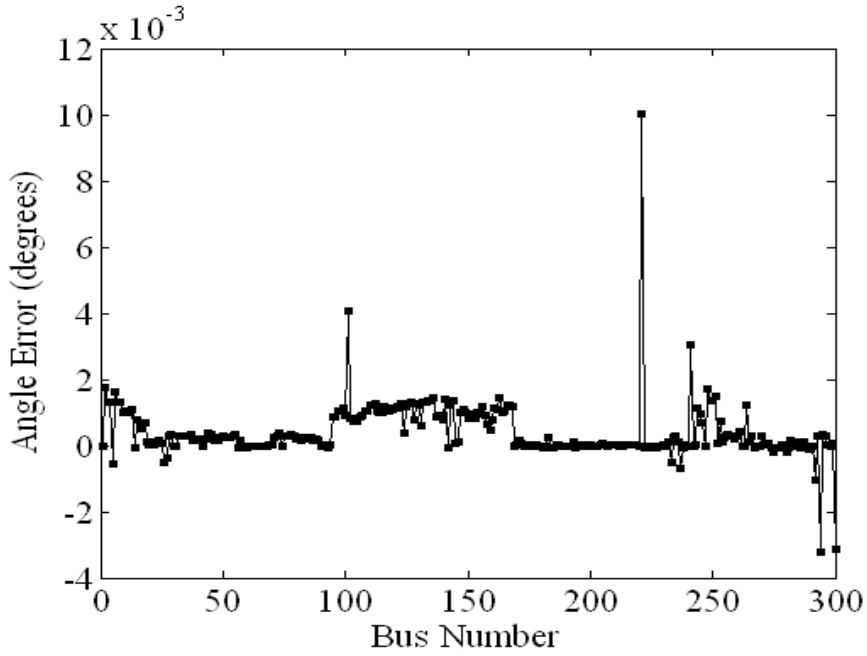

Figure 4-7 Error Difference in Voltage Angle between the Results of Figures 4-3 and 4-5

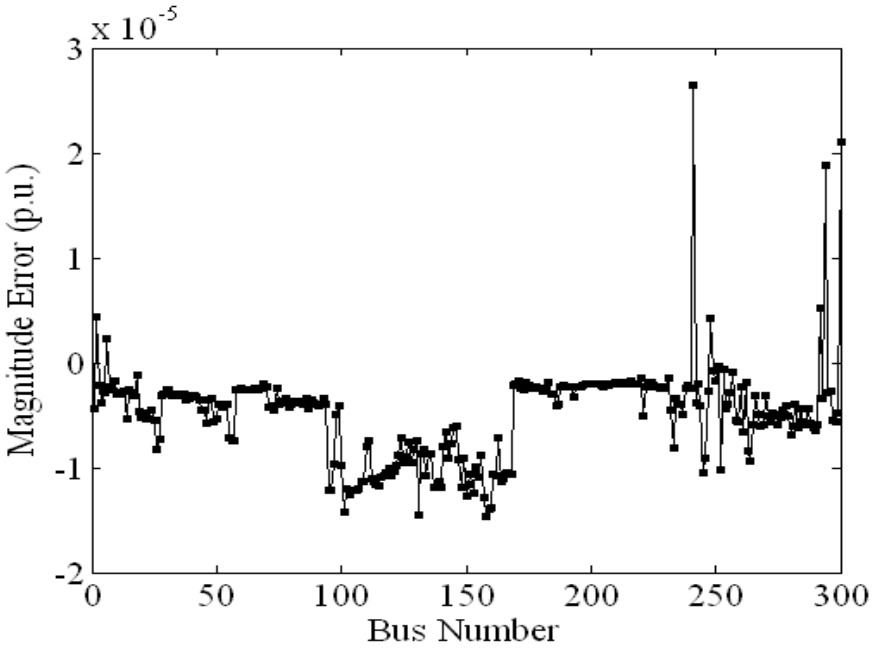

Figure 4-8 Error Difference in Voltage Magnitude between the Results of Figures 4-4 and 4-6

Finally, Figures 4-7 and 4-8 show the difference between Figures 4-3 and 4-5, 4-4 and 4-6 respectively, i.e. the difference between the estimates obtained by the methods of Sections 4.2 and 4.3. It is obvious from Figures 4-7 and 4-8 that the two results are practically identical.

The effect of adding different number of PMUs to the system is shown in Figure 4-9. Here the number of PMUs is varied between 0, 30, 100, and 250. The RMS errors of estimation for each of the estimates are plotted as a function of the number of PMUs added. It is clear that the PMU data is beneficial to the state estimation process, with the benefit increasing as the number of PMUs in the system increases.

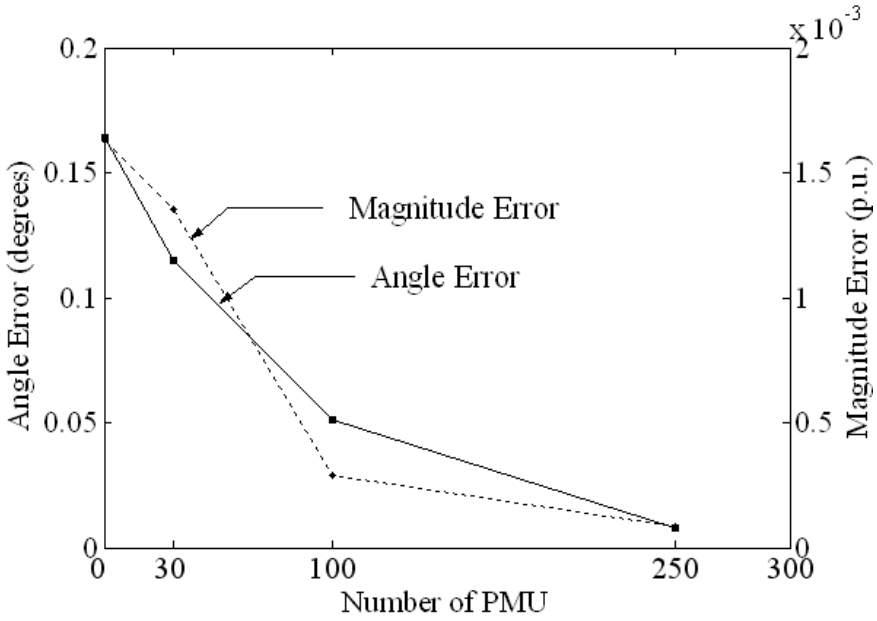

Figure 4-9 Effect of Adding Increasing Number of PMUs to the System on Errors of Estimation

Table 4-1 Processing Parameters of Two Techniques

Number	Processing time (s)	
	Technique 1	Technique 2
1	7	5.172
2	6.984	5.156
3	6.937	5.11
4	6.937	5.296
5	7.109	5.172
6	7	5.187
7	7	5.094
8	6.953	5.203
9	6.985	5.125
10	6.937	5.062
Average	6.9842	5.1577
Iteration number	9 iteration	6 iteration

For the same system with the same number and distribution of conventional and phasor measurements, the described techniques require different computational time to accomplish the state estimation. Considering the case of 100 PMUs distributed evenly in

the system, as is listed in Table 4-1, the average processing time for technique 1 over ten simulations on a computer with 1.6 GHz processor and 1.24 GB of RAM is 6.9842 seconds, while the average processing time for technique 2 on the same computer is 5.1577 seconds, 26.15% less. Nine iterations are needed for the 300 bus system to converge with technique 1, mixing phasor measurements with traditional measurements. But, only 6 iterations are needed if using technique 2, adding phasor measurements through a post-processing step.

When comparing the difference in computational time, it is not difficult to conclude that technique 2 can save more time for the applications with critical real time requirement, and could buy valuable seconds for system operators to avoid a system collapse or blackout. The time saving in technique 2 comes from dividing the process into two steps, one of which is linear, so that no iteration is needed to achieve the linear estimation. Moreover, the separation of phasor measurements from traditional measurements avoids the enlargement of non-linear Jacobian matrix, thus further decreases the calculation time through fewer iterations and less processing time per iteration on a much smaller sized Jacobian matrix. This situation is more noticeable as the number of installed PMUs increases, which is the current trend in power systems all over the world.

4.6. Conclusion

An alternative technique for using synchronized phasor measurements as additional data in traditional state estimator software in modern Energy Management Systems has been presented in this chapter. The following results have been established with supporting theory and simulations on a 300 bus power system:

A mathematically equivalent, and far more attractive option to incorporate phasor measurements in state estimation is to use them in a post-processing step. Thus, the results of the traditional state estimate and the phasor measurements with their respective error covariance matrices are considered to be a set of measurements which are linear functions of the state vector. This leads to a linear (non-iterative) estimation step, which

requires no modification of the traditional EMS software. This technique can be implemented quickly as an additional application software and produces results which are practically identical to the results obtained by the method of combining the traditional and phasor measurements in a non-linear measurement set.

Results also showed that as the number of phasor measurements on a power system is increased, the quality of the estimated state is progressively improved.

The proposed post-processing technique provides a better alternative to conveniently take full advantage of phasor measurements without tremendous modification of existing state estimators. In addition, it separates the processing of traditional measurements and phasor measurements, largely reducing the scale of non-linear estimation problem, as well as the number of iteration and the processing time per iteration. Therefore, it is also better for the stringent real time requirement of some advanced applications.

Chapter 5. Calibrating Instrument Transformers with Phasor Measurements

5.1. Introduction

The usage of instrument transformers is an essential feature in modern measurement techniques. It became a standard practice at the end of the nineteenth century, when currents and voltages increased rapidly in magnitude due to the growth in power generation and transmission [36]. There are two types of instrument transformers, current transformers (CTs) and voltage transformers (VTs). Instrument transformers reduce high voltages and currents into lower standardized values that are more convenient and safer for measurement.

An ideal instrument transformer magnetically couples to the secondary circuit with a signal magnitude exactly proportional to its turns ratio and in phase with the primary signals. But instrument transformers in the real world always have a Ratio Correction Factor (RCF) and a Phase Angle Correction Factor (PACF) that are not exactly 1 and 0º, making them a source of biased measurements if they are not properly calibrated.

The next two sections provide a general introduction to the errors of CTs, VTs, and Capacitive-Coupled Voltage Transformers (CCVTs) and a literature review of measurement calibration. After that, a method of calibrating instrument transformers with phasor measurements is proposed. At last, simulation results of the proposed method and conclusions are presented.

5.2. Instrument Transformer Errors

The importance of instrument transformers as accurate measuring units has been recognized for a long time. Most major countries have developed their own industry standards [37] on instrument transformers. In the U.S., the utility industry relies heavily

on the IEEE C57.13 [38], “Requirements for Instrument Transformers”, to design and select appropriate CTs and VTs. This standard defines the accuracy classes of different instrument transformers, and is used as the foundation for performance, interchangeability and safety of equipment in the U.S. power systems.

5.2.1. Instrument Current Transformers

Instrument current transformers are connected in series with the circuit they monitor. According to their application, CTs are categorized into metering and relaying devices. The accuracy classes for metering CTs is determined by a group of parallelograms with the limiting values for RCFs and PACFs, as shown in Figure 5-1 [38] and tabulated in Table 5-1. A certain accuracy class is satisfied when the correction vector, with the magnitude (RCF) and angle (PACF), dwells inside the parallelogram prescribed in the standard.

Table 5-1 Standard Accuracy Class for Metering Service and Corresponding Limits of RCF

Metering accuracy class	Voltage transformers (at 90% to 100% rated voltage)		Current transformers			
	Min	Max	At 100% rated current		At 10% rated current	
			Min	Max	Min	Max
0.3	0.997	1.003	0.997	1.003	0.994	1.006
0.6	0.994	1.006	0.994	1.006	0.988	1.012
1.2	0.988	1.012	0.988	1.012	0.976	1.024

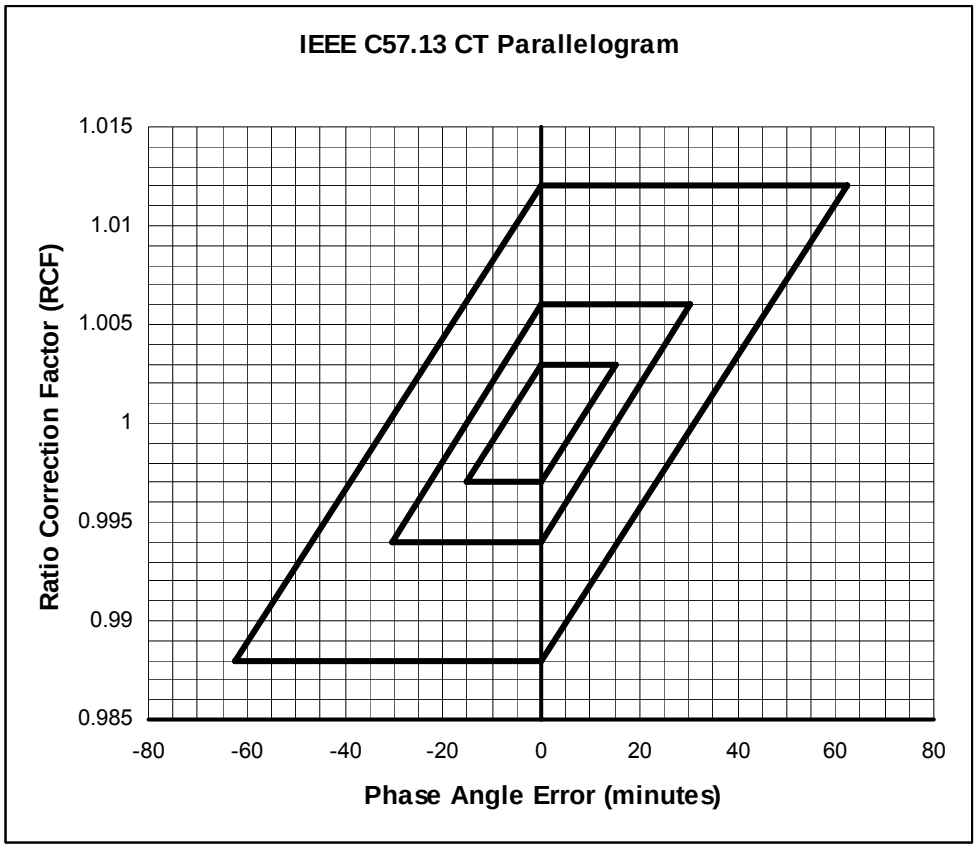

Figure 5-1 Accuracy Coordinates for CTs

Relaying CTs have RCF ranges of 90% to 110%, at any current from 1 to 20 times the rated one at the standard or lower burden. According to experiments performed on the Nissin Electric 345 kV Relaying CT, the maximum PACF detected was less than 0.5 degrees over the frequency range from 60 to 1800 Hz and the magnitude error was negligible [39]. Meliopoulos extracted steady state response from a test on a wide range of frequency responses of conventional relaying CTs. He concluded that conventional relaying CTs have an accurate performance at steady state, though no explicit data was provided [40].

The International Electrotechnical Commission (IEC) compared the various national rules and published the standard 60044-1 [41], "Instrument Transformers-Part 1: Current Transformer". This standard specifies the limit values of RCFs and PACFs that may be introduced by relaying CTs at rated current under the nominal working condition, as is

tabulated in Table 5-2. This information is useful for determining the error range of PMUs whose measurement are obtained through relaying instrument transformers rather than metering ones. In general, errors from relaying instrument transformers are larger than those from metering devices, as can be observed by comparing Table 5-2 with Table 5-1.

Table 5-2 Limits of Error for Relaying CTs

Accuracy Class	Current error at rated primary current %	Phase displacement at rated primary current		Composite error at rated accuracy limit primary current %
		Minutes	Centiradians	
5P	±1	±60	±1.8	5
10P	±3	--	--	10

5.2.2. Voltage Transformers

Voltage transformers are connected in parallel with the circuit they monitor. Generally, a higher transformation ratio of VT corresponds to higher errors in RCFs. Sensitivity to burden impedance is small over most of the frequency range, including working frequency, 60 Hz [39]. The accuracy classes of metering instrument transformers are listed in Table 5-1 and the accuracy classes for relaying are listed in Table 5-3, as quoted from IEC 60044-2 [42], "Instrument Transformers-Part 2: Inductive Voltage Transformers".

Table 5-3 Limits of Voltage Error and Phase Displacement for Relaying Voltage Transformers

Class	Percentage voltage (ratio) error + or -	Phase displacement + or -	
		Minutes	Centiradians
3P	3.0	120	3.5
6P	6.0	240	7.0

5.2.3. Capacitive-Coupled Voltage Transformer

CCVTs are a class of VTs popularly used in high voltage systems for voltage

measurements. They were developed in the early 1920s and are a combination of a capacitance voltage divider and an electromagnetic VT. They are mostly used for relaying application due to their low cost and stable performance. However, the accuracy of CCVTs drifts with time and temperature and routine maintenance and calibration is required.

5.3. Literature Review

Ways of calibrating measurements have been extensively researched in many papers and standards. The most instinctive way to eliminate the errors introduced by instrument transformers is to calibrate them in the field periodically. IEEE Standard Requirements for Instrument Transformers lists two general categories of calibration methods: null and deflection. The null method could be further classified into direct-null and comparative-null methods [38]. If in-situ calibration is required, special considerations of proper location of grounds, current (or voltage) value, burden, frequency etc. are needed, in addition to highly accurate calibration devices. And this is a very demanding and labor intensive way to calibrate instrument transformers in the field. Reference [43] shows that the accuracy of CTs is a few tenths of one percent in the field after they are calibrated by comparing with an accurate reference CT on the site. However, in order to get the CTs calibrated for use with PMUs, one reference CT, 4 or 5 times more accurate than the requirement, needs to be transported to the substation control house together with other field calibration equipments. In the field instrument transformers are calibrated one by one. Each calibration procedure requires connecting and disconnecting of the instrument terminals, collecting readings and making adjustments, that sums up to huge amount of work [44].

M. M. Adibi introduced the concept of Remote Measurement Calibration in 1986. Telemetered values of power system traditional measurements over a period of several days were used to estimate the calibration parameters like off-set, gain at the origin, non-linearity coefficients etc. in substations [44-47]. Shan Zhong and Ali Abur proposed a method of calibrating measurements by including calibration parameters into the state vector of state estimation in paper [48]. Both Adibi and Zhong assumed that it was

possible to establish parametric models of the measurements either as quadratic functions or linear functions of the true measurement. These functions applied to the conventional measurements exclusively and no phasor measurements were considered. Therefore, the phase angle displacements were not included in the calibration parameters. A. P. Sakis Meliopoulos created the concept of SuperCalibrator [40, 49, 50], which was based on the decentralized, detailed state estimators operating on substation level. Precise model of the power system, the instrument transformer, the instrumentation channels and the interconnected transmission lines were assumed to be available to operate the SuperCalibrator [51].

An instrument transformer calibration method with phasor measurements that takes the phase angle displacements into account and avoids the necessity of detailed and concise instrument transformer models is proposed in this chapter. By taking advantage of multiple scans of phasor measurements of diverse system operating states, this method will automatically tune RCFs and PACFs of instrument transformers and greatly improve the accuracy of system state estimation.

5.4. Instrument Transformer Calibration with Multiple Scans of Phasor Measurements

Given the fact that instrument transformers are not ideal ones, if they are not properly calibrated, the measurement contaminations in their effect on magnitude and angle measurement are significant. Therefore, by taking the RCFs and PACFs of instrument transformers into account, the phasor measurements acquired from PMUs are the summation of the random errors and the products of the true phasors with the complex correction factors, as shown in the following equations:

$$E = E_0 \times (a + jb) + \varepsilon_E \tag{5.1}$$

$$\begin{bmatrix} E_r \\ E_i \end{bmatrix} = \begin{bmatrix} a & -b \\ b & a \end{bmatrix} \times \begin{bmatrix} E_{0r} \\ E_{0i} \end{bmatrix} + \begin{bmatrix} \varepsilon_{Er} \\ \varepsilon_{Ei} \end{bmatrix} \tag{5.2}$$

where, E_0 represents true voltage phasor; E represents voltage phasor measurements; a+jb represents complex VT correction factors to be calculated; subscript r and i indicate real part and imaginary part; and ε_E represents Gaussian errors caused by quantization errors of PMU and synchronization inaccuracies.

Equation (5.2) shows the relationship between the voltage phasor measurements and the true system state in rectangular coordinates. The current phasor measurements are given by equations (5.4). Since current phasors are able to be calculated from system state, as shown in equation (5.3), the relationship between the current phasor measurements and the true system state is given in equation (5.5).

$$\begin{bmatrix} I_{0(pq)r} \\ I_{0(pq)i} \end{bmatrix} = \begin{bmatrix} g_{(pq)} & -g_{(pq)} & \{-b_{(pq)} - b_{(p0)}\} & b_{(pq)} \\ \{b_{(pq)} + b_{(p0)}\} & -b_{(pq)} & g_{(pq)} & -g_{(pq)} \end{bmatrix} \times \begin{bmatrix} E_{0(p)r} \\ E_{0(q)r} \\ E_{0(p)i} \\ E_{0(q)i} \end{bmatrix} \tag{5.3}$$
$$= Y \times E_0 = \begin{bmatrix} Y_r & -Y_i \\ Y_i & Y_r \end{bmatrix} \times \begin{bmatrix} E_{0r} \\ E_{0i} \end{bmatrix}$$

$$I = I_0 \times (c + jd) + \varepsilon_I \tag{5.4}$$

$$\begin{bmatrix} I_{(pq)r} \\ I_{(pq)i} \end{bmatrix} = \begin{bmatrix} c & -d \\ d & c \end{bmatrix} \times \begin{bmatrix} I_{0(pq)r} \\ I_{0(pq)i} \end{bmatrix} + \begin{bmatrix} \varepsilon_{Ir} \\ \varepsilon_{Ii} \end{bmatrix} = \begin{bmatrix} c & -d \\ d & c \end{bmatrix} \times \begin{bmatrix} Y_r & -Y_i \\ Y_i & Y_r \end{bmatrix} \times \begin{bmatrix} E_{0r} \\ E_{0i} \end{bmatrix} + \begin{bmatrix} \varepsilon_{Ir} \\ \varepsilon_{Ii} \end{bmatrix} \tag{5.5}$$

where, I_0 represent true voltage and current phasors; I represent voltage and current phasor measurements; c+jd represent complex VT and CT correction factors to be calculated; subscript r and i represent real part and imaginary part; ε_I represent Gaussian errors caused by quantization errors of PMU and synchronization inaccuracies; $g_{(pq)}+jb_{(pq)}$ represents conductance of line pq; $b_{(p0)}$ and $b_{(q0)}$ represent susceptances summation on bus p and bus q; and Y represents conductance matrix composed of line conductances and bus susceptances, indicating the relationship between line currents and bus voltages.

Given that RCF and PACF are not identified, they can be converted from model parameters into independent state variables and be estimated together with the system

states if abundant measurement redundancy is available. However, with the additional model parameters as unknowns, estimators become unsolvable since they are underdetermined. Consider the simplest example of 2 bus system in Figure 5-2,

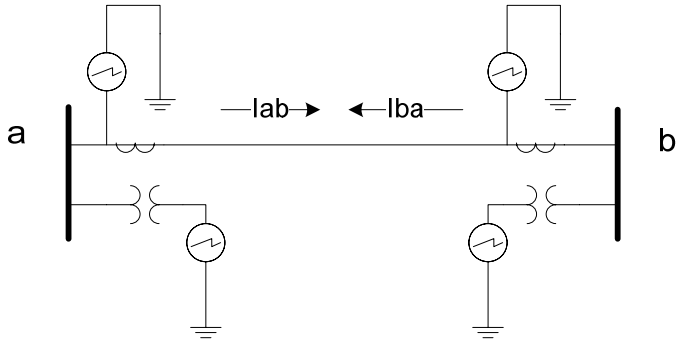

Figure 5-2 Two Bus System for Demonstration

Four measurements are available as voltage and current phasors (V_a, V_b, I_{ab} and I_{ba}). In addition to the four correction factors (CF_{Va}, CF_{Vb}, CF_{Iab}, CF_{Iba}), there are two more unknowns from the system state (V_a, V_b). That is a total of 6 unknowns. Apparently, this is an underdetermined system with more unknowns (6) than equations (4) and it can be consistent with infinitely many solutions. In order to find the appropriate estimation of the true correction factors of instrument transformers and the system state, a method of increasing the number of phasor measurements is required. Generally, instrument transformers work in the linear portion of their characteristic curve under normal conditions [37] and correction factors are predictable and repeatable. Therefore, although system operating conditions and corresponding system states may vary, instrument transformer correction factors remain constant under different operating conditions. As a result, reformulating the conventional system state estimation problem to incorporate phasor measurements of several scans of different conditions would provide the essential redundancy to the inclusion of calibration parameters. Profiting from this fact, a method of calibrating instrument transformers with phasor measurements is proposed in the following paragraphs.

To convert correction factors of instrument transformers into independent variables, the augmented Jacobian Matrix H, integrated by both VT and CT RCFs and PACFs is

depicted in the equation (5.7).

$$H = \begin{bmatrix} \frac{\partial E_r}{\partial E_{0r}} & \frac{\partial E_r}{\partial E_{0i}} & \frac{\partial E_r}{\partial a} & \frac{\partial E_r}{\partial b} & \frac{\partial E_r}{\partial c} & \frac{\partial E_r}{\partial d} \\ \frac{\partial I_{(pq)r}}{\partial E_{0r}} & \frac{\partial I_{(pq)r}}{\partial E_{0i}} & \frac{\partial I_{(pq)r}}{\partial a} & \frac{\partial I_{(pq)r}}{\partial b} & \frac{\partial I_{(pq)r}}{\partial c} & \frac{\partial I_{(pq)r}}{\partial d} \\ \frac{\partial E_i}{\partial E_{0r}} & \frac{\partial E_i}{\partial E_{0i}} & \frac{\partial E_i}{\partial a} & \frac{\partial E_i}{\partial b} & \frac{\partial E_i}{\partial c} & \frac{\partial E_i}{\partial d} \\ \frac{\partial I_{(pq)i}}{\partial E_{0r}} & \frac{\partial I_{(pq)i}}{\partial E_{0i}} & \frac{\partial I_{(pq)i}}{\partial a} & \frac{\partial I_{(pq)i}}{\partial b} & \frac{\partial I_{(pq)i}}{\partial c} & \frac{\partial I_{(pq)i}}{\partial d} \end{bmatrix} \tag{5.7}$$

$$= \begin{bmatrix} a & -b & E_{0r} & -E_{0i} & 0 & 0 \\ cY_r - dY_i & -(cY_i + dY_r) & 0 & 0 & Y_rE_{0r} - Y_iE_{0i} & -(Y_iE_{0r} + Y_rE_{0i}) \\ b & a & E_{0i} & E_{0r} & 0 & 0 \\ cY_i + dY_r & cY_r - dY_i & 0 & 0 & Y_iE_{0r} + Y_rE_{0i} & Y_rE_{0r} - Y_iE_{0i} \end{bmatrix}$$

Equation (5.7) is composed of the derivatives of voltage and current phasor measurements, to system states, and complex VT and CT correction factors. Both the phasor measurements (voltage and current) and the estimated values (system states and complex correction factors) are in rectangular coordinates.

Assume that

$$T_1 = \begin{bmatrix} \frac{\partial E_r}{\partial E_{r0}}(E_1) & \frac{\partial E_r}{\partial E_{i0}}(E_1) \\ \frac{\partial I_r}{\partial E_{r0}}(E_1) & \frac{\partial I_r}{\partial E_{i0}}(E_1) \\ \frac{\partial E_i}{\partial E_{r0}}(E_1) & \frac{\partial E_i}{\partial E_{i0}}(E_1) \\ \frac{\partial I_i}{\partial E_{r0}}(E_1) & \frac{\partial I_i}{\partial E_{i0}}(E_1) \end{bmatrix}, \cdots, T_n = \begin{bmatrix} \frac{\partial E_r}{\partial E_{r0}}(E_n) & \frac{\partial E_r}{\partial E_{i0}}(E_n) \\ \frac{\partial I_r}{\partial E_{r0}}(E_n) & \frac{\partial I_r}{\partial E_{i0}}(E_n) \\ \frac{\partial E_i}{\partial E_{r0}}(E_n) & \frac{\partial E_i}{\partial E_{i0}}(E_n) \\ \frac{\partial I_i}{\partial E_{r0}}(E_n) & \frac{\partial I_i}{\partial E_{i0}}(E_n) \end{bmatrix} \tag{5.8}$$

and

$$F_1=\begin{bmatrix}\frac{\partial E_r}{\partial a}(E_1) & \frac{\partial E_r}{\partial b}(E_1) & \frac{\partial E_r}{\partial c}(E_1) & \frac{\partial E_r}{\partial d}(E_1)\\ \frac{\partial I_r}{\partial a}(E_1) & \frac{\partial I_r}{\partial b}(E_1) & \frac{\partial I_r}{\partial c}(E_1) & \frac{\partial I_r}{\partial d}(E_1)\\ \frac{\partial E_i}{\partial a}(E_1) & \frac{\partial E_i}{\partial b}(E_1) & \frac{\partial E_i}{\partial c}(E_1) & \frac{\partial E_i}{\partial d}(E_1)\\ \frac{\partial I_i}{\partial a}(E_1) & \frac{\partial I_i}{\partial b}(E_1) & \frac{\partial I_i}{\partial c}(E_1) & \frac{\partial I_i}{\partial d}(E_1)\end{bmatrix},\cdots,F_n=\begin{bmatrix}\frac{\partial E_r}{\partial a}(E_n) & \frac{\partial E_r}{\partial b}(E_n) & \frac{\partial E_r}{\partial c}(E_n) & \frac{\partial E_r}{\partial d}(E_n)\\ \frac{\partial I_r}{\partial a}(E_n) & \frac{\partial I_r}{\partial b}(E_n) & \frac{\partial I_r}{\partial c}(E_n) & \frac{\partial I_r}{\partial d}(E_n)\\ \frac{\partial E_i}{\partial a}(E_n) & \frac{\partial E_i}{\partial b}(E_n) & \frac{\partial E_i}{\partial c}(E_n) & \frac{\partial E_i}{\partial d}(E_n)\\ \frac{\partial I_i}{\partial a}(E_n) & \frac{\partial I_i}{\partial b}(E_n) & \frac{\partial I_i}{\partial c}(E_n) & \frac{\partial I_i}{\partial d}(E_n)\end{bmatrix} \quad (5.9)$$

the augmented Jacobian matrix with n scans is denoted as H_2 in equation (5.10). The complex VT and CT correction factors are constant at different load conditions. Therefore, the number of unknown instrument transformer parameters is not growing with the increase of phasor measurement scans used.

$$H_2=\begin{bmatrix}T_1 & & & F_1\\ & T_2 & & F_2\\ & & \ddots & \vdots\\ & & T_n & F_n\end{bmatrix},W=\begin{bmatrix}W_1 & & & \\ & W_2 & & \\ & & \ddots & \\ & & & W_n\end{bmatrix},\Delta z=\begin{bmatrix}\Delta z_1\\ \Delta z_2\\ \vdots\\ \Delta z_n\end{bmatrix} \quad (5.10)$$

The covariance matrix of n scans is simply a diagonal matrix with each diagonal element filled by the covariance matrix of that scan. And the measurement incremental array is the vector obtained by appending each incremental array in the same order as is in the covariance matrix.

$$\begin{bmatrix}\Delta E_{r1}\\ \Delta E_{i1}\\ \vdots\\ \Delta E_{rn}\\ \Delta E_{in}\\ \Delta a\\ \Delta b\\ \Delta c\\ \Delta d\end{bmatrix}=\left[H_2^T W^{-1} H_2\right]^{-1} H_2^T W^{-1}\Delta z \quad (5.11)$$

Assuming a starting value for $\begin{bmatrix}E_{r1} & E_{i1} & \cdots & E_{rn} & E_{in} & a & b & c & d\end{bmatrix}^T$, one proceeds with iterations to obtain the weighted least squares solution for the state vectors

and instrument transformer parameters. Iteration continues until the incremental of unknowns change as little as a prescribed low value.

5.5. Instrument Transformer Calibration for Systems Sparsely Installed with PMUs

Redundancy is one of the keys for calibration, the lack of which will turn measurements into critical measurements or critical k-tuples that are impossible to detect and/or identify from any systematic errors. A critical measurement is defined as the one whose loss would render the system un-observable. A critical k-tuple is a set of k redundant measurements, the elimination of which will make the associated system lose observability [32]. Due to the lack of redundancy, the bad data detection of a critical measurement is unachievable. In addition, although the existence of bad data for any k-1 member subset of a critical k-tuple is detectable, it is impossible to identify which ones are the bad data. Therefore, only the redundant measurements and any k-2 measurements out of a critical k-tuple can be calibrated. Otherwise, the augmented Jacobian matrix with instrument transformer correction factors would be singular, which leads to an unsolvable estimator.

When the system is covered with a minimal set of PMUs providing the system state through either measurements or calculations, redundancy is generally available, although it is minimized for the sake of cost saving. By looking into the structure of the residual covariance matrix, one can tell critical measurements or critical k-tuples from redundant measurements. The residual covariance matrix S, defined as $S = I - H\left(H^T W^{-1} H\right)^{-1} H^T W^{-1}$, reflects the sensitivity of measurement residual to errors [32] (Here, I is an identity matrix.). The column of S corresponding to a critical measurement will have all null elements, since the residual of a critical measurement will always equal zero, regardless of the correctness of the measurement. K columns of the residual covariance matrix corresponding to the k measurements belonging to a critical k-tuple will be linearly dependent [52]. For example, if k equals 2, the normalized residuals of these two measurements are always identical; therefore, it is not possible to

tell the good data from the bad one.

The existence and distribution of critical measurements and critical k-tuples depend on the number and the allocations of the telemetered measurements, independent of the measurement value, its weight, and the parameters of the system model. Therefore, simplifying the weight matrix to an identity matrix and applying it in the calculation of residual covariance matrix is preferable for computational saving, and it will be used in the following simulations.

5.6. Simulation Results

The simulations were carried out on the IEEE 14 bus system [34]. The different load scenarios were created by multiplying both the generations and the loads of the base case with a coefficient. It was assumed that the load flow solutions of each load scenarios are the basis for generating phasor measurements by multiplying the values with randomly assigned correction factors and then adding appropriate measurement errors following a normal distribution.

5.6.1. Error Model

Phasor measurements are assumed to deviate from their true values due to un-calibrated instrument transformers with complex correction factors, in addition to the Gaussian errors caused by the per unit quantization errors of the digitizing process and synchronization inaccuracies.

In this research, it is assumed that the complex correction factors of CTs and VTs are within the ranges shown in Table 5-4 [37], and that VTs and CTs adopt accuracy classes 2.4 and 1.2 respectively. Namely, RCF and PACF of CT are values randomly selected from the range $[0.988,1.012]$ and $[-1°,1°]$ respectively. Similarly, RCF and PACF of VT are randomly selected from the range $[0.976,1.024]$ and $[-2°,2°]$.

Table 5-4 CT and VT Correction Factor Ranges of Different Accuracy Classes

	Accuracy Class	RCF Range	Phase Range (min)
New	**0.15**	**1.0015-0.9985**	**±7.8**
IEEE C57.13	**0.3**	**1.003-0.997**	**±15.6**
IEEE C57.13	**0.6**	**1.006-0.994**	**±31.2**
IEEE C57.13	**1.2**	**1.012-0.988**	**±62.4**
IEEE C57.13	**2.4**	**1.024-0.976**	**±124.8**

The Gaussian error of PMUs essentially is the quantization error due to analog to digital conversion [53]. For a well-designed commercial PMU, the effects of quantization errors in the magnitude of the measurement are generally negligible. Monte Carlo simulation with 400 trials were performed in report [53] to get the standard deviation of errors, in the phasor magnitude, of 0.825×10^{-5} p.u. with a 12 bit A/D converter acquiring 12 samples per cycle from a 10 volt peak input signal. In this research, considering other error factors, e.g., errors caused by anti-aliasing filters and non-harmonic noises, the PMU phasor magnitude measurements are assumed to have a standard deviation of 1×10^{-5} p.u.. Suppose the PMU phase angle measurements are in error only because of time synchronization inaccuracies. With the synchronization as precise as 1 μs, the PMU phase angle error is presumed to have a standard deviation of 0.00667º, where 0.00667 º is 1/3 of 0.02º, the largest PMU phase angle error in a 60 Hz system.

5.6.2. Simulation Results

The IEEE 14 bus system with 14 buses and 20 lines was chosen as the test bed for this research. Only the instrument transformers providing voltage and current phasor measurements are candidates to be calibrated. Assuming the load flow solution provides the true value of the system state vector. A normal random number generator with proper standard deviation was used to add errors to the measurements from the instrument transformers, which are deviated from their true values by multiplying by the corresponding complex correction factors. Therefore, the composition of phasor measurements is

$$\begin{bmatrix} I \\ V \end{bmatrix} = \begin{bmatrix} I_t & 0 \\ 0 & V_t \end{bmatrix} \times \begin{bmatrix} CF_I \\ CF_V \end{bmatrix} + \begin{bmatrix} \varepsilon_I \\ \varepsilon_V \end{bmatrix} \tag{5.12}$$

where, subscript t denotes the true value; and ε represents errors following Gaussian distribution.

It is assumed that the phasor angles are adjusted so that they are consistent with the traditional assumption of 0º for the swing bus angle. And similar to the effect of swing bus, at least one VT or CT is already calibrated for reference purpose.

The results of simulations are presented in the following subsections.

5.6.2.1. Calibration Performance with Different Numbers of Scans

The calibration performance is closely related to the number of measurement scans used and the load condition of each scan. Assume that PMUs are installed on every single bus throughout the system, and each PMU measures not only the bus voltage phasor, but also the current phasors in the lines that originate from that bus. Figure 5-3 to Figure 5-10 show the errors and standard deviations of CT and VT PACFs and RCFs calibrated in three different cases (A, B, and C) with the number of scans increases from 3, 5, to 7. Each situation adopts 3 basic scans, a heavy-load scan (1.5 times the base load), a normal-load scan (base case), and a light load scan (0.1 times the base load). It is assumed that more light-load and heavy-load scans with random errors are employed to enhance the measurement redundancy. Namely, 3, 5, and 7 scans are composed of one normal-load scan and 1, 2, and 3 pairs of light-load and heavy-load scans respectively.

The standard deviations of errors of estimated CT and VT RCFs and PACFs were calculated from the results of Monte Carlo simulation with 100 trails. In each trail, the complex instrument transformer correction factors were kept unchanged.

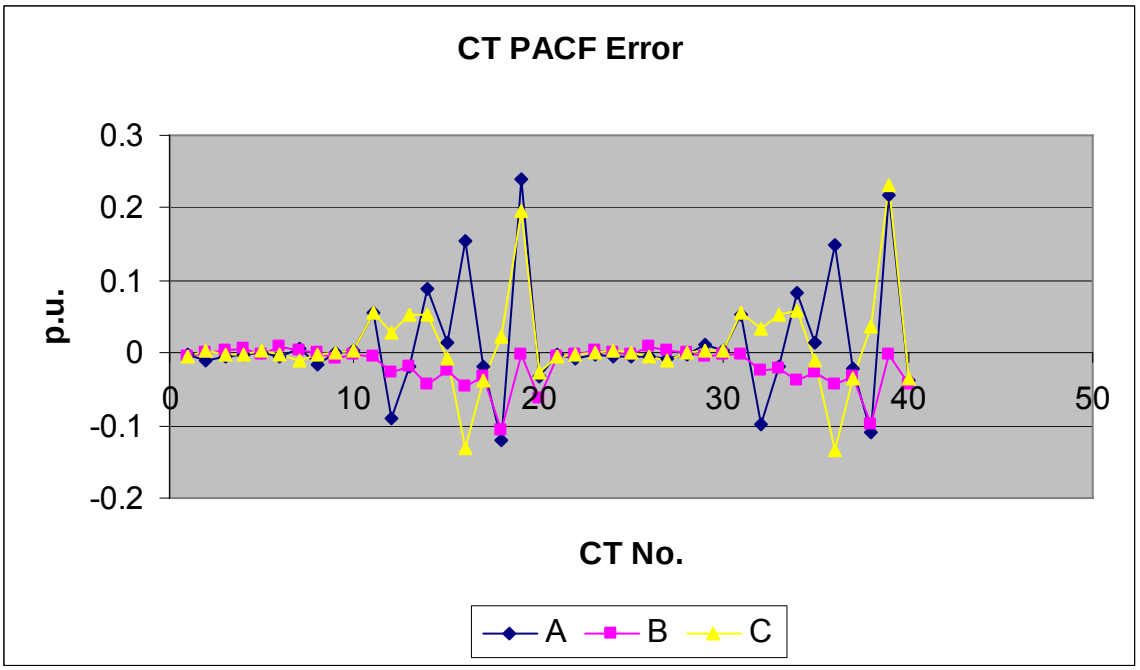

Figure 5-3 CT PACF Errors

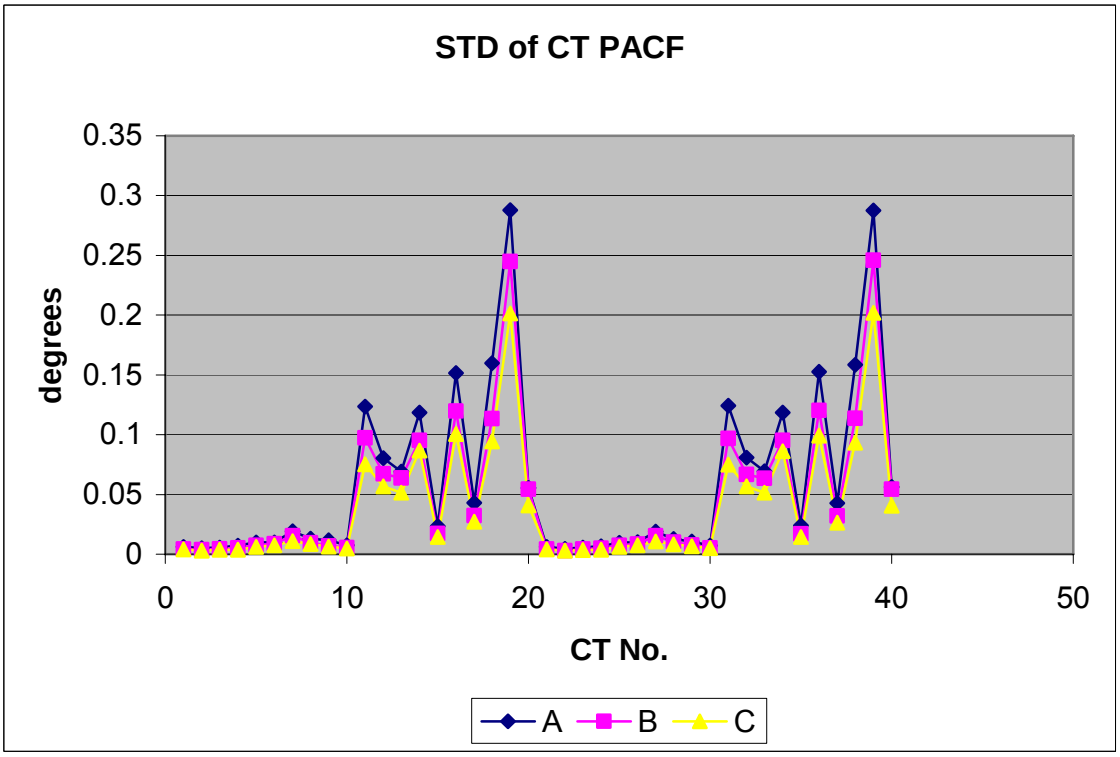

Figure 5-4 Standard Deviations of CT PACF

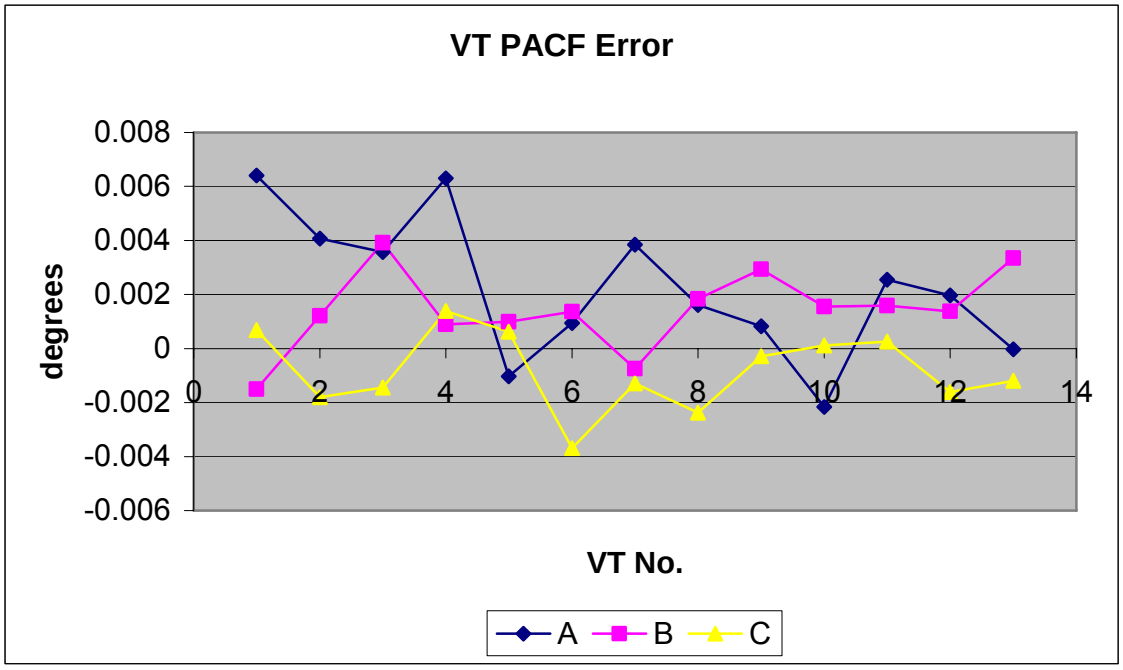

Figure 5-5 VT PACF Errors

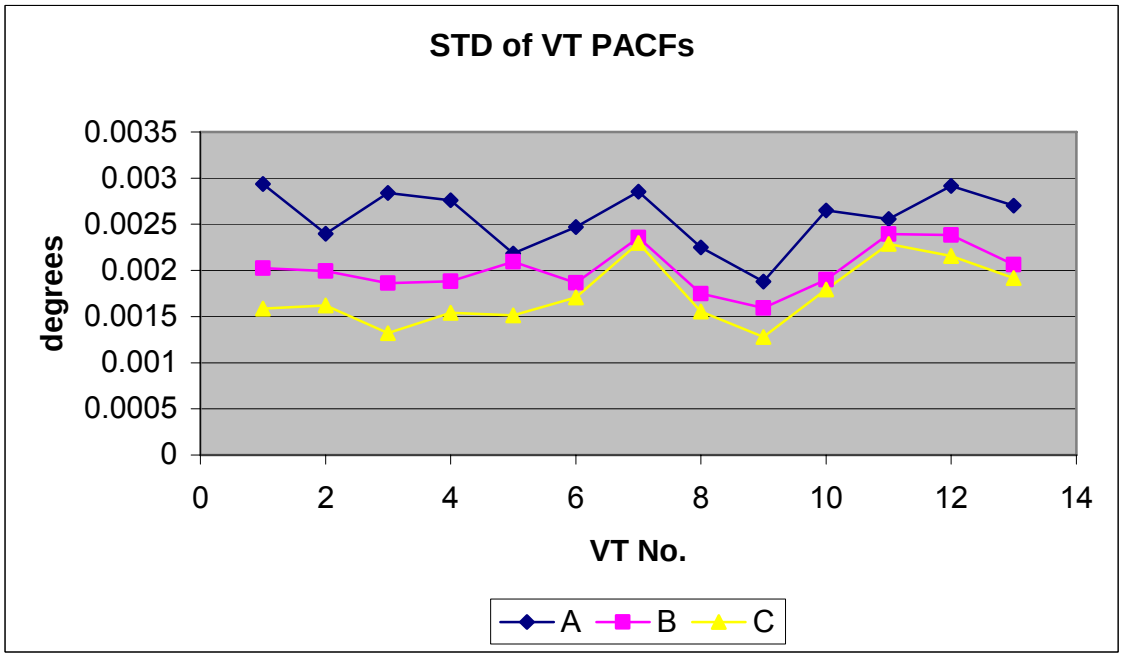

Figure 5-6 Standard Deviations of VT PACF

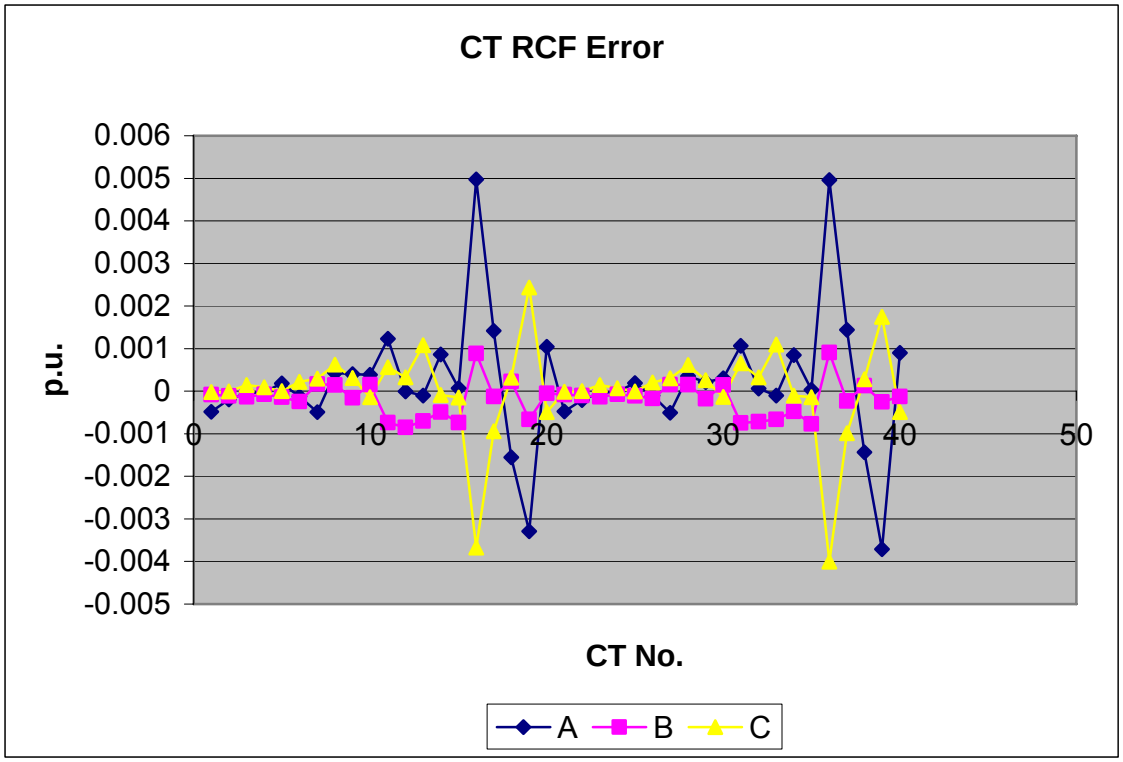

Figure 5-7 CT RCF Errors

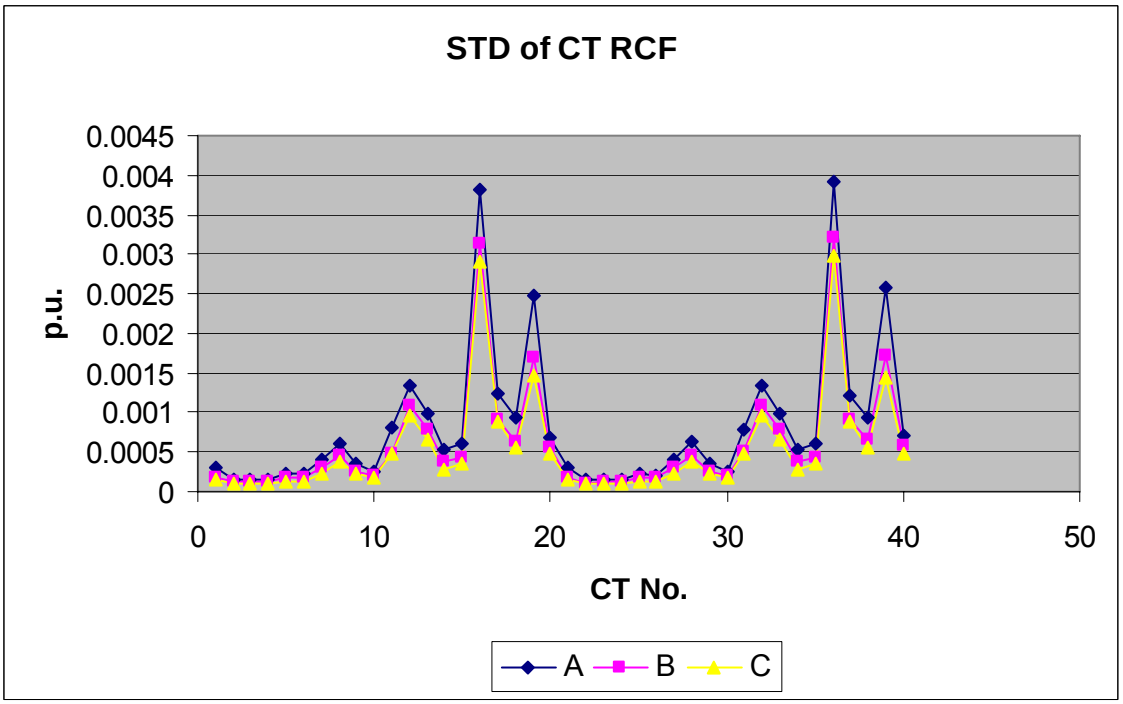

Figure 5-8 Standard Deviations of CT RCF

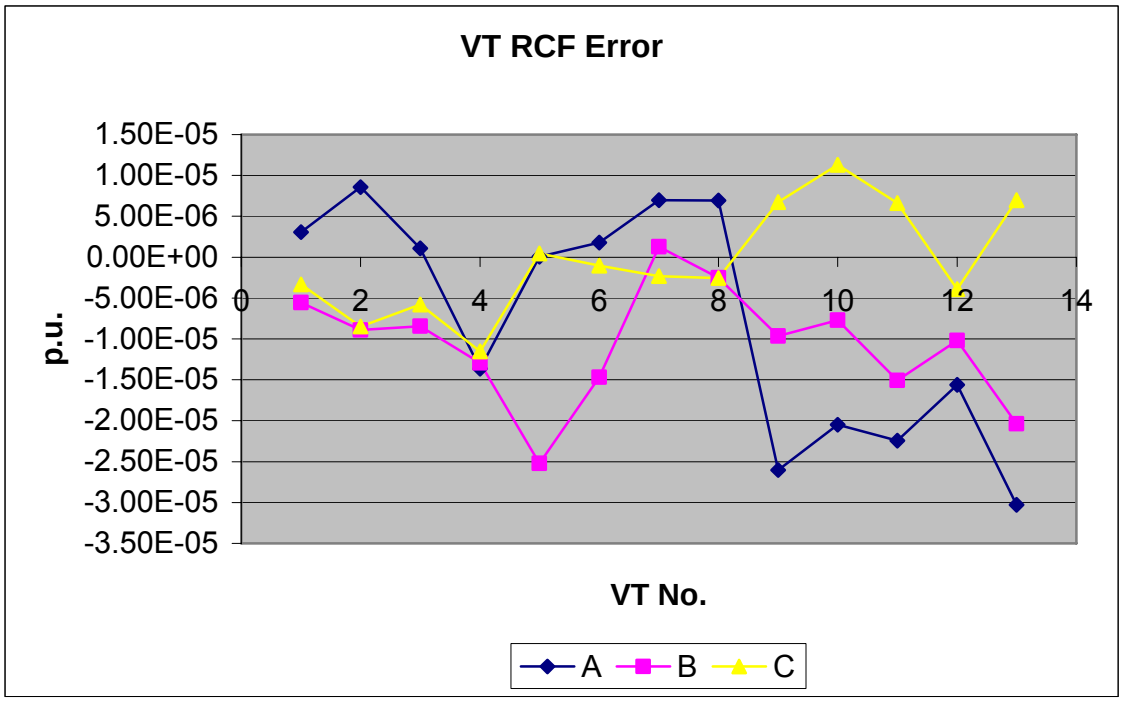

Figure 5-9 VT RCF Errors

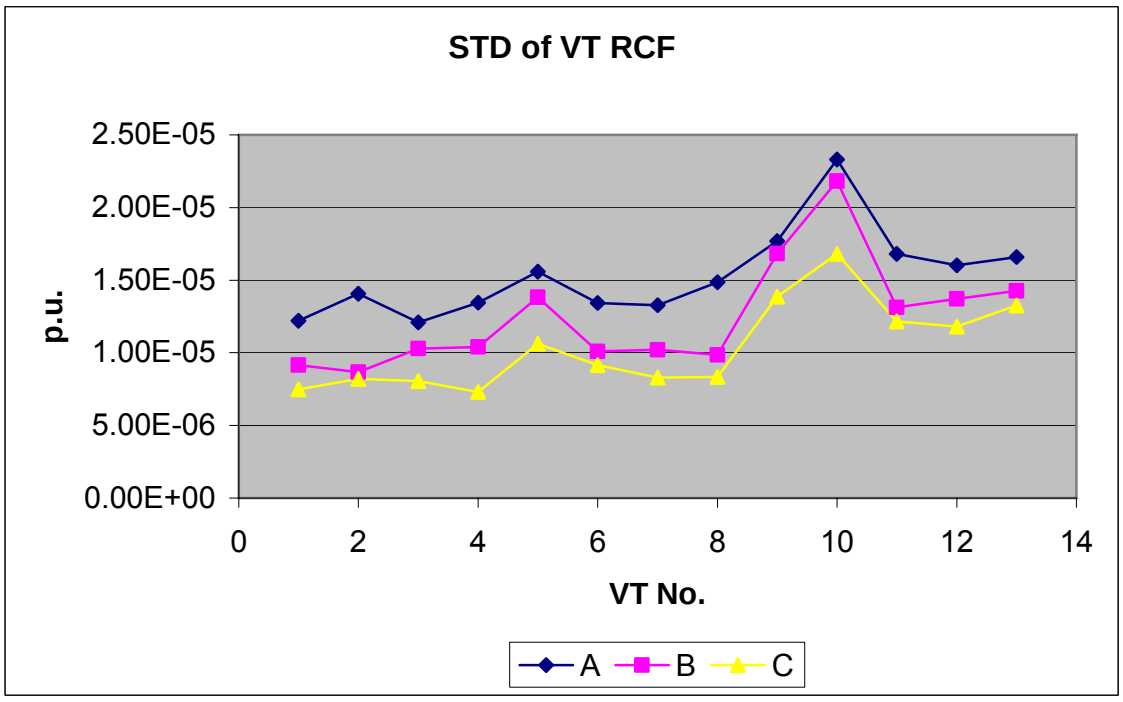

Figure 5-10 Standard Deviations of VT RCF

As expected, utilizing more scans leads to more accurate result of instrument transformer calibration, which can be observed from the decrease in standard deviations with the increase in the number of scans shown in Figures 5-4, 5-6, 5-8 and 5-10.

5.6.2.2. Relationship of Calibration Performance with Scans of Different Load Condition

Besides the number of scans used in the calibration process, the ranges of load covered by the scans greatly affect the accuracy of the calibration.

This phenomenon could be explored by comparing the cases of adopting 3 different groups of scans in the simulation tabulated in Table 5-5. Assume that PMUs are installed on every single bus throughout the system, and each PMU measures not only the bus voltage phasor, but also the current phasors in the lines that originate from that bus. Case A takes the scans that cover the largest operating ranges, which are the load difference between the lightest load scan and the heaviest load scan. While case C takes the scans that cover the narrowest operating ranges.

Table 5-5 System Load Condition for Each Scans Taken in 3 Cases

Case	Load Condition (*base case)		
	Scan 1	Scan 2	Scan 3
A	0.1	1	1.5
B	0.25	1	1.25
C	0.5	1	1.05

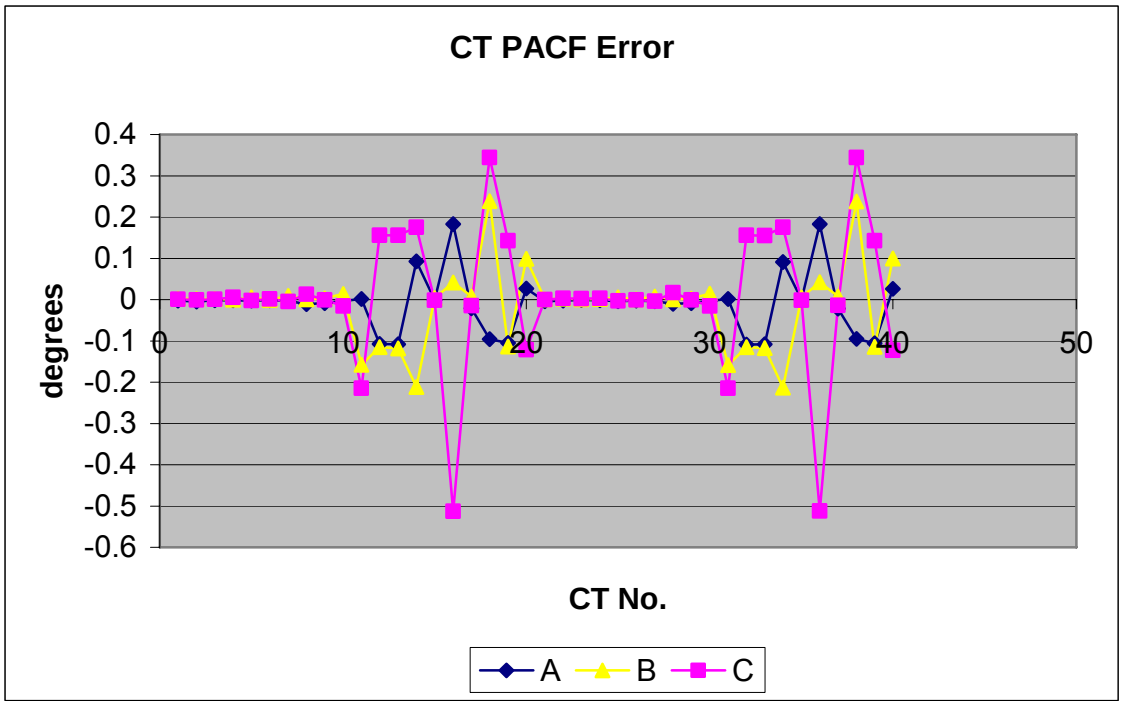

Figure 5-11 CT PACF Errors

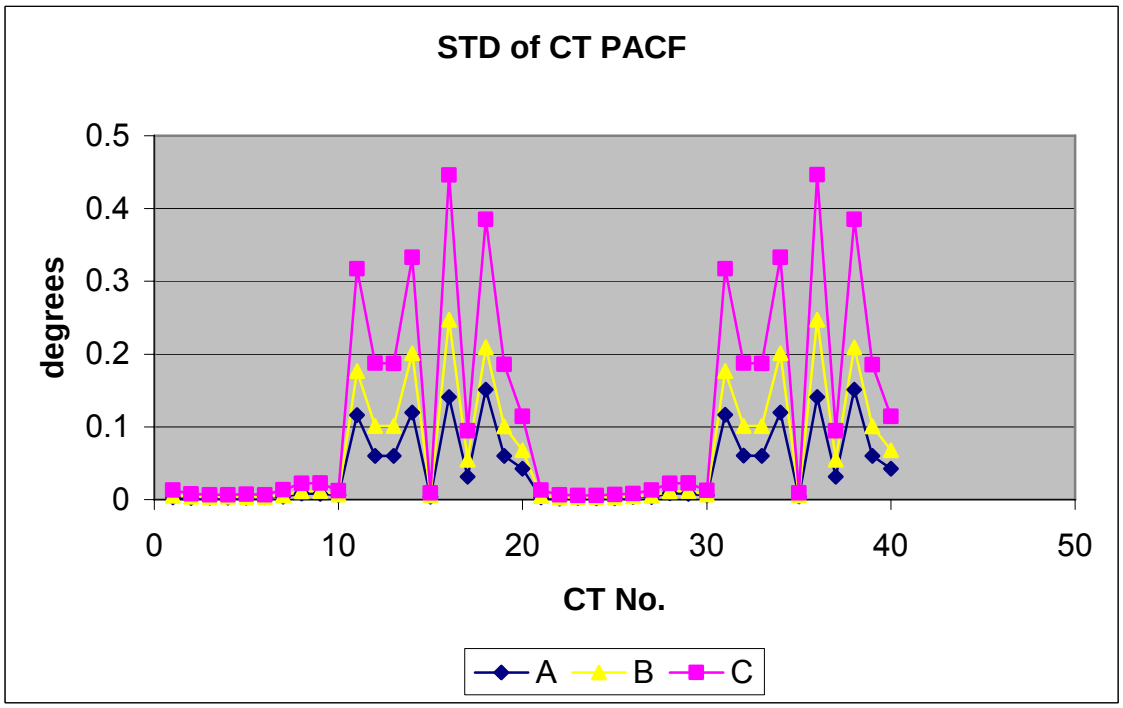

Figure 5-12 Standard Deviations of CT PACF

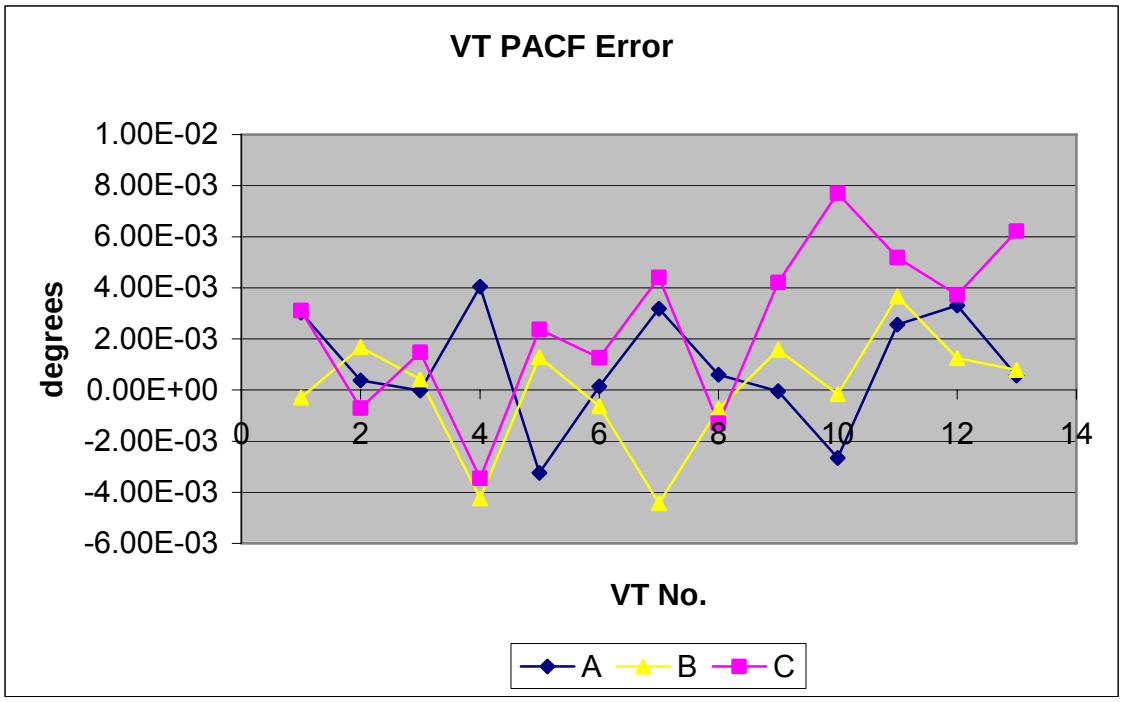

Figure 5-13 VT PACF Errors

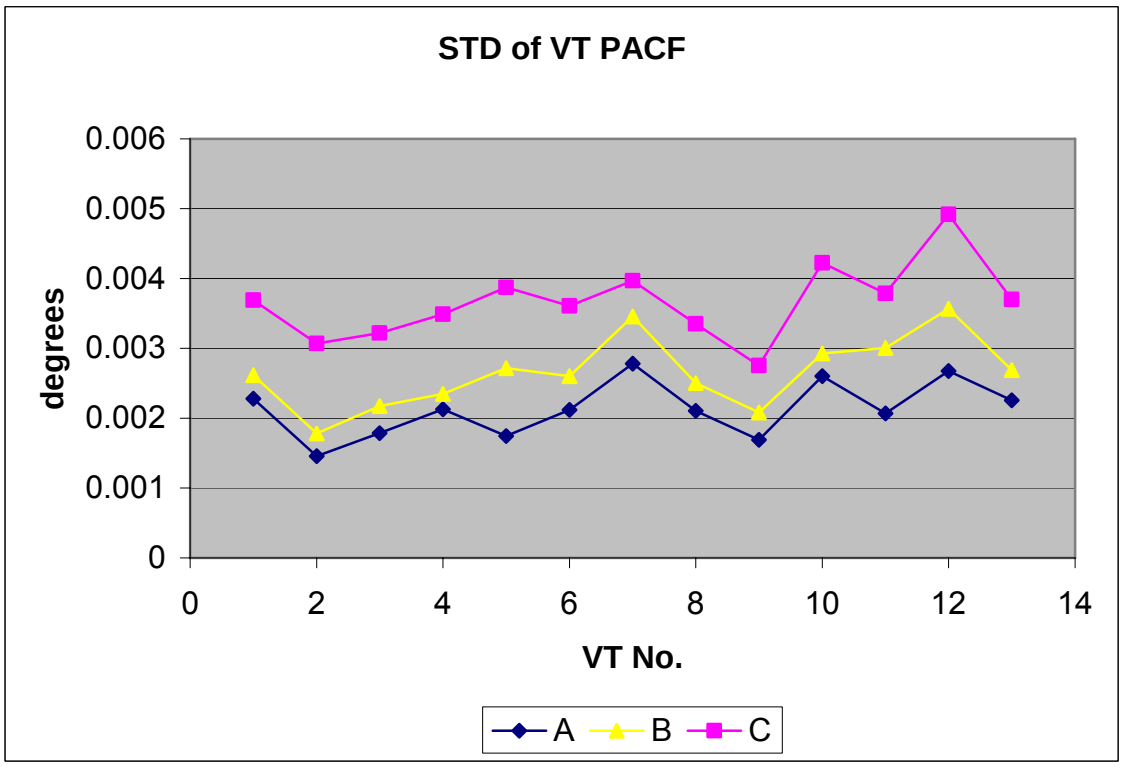

Figure 5-14 Standard Deviations of VT PACF

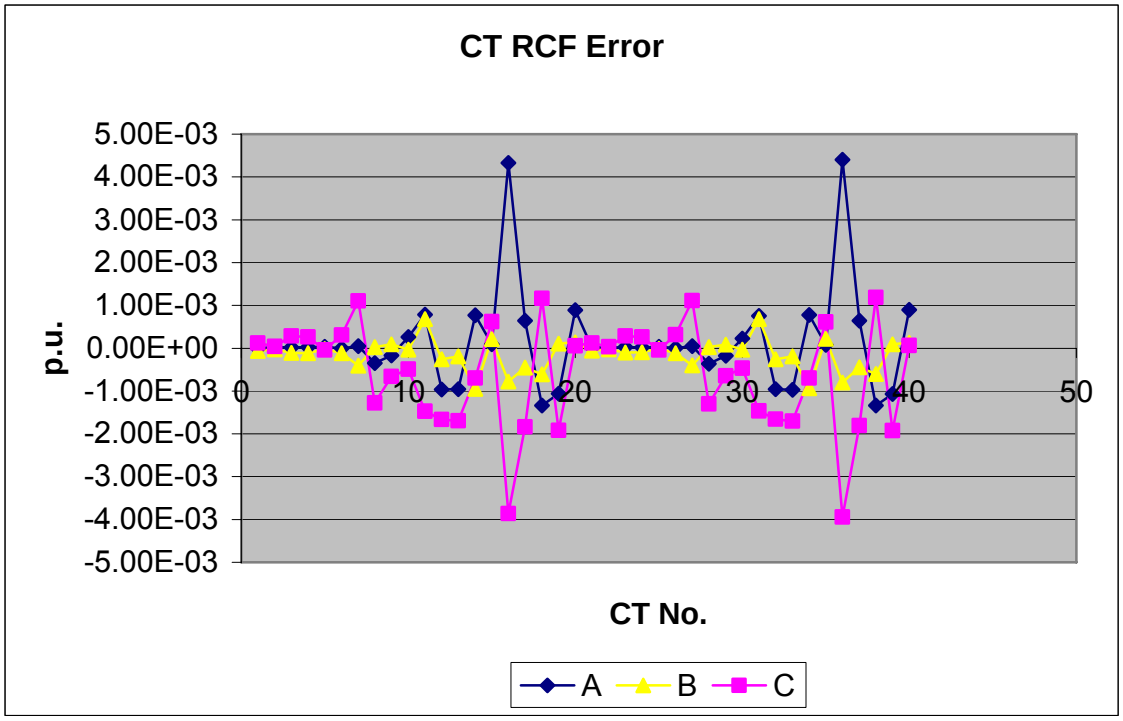

Figure 5-15 CT RCF Errors

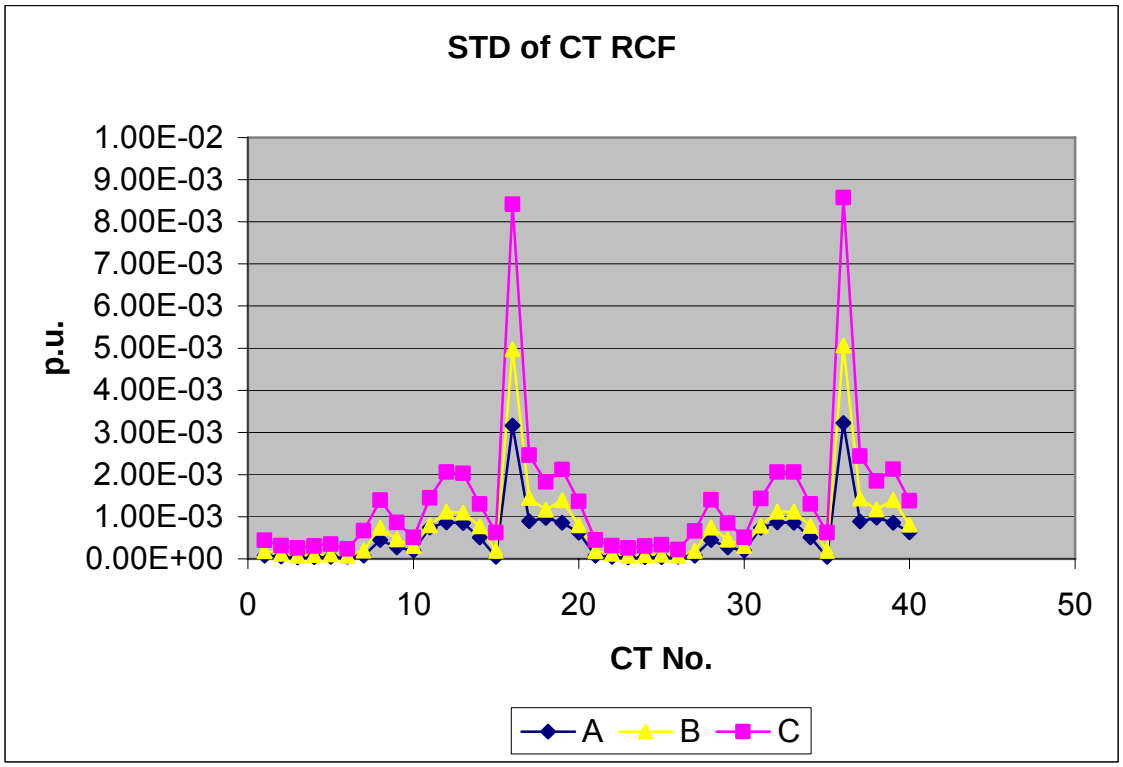

Figure 5-16 Standard Deviations of CT RCF

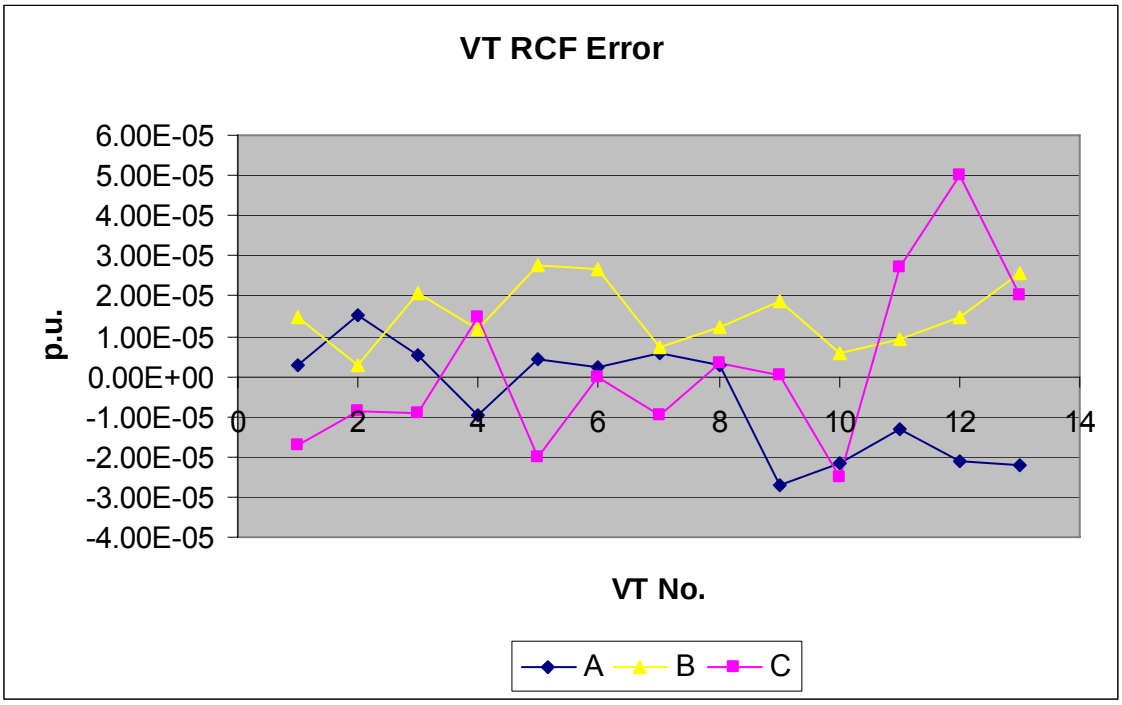

Figure 5-17 VT RCF Errors

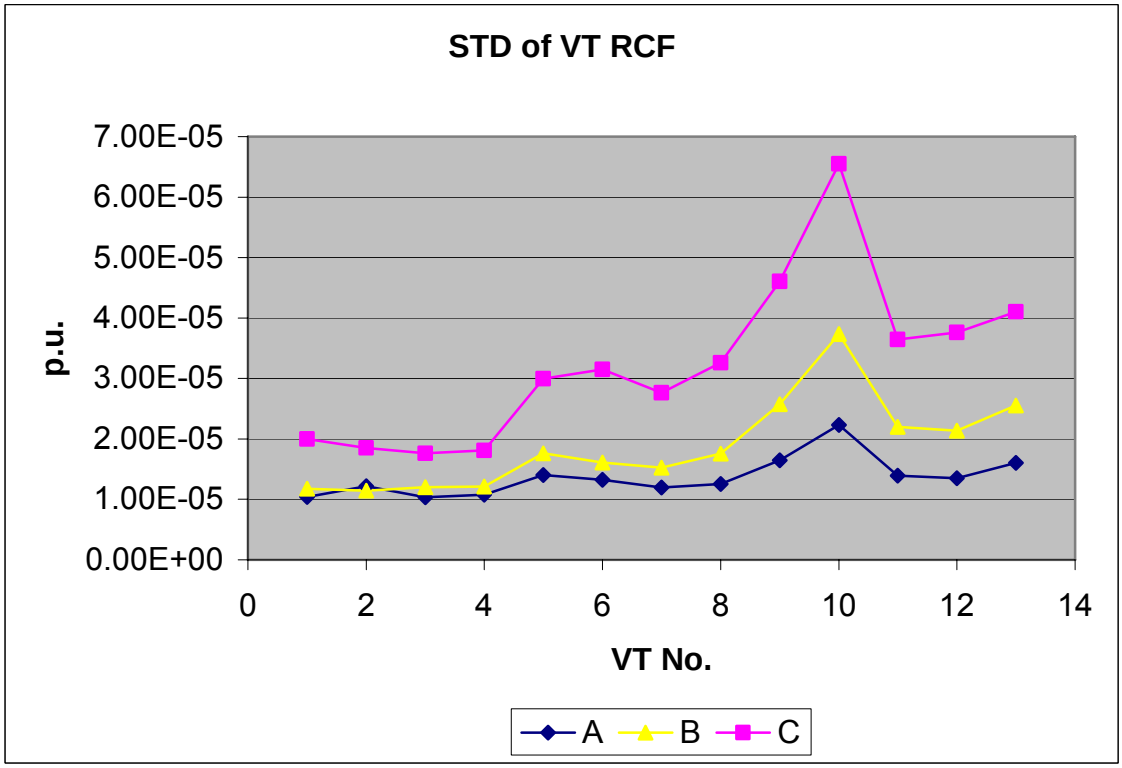

Figure 5-18 Standard Deviations of VT RCF

From Figure 5-11 to Figure 5-18, it is obvious that scans covering wider range of operation situations help determine a more accurate instrument calibrator. Explicitly, it is beneficial to include scans of system measurements under various working conditions.

The estimation of some CT correction factors is more accurate than others. The reason behind it can be explained as a "load problem". When the system is under certain working conditions, heavy loaded or light loaded, power flow may not distribute evenly due to the topology and parameters of generators, loads, lines and etc.. If the change of power flows going through a line for different scans is large, the estimation of both the VT and CT RCFs and PACFs will become more accurate, which is indicated by the decrease in the error standard deviations.

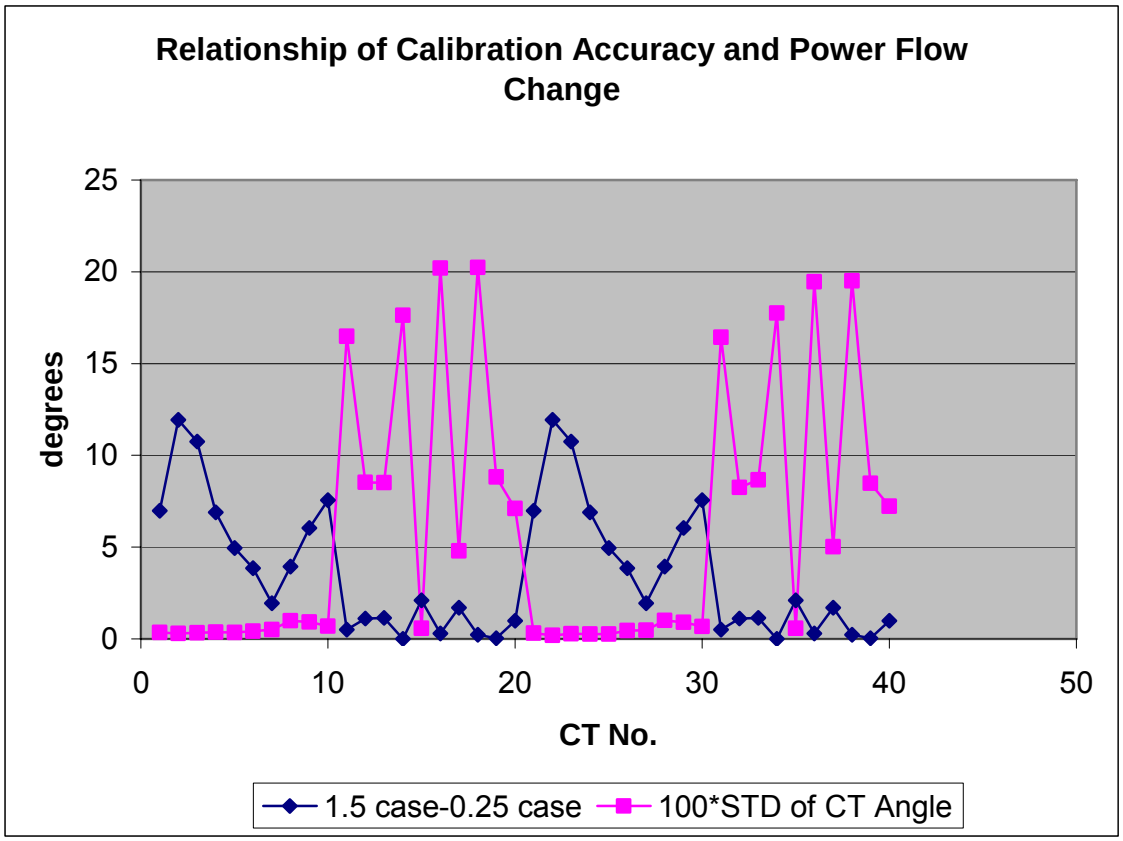

Figure 5-19 Relationship of Calibration Accuracy and Power Flow Change

As shown in Figure 5-19, the calibration accuracy of CT PACF is roughly inversely proportional to the value of power flow change through the CT. Calibration accuracy of

CT PACF can be explained by the corresponding standard deviation, and the load condition of a line can be interpreted by the angle difference of the two buses at the ends of the line. In order to show the change of load conditions in different scans, the line angle difference between heavy-load and light-load scans is used.

5.6.2.3. Instrument Transformer Calibration with Sparsely Distributed Phasor Measurements

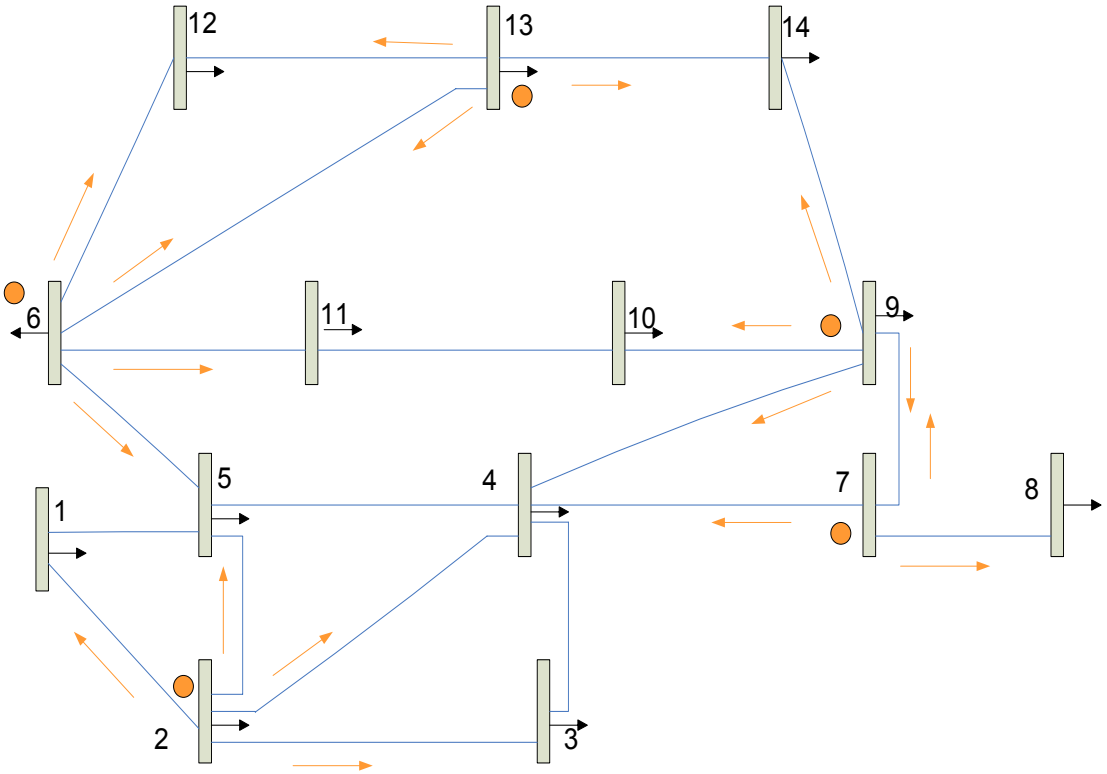

Figure 5-20 Phasor Measurements in 14 Bus System

Assume that there are 5 PMUs installed on buses {2, 6, 7, 9, 13} in the IEEE 14 bus system. Each PMU measures not only the voltage phasor on the bus, but also the current phasors in all the lines that originate from the bus. So, current phasors measurements {I2-1, I2-3, I2-4, I2-5, I6-5, I6-11, I6-12, I6-13, I7-4, I7-8, I7-9, I9-4, I9-7, I9-10, I9-14, I13-6, I13-12, I13-14} are available in addition to voltage measurements {V2, V6, V7, V9, V13}, as is marked in orange in Figure 5-20.

Critical measurements could be identified through the structure of simplified residual covariance matrix $S = I - H\left(H^T H\right)^{-1} H^T$. The analysis of the matrix shows that other than {V2, V6, V7, V9, V13, I2-4, I2-5, I6-12, I6-13, I7-9, I9-14, I13-14, I7-4, I9-4, I6-5, I13-6, I9-7, I13-12}, all the other phasor measurements are critical ones, since the columns in S corresponding to those measurements are null vectors.

Assume that critical measurements have been calibrated beforehand. The proposed method would take care of the remaining ones, whose calibration by software is only allowed due to the available redundancy.

Figures 5-21 to 5-28 illustrate the estimation errors and standard deviations of VT and CT RCFs and PACFs. Each case employs 3 scans, and the load conditions are listed in Table 5-6.

Table 5-6 Load Conditions

Case	Load Conditions (*base case)		
	Scan 1	Scan 2	Scan 3
A	0.1	1	1.5
B	0.25	1	1.25
C	0.3	1	1.2

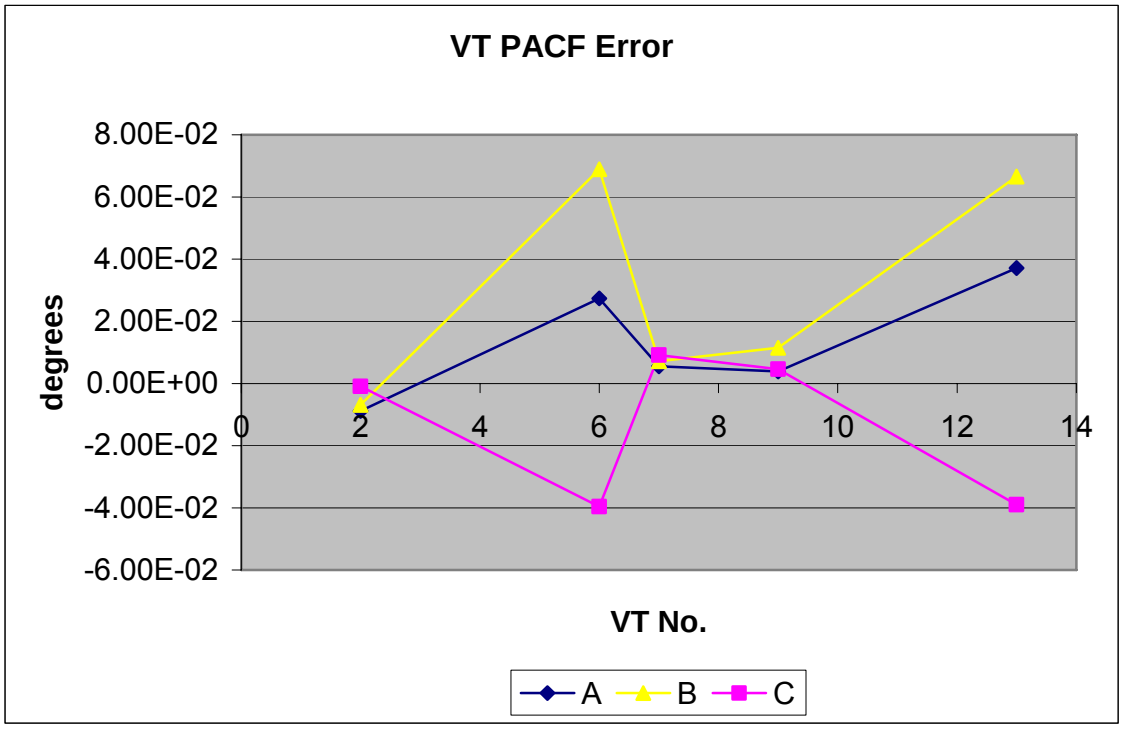

Figure 5-21 VT PACF Errors

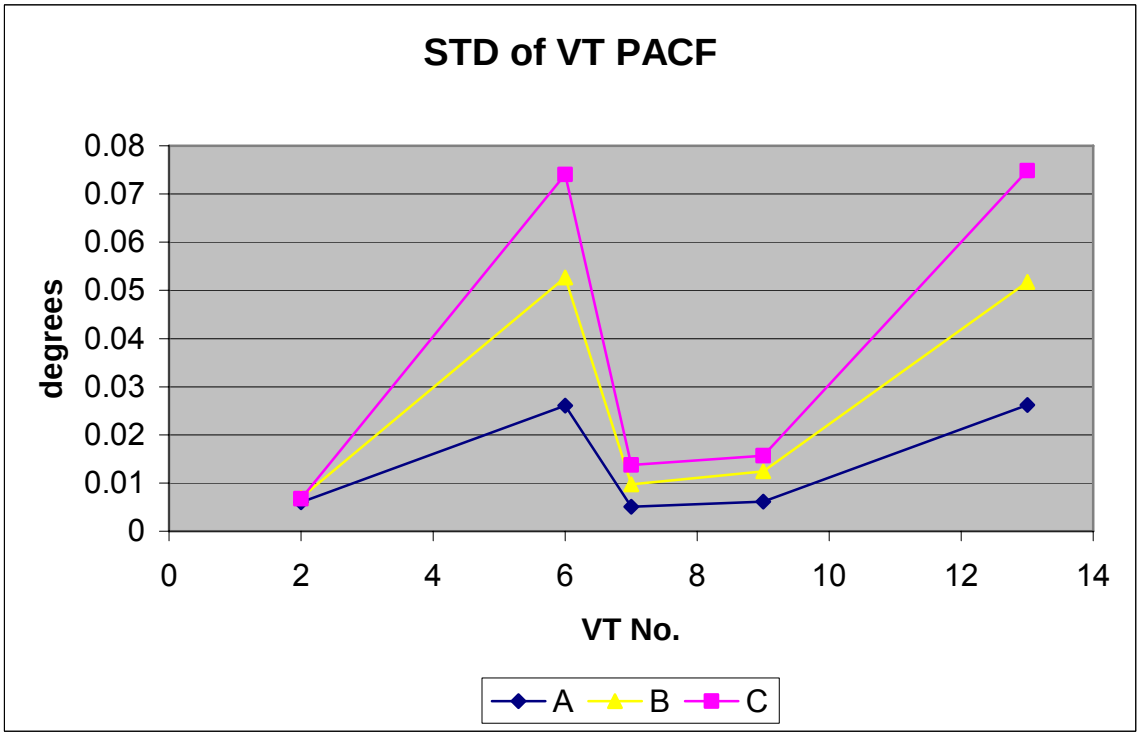

Figure 5-22 Standard Deviations of VT PACF

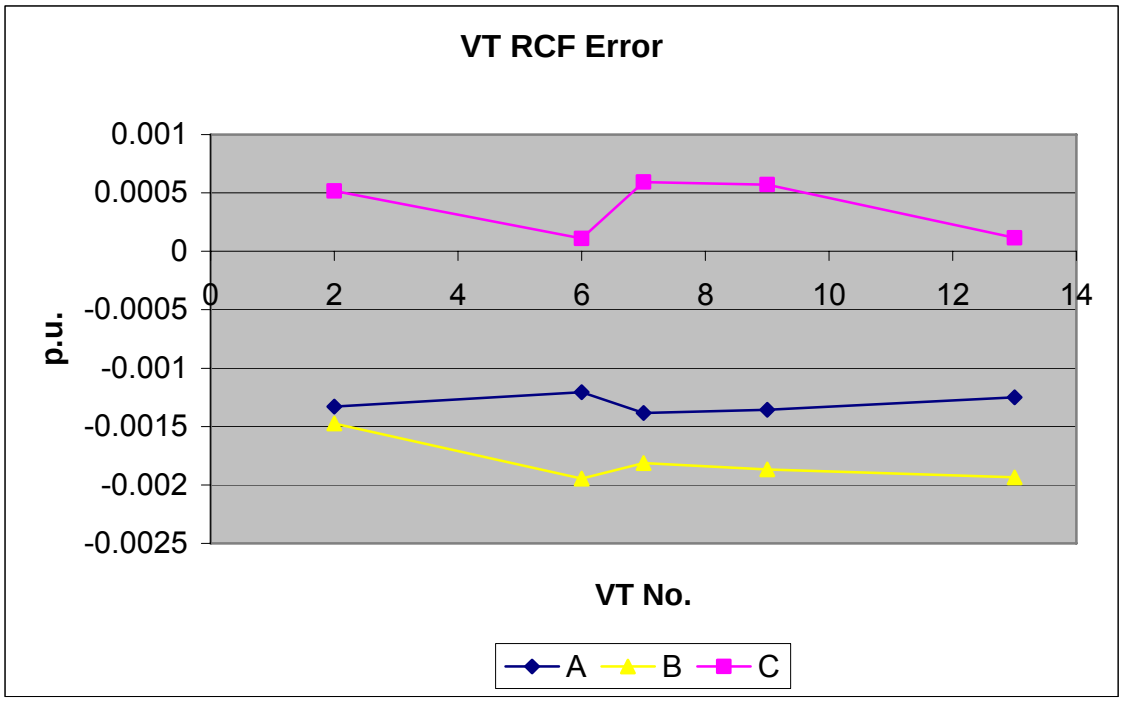

Figure 5-23 VT RCF Errors

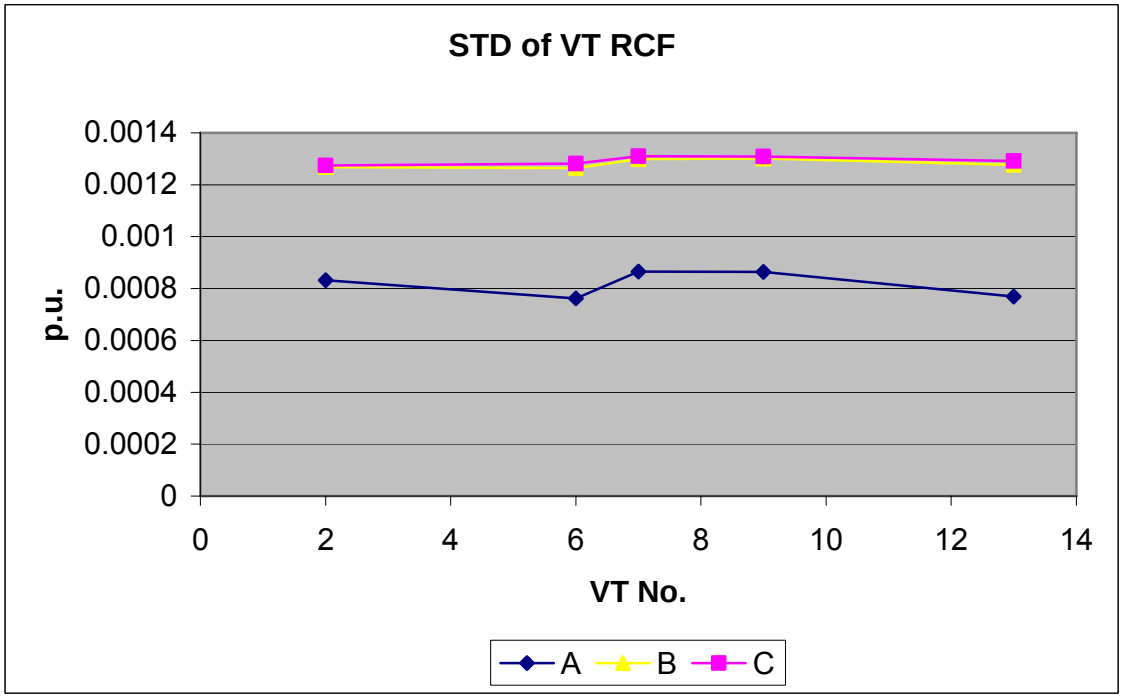

Figure 5-24 Standard Deviations of VT RCF

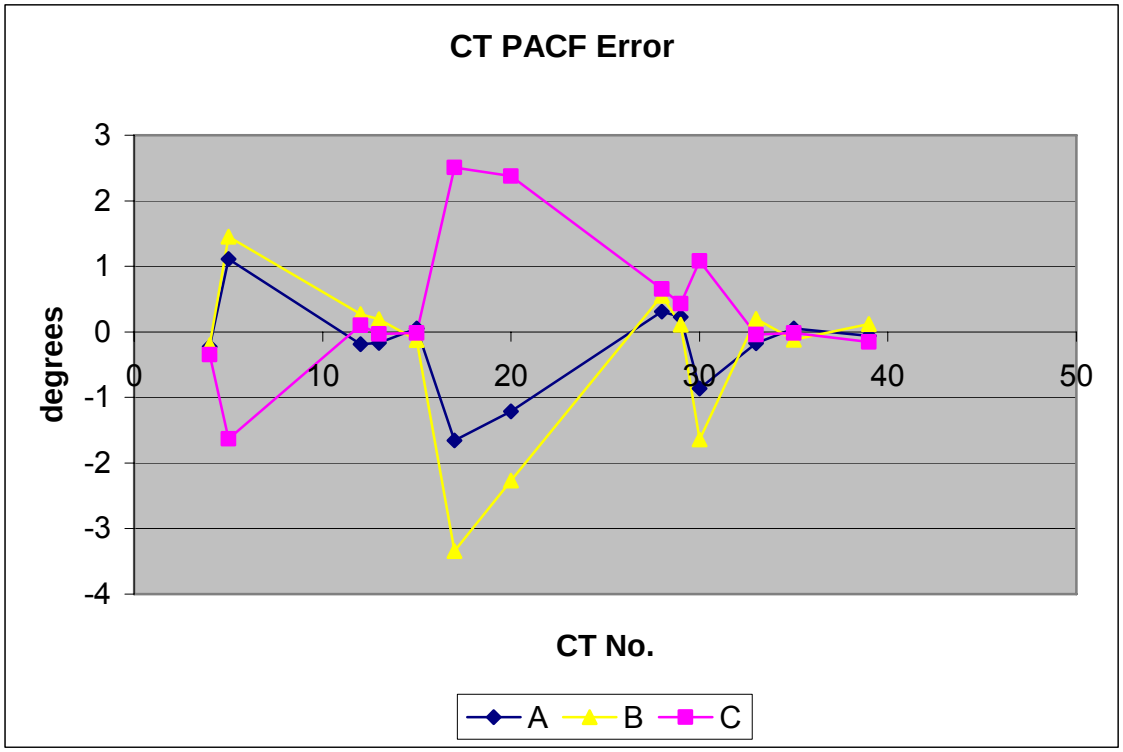

Figure 5-25 CT PACF Errors

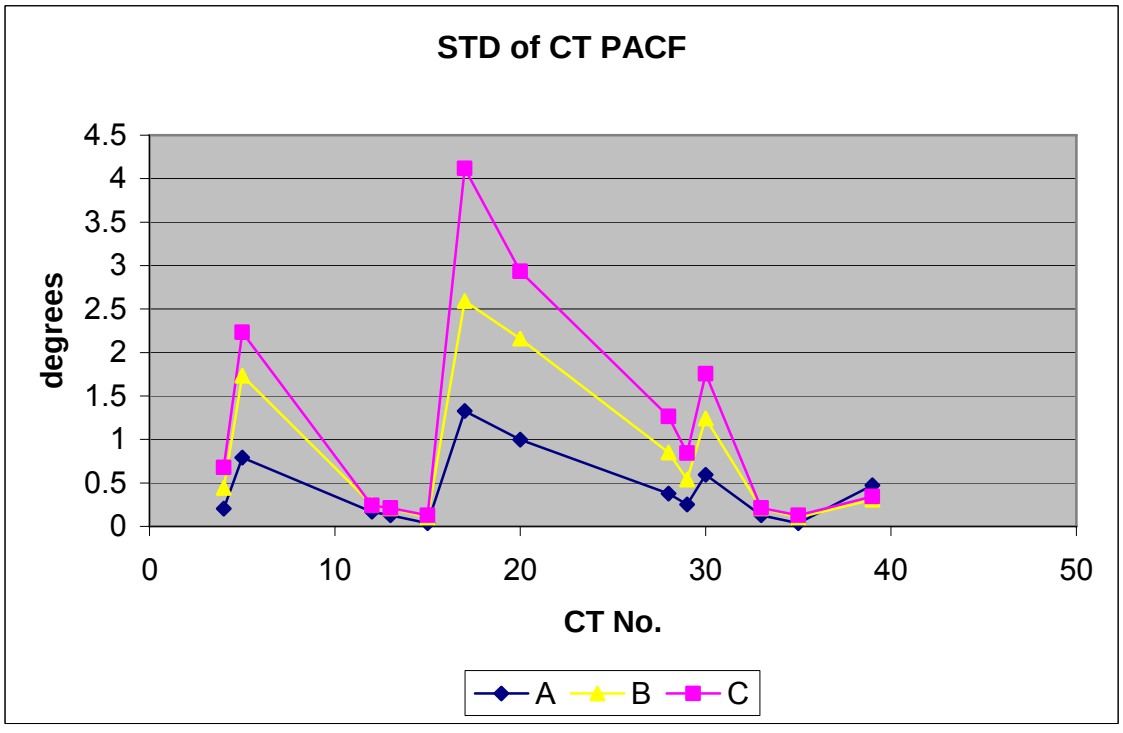

Figure 5-26 Standard Deviations of CT PACF

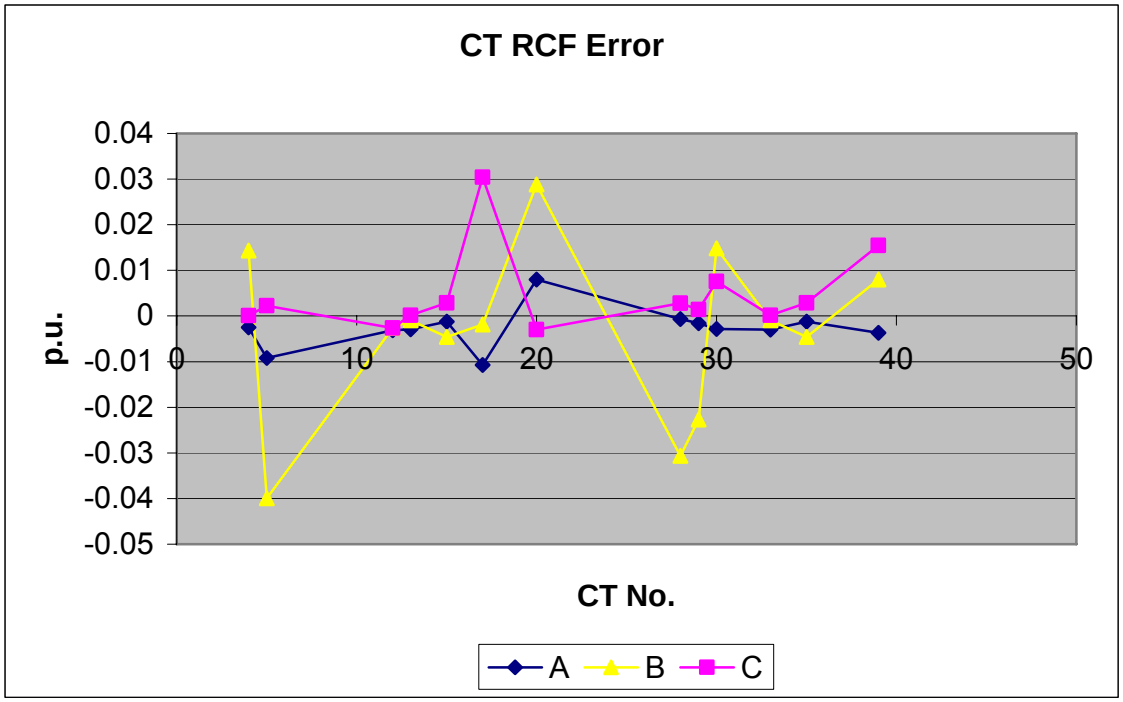

Figure 5-27 CT RCF Errors

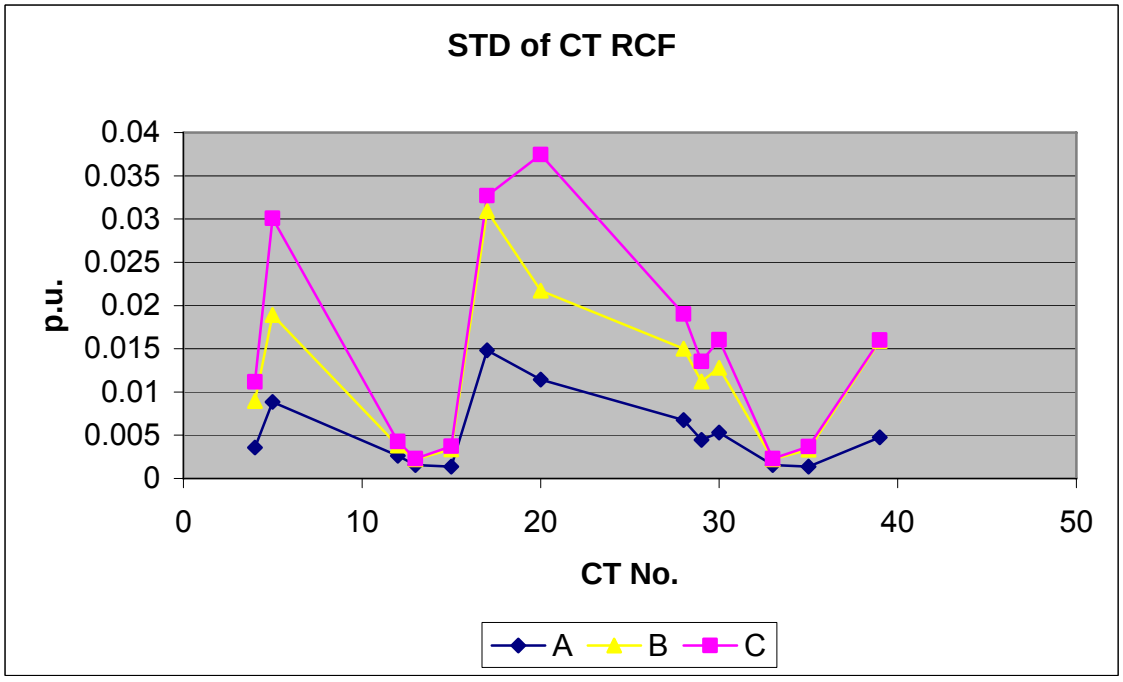

Figure 5-28 Standard Deviations of CT RCF

Figures 5-29 to 5-32 show the standard deviations of estimation when using different

number of scans in three cases (A, B, and C), with the number of scans increases from 3, 5 to 7. Each case adopts 3 basic scans, a heavy-load scan (1.5 times the base load), a normal-load scan (base case), and a light load scan (0.1 times the base load). It is assumed that more light-load and heavy-load conditions with random errors are employed to enhance the measurement redundancy. Namely, 3, 5, and 7 scans are composed of one normal-load scan and 1, 2, and 3 pairs of light-load and heavy-load scans respectively.

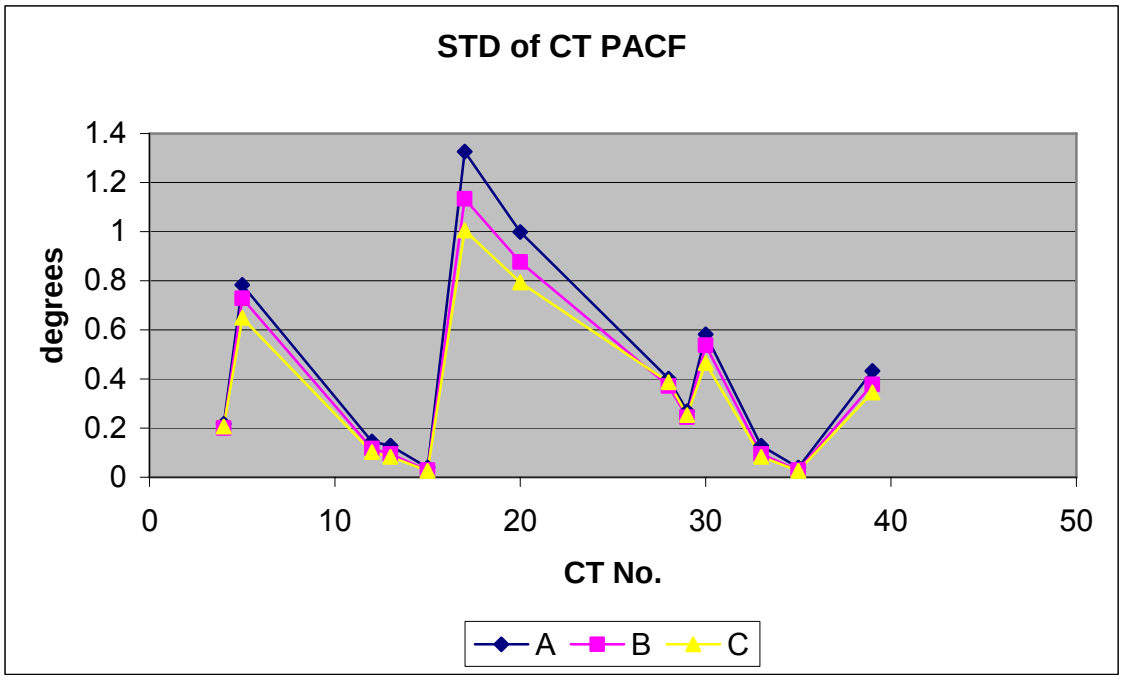

Figure 5-29 Standard Deviations of CT PACF

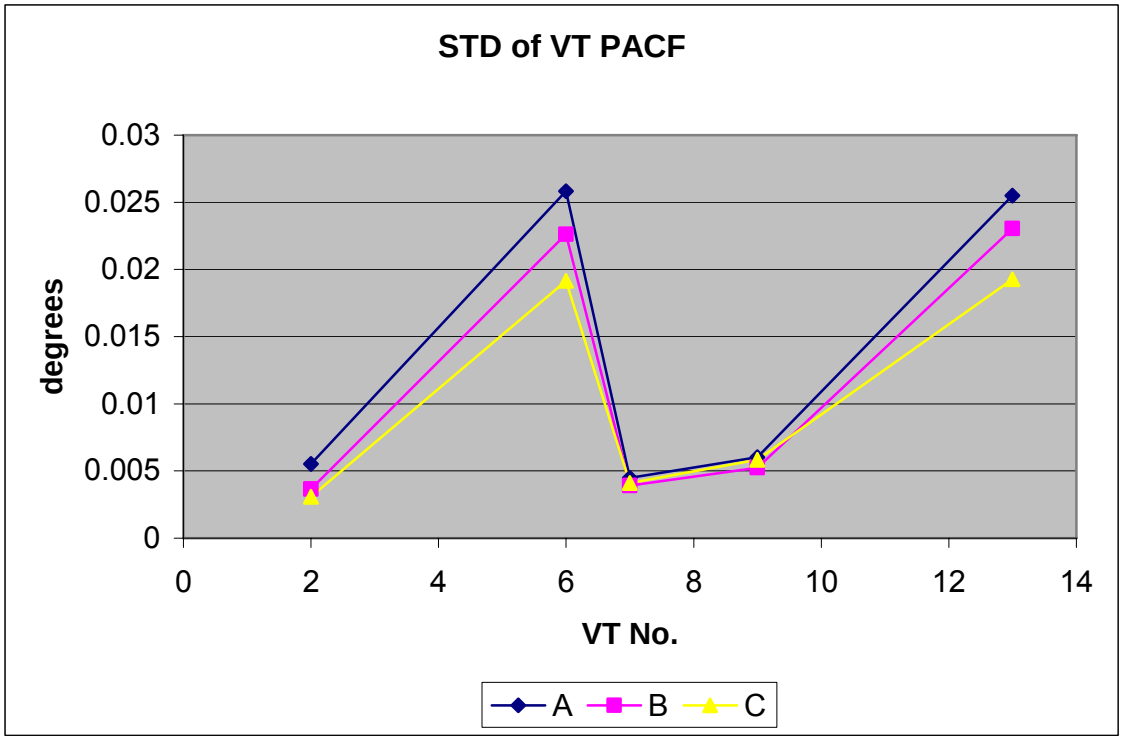

Figure 5-30 Standard Deviations of VT PACF

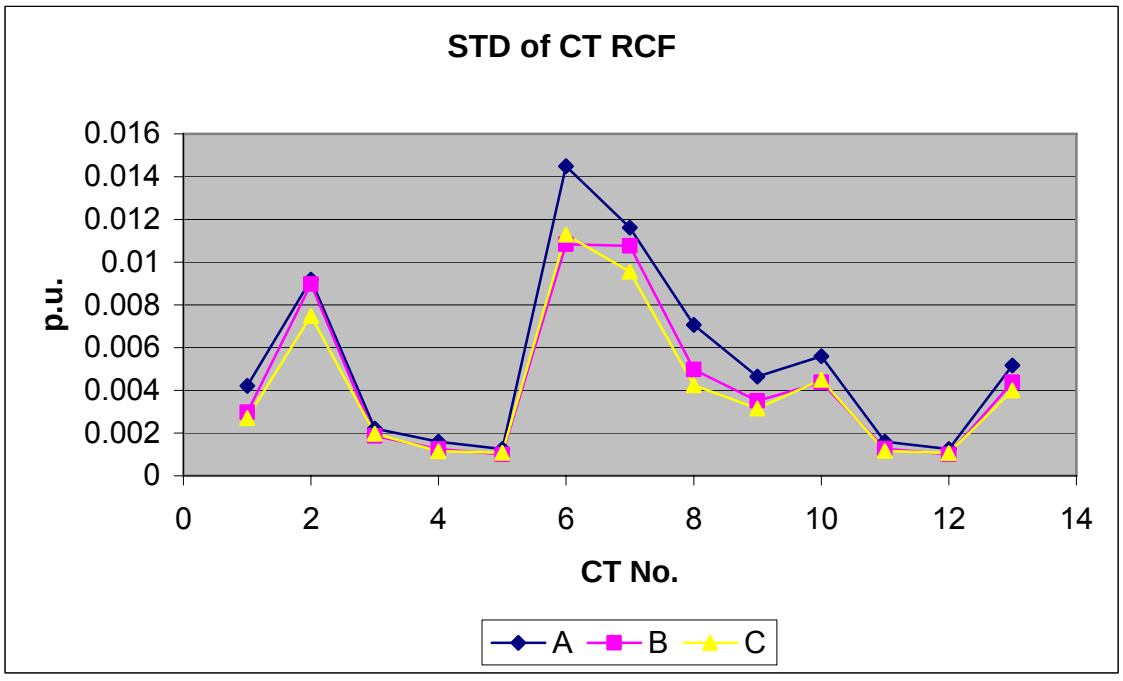

Figure 5-31 Standard Deviations of CT RCF

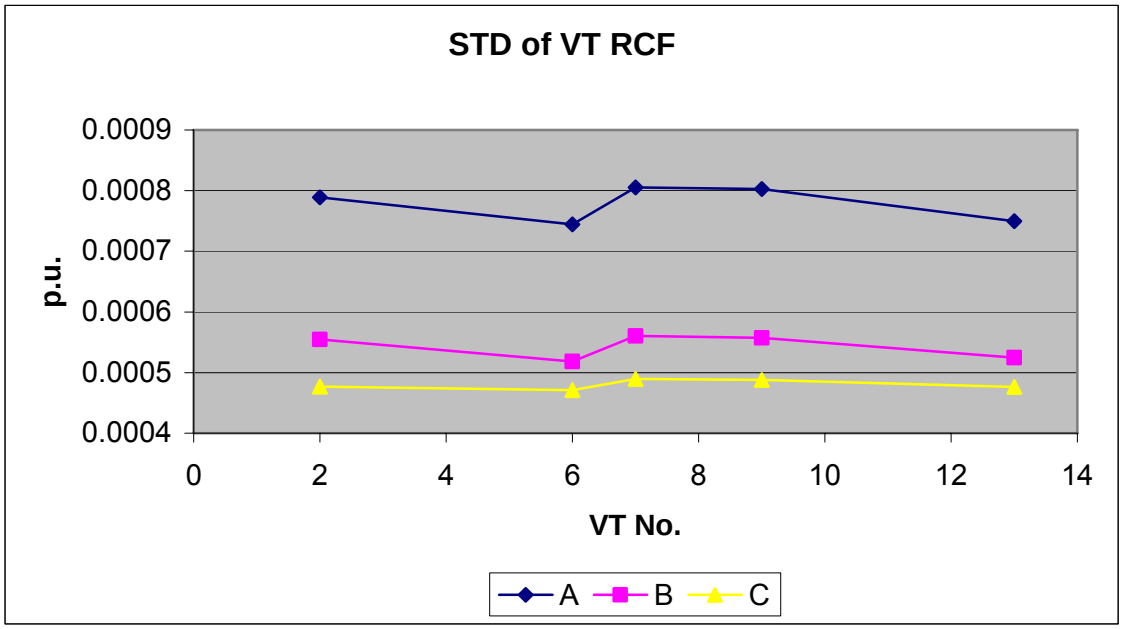

Figure 5-32 Standard Deviations of VT RCF

One can draw the same conclusion from these simulation results as before. The calibration effects are influenced by the load condition and the number of scans used in the estimator. Wider load range and more measurement scans increase largely the calibration accuracy.

The objective of estimating complex correction factors is to calibrate instrument transformers and to improve the accuracy of system state estimation through compensating the phasor measurements with the estimated error values. Figure 5-33 and Figure 5-34 compare the system states estimation with and without calibration through the proposed method.

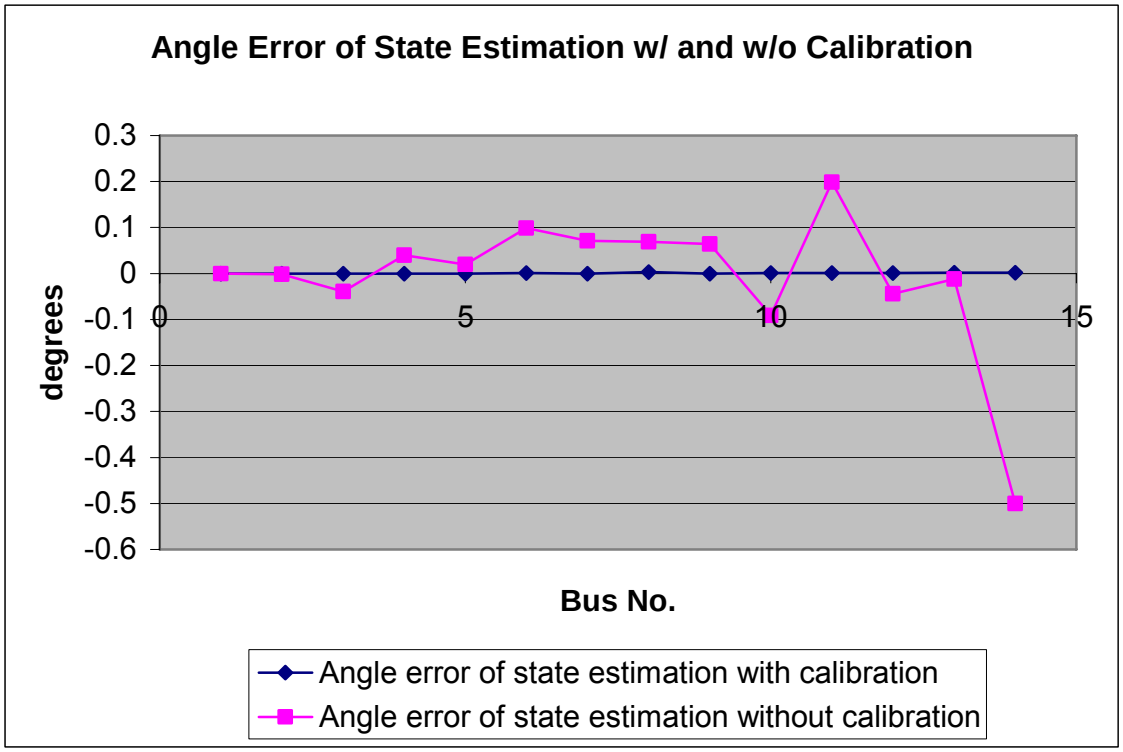

Figure 5-33 Angle Error of State Estimation with and without Calibration

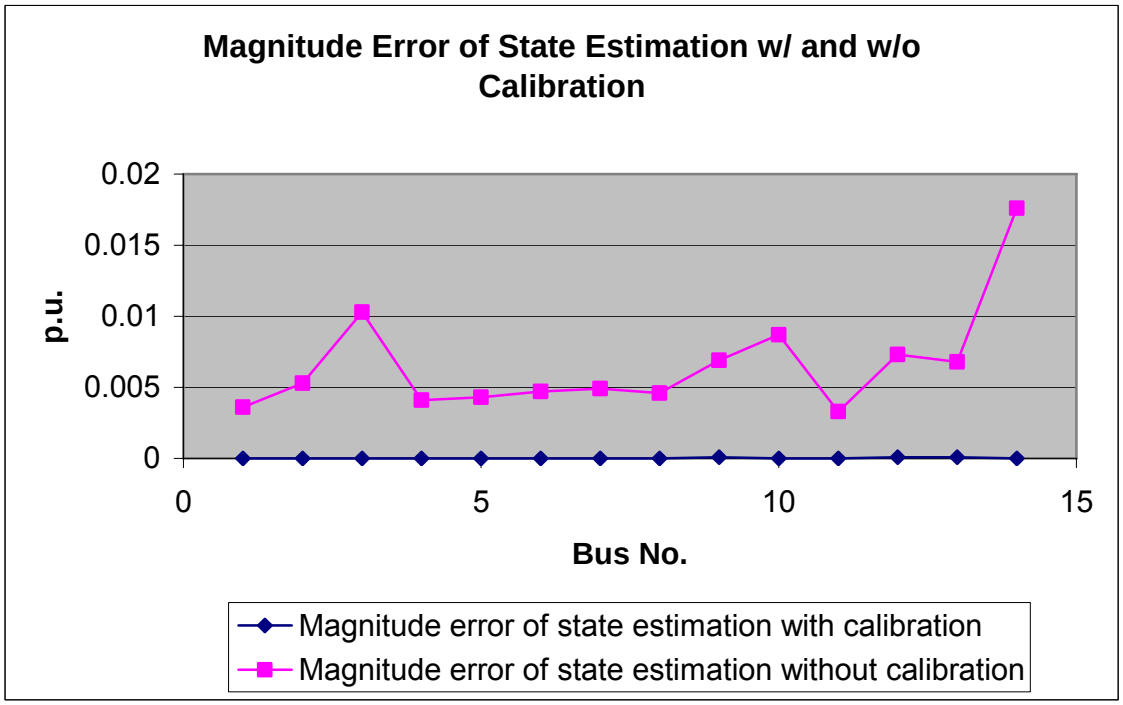

Figure 5-34 Magnitude Error of State Estimation with and without Calibration

Assume that a system under normal load condition has PMUs installed on every bus in the system. PMU measurements are collected as the input of state estimator. When calibration service is not available, it is assumed that the complex correction factors of CTs and VTs are all $1\angle 0$ s in default and estimators consider measurements as the ones with Gaussian errors only. However, phasor measurements are actually biased due to the un-calibrated instrument transformers, and so are the estimated states. After compensating with the complex VT and CT correction factors determined by the proposed method, (two scans, 0.25*base case and 1.5*base case, are employed to calibrate instrument transformers), the estimation is greatly improved. The difference between the estimated state and the true state stays close to zero and is presented in dark color in Figure 5-33 and 5-34. And the estimation results are also tabulated below. The calibration ensures the quality of measurement inputs, consequently, tremendously improves the estimation accuracy.

Table 5-7 Estimation Results w/ and w/o Calibration

Bus No.	True State		Est. State w/ Cali.		Est. State w/o Cali.	
	θ	|V|	θ	|V|	θ	|V|
1	0	1.06	0	1.06	0	1.0636
2	-4.9809	1.045	-4.981	1.045	-4.9823	1.0503
3	-12.718	1.01	-12.718	1.01	-12.757	1.0203
4	-10.324	1.0186	-10.324	1.0186	-10.284	1.0227
5	-8.7826	1.0203	-8.7825	1.0203	-8.7628	1.0246
6	-14.223	1.07	-14.222	1.07	-14.124	1.0747
7	-13.368	1.062	-13.368	1.062	-13.297	1.0669
8	-13.368	1.09	-13.365	1.09	-13.299	1.0946
9	-14.947	1.0563	-14.947	1.0564	-14.883	1.0633
10	-15.104	1.0513	-15.103	1.0513	-15.195	1.06
11	-14.795	1.0571	-14.794	1.0571	-14.596	1.0604
12	-15.077	1.0552	-15.076	1.0553	-15.121	1.0626
13	-15.159	1.0504	-15.157	1.0505	-15.171	1.0573
14	-16.039	1.0358	-16.037	1.0358	-16.539	1.0534

5.7. Conclusion

The PMU is one of the most accurate measurement devices in power systems. However, the overall phasor precision is significantly reduced by the error accumulation through the measurement channel, and it is especially influenced by the absence of calibration of instrument transformers.

A method for calibrating CTs and VTs remotely has been proposed in this chapter. This method incorporates several scans of phasor measurements in the estimator and estimates complex correction factors for instrument transformers along with the system states of each scan. No precise models of instrument transformers are required to accomplish the calibration process, and as a "soft" calibration, it can be executed several times per day to timely adjust the parameters. After implementing the simulations on a 14 bus system, it has been verified that this method effectively improves the accuracy of phasor measurements, and hence the advanced applications such as state estimation that can be improved with PMU data. Moreover, the calibration accuracy grows with the increasing number of scans and/or the load range covered by the scans. In addition,

phasor measurements attained from the sparsely installed PMUs can assist the calibration of instrument transformers that facilitate measuring the redundant phasors.

Chapter 6. Conclusions

1.1. Summary

Four important technical topics for phasor measurement applications have been addressed in this dissertation. These topics are important for the use of synchronized phasor measurements in advanced power system monitoring and control applications. PMU placement, staged PMU deployment, inclusion of phasor measurements in state estimators, and instrument transformer calibration with phasor measurements. The main objective of these researches is to enhance the deployment and usage of phasor measurements to improve the precision of power system monitoring and serve as the foundation for future applications to strengthen system operation, planning and control in the new deregulated power markets.

Subjects have been presented with thorough theoretical and numerical analysis, and are summarized as follows:

Five categories of virtual buses that either do not exist physically or are not practical locations to install PMUs have been identified from the study of practical system models used for power flow calculation purpose. The reasons of invalidity of these virtual buses in topology analysis for PMU placement have been presented. Methods of achieving equivalent models after removing these virtual buses and their corresponding causes for removal have been suggested and analyzed. Reduction of virtual buses decreases system scale by 1/3, according to the experiment result on a large system in the real world. In addition, a set of PMUs covering this reduced system model will guarantee the observability of the real system. No PMUs will be assigned to a bus that does not exist or lacks equipments or facilities for measuring and communicating.

A pre-processing method of matrix reduction algorithm that can be adapted to most of the optimal PMU placement algorithms available in the literature has been presented.

The method is applied to system data before the process of optimal PMU placement. Independent of the algorithm used to determine the optimal PMU placement set, this method is able to reduce the scale of the optimization problem and thus the computational requirements. Four IEEE sample systems and a large real world system were used to test this pre-processing method. The feasibility of the proposed method has been verified by comparing numbers of minimum PMUs needed for full observability with the ones achieved by other methods previously proposed. In addition, Lagrangian relaxation has been employed to confirm the performance feasibility for the real world large system that was not part of any earlier study.

Staged PMU installations have been introduced using depth of un-observability as one of the criteria to determine a preferred sequence of PMU installation. The installation procedure, aimed at decreasing the depth of un-observability, focuses on maximizing the number of buses that benefit from the limited PMUs deployed as well as the overall "benefit degree" at each stage. Incidence matrix of depth n was used as the matrix product of n copies of the original incidence matrix. Integer programming was applied to the incidence matrices of depth 1 to n to achieve a staged installation.

An alternative of combining phasor measurements with traditional P, Q, and |V| measurements in a post-processing linear hybrid state estimator instead of mixing them with conventional measurements as one set and developing a non-linear state estimator has been developed. This alternative allows keeping the conventional state estimator software intact, and does not require iterations in the post-processing step. It also leads to practically the same results as estimators mixing phasor measurements in a non-linear measurement set and is computationally more attractive.

A method has been proposed for calibrating instrument transformers with phasor measurements. The method estimates ratio correction factors and phase angle correction factors along with system states through the incorporation of several scans of phasor measurements during diverse system operating conditions. This method requires no accurate instrument transformer models and can be executed several times a day to keep the calibration of the instrument transformers up to date. Studies on factors that improve

the calibration accuracy like a large number of scans and a large range of load conditions have been presented. In addition, systems with sparsely installed PMUs are able to provide phasor measurements enabling the calibration of instrument transformers of redundant phasors. Those redundant phasors could be identified as corresponding to the structure of a sensitivity covariance matrix.

1.2. Future Work

The work reported in the dissertation could be the foundation for future researches associated with PMU placement and applications in state estimation and control applications. The followings are recommended for further investigation:

The PMU placement problems assume that a PMU installed on one bus is able to measure the voltage and all the currents in the lines that originate on that bus. However, even if a single PMU is able to measure all the currents, there is a larger possibility at these buses that some of the current measurement might be lost. For instance, the largest number of connecting lines in the large real world system with 1457 buses is 14 lines. Several PMUs may be needed to measure all the current phasor measurements. Therefore, taking into consideration the larger possibility of failure when determining the minimal number of PMUs is one of the practical problems that need further exploration.

For the inclusion of phasor measurements in state estimation, further studies are needed on better bad data identification and topology error detection techniques.

For the proposed estimators with the ability to include phasor measurements or calibrate instrument transformers, tests on practical systems with real measurements are needed to validate the proposed algorithm. Due to the lack of real measurement data, the proposed estimators that include phasor measurements or calibrate instrument measurements were tested with simulated data only. In the future, the proposed estimators should be tested in practical systems and with real measurement data.

For time skewed real conventional measurements a study needs to be performed to determine how well adding PMUs using the proposed post-processing method will

alleviate the skew problem and help achieve the accuracy requirements for certain applications.

References

[1] A. G. Phadke, "Synchronized phasor measurements in power systems," *Computer Applications in Power, IEEE,* vol. 6, pp. 10-15, 1993.

[2] A. G. Phadke, "Synchronized phasor measurements-a historical overview," in *Transmission and Distribution Conference and Exhibition 2002: Asia Pacific. IEEE/PES*, 2002, pp. 476-479 vol.1.

[3] A. G. Phadke and J. S. Thorp, "HISTORY AND APPLICATIONS OF PHASOR MEASUREMENTS," in *Power Systems Conference and Exposition, 2006. PSCE '06. 2006 IEEE PES*, 2006, pp. 331-335.

[4] A. G. Phadke, J. S. Thorp, and M. G. Adamiak, "A New Measurement Technique for Tracking Voltage Phasors, Local System Frequency, and Rate of Change of Frequency," *IEEE Transactions on Power Apparatus and Systems,* vol. PAS-102, pp. 1025-1038, 1983.

[5] L. Mili, T. Baldwin, and R. Adapa, "Phasor measurement placement for voltage stability analysis of power systems," in *Decision and Control, 1990., Proceedings of the 29th IEEE Conference on*, 1990, pp. 3033-3038 vol.6.

[6] G. Mueller, P. Komarnicki, I. Golub, Z. Styczynski, C. Dzienis, and J. Blumschein, "PMU placement method based on decoupled newton power flow and sensitivity analysis," in *Electrical Power Quality and Utilisation, 2007. EPQU 2007. 9th International Conference on*, 2007, pp. 1-5.

[7] T. L. Baldwin, L. Mili, M. B. Boisen, Jr., and R. A. Adapa, "Power system observability with minimal phasor measurement placement," *Power Systems, IEEE Transactions on,* vol. 8, pp. 707-715, 1993.

[8] A. Abur and A. G. Exposito, *Power System State Estimation- Theory and Implementation*: CRC, 2004.

[9] F. C. Schweppe, "Power System Static-State Estimation, Part III: Implementation," *IEEE Transactions on Power Apparatus and Systems,* vol. PAS-89, pp. 130-135, 1970.

[10] F. C. Schweppe and J. Wildes, "Power System Static-State Estimation, Part I: Exact Model," *IEEE Transactions on Power Apparatus and Systems,* vol. PAS-89, pp. 120-125, 1970.

[11] F. C. Schweppe and D. B. Rom, "Power System Static-State Estimation, Part II: Approximate Model," *IEEE Transactions on Power Apparatus and Systems,* vol. PAS-89, pp. 125-130, 1970.

[12] R. E. Larson, W. F. Tinney, and J. Peschon, "State Estimation in Power Systems Part I: Theory and Feasibility," *IEEE Transactions on Power Apparatus and Systems,* vol. PAS-89, pp. 345-352, 1970.

[13] R. E. Larson, W. F. Tinney, L. P. Hajdu, and D. S. Piercy, "State Estimation in Power Systems Part II: Implementation and Applications," *IEEE Transactions on Power Apparatus and Systems,* vol. PAS-89, pp. 353-363, 1970.

[14] A. Abur, "Optimal Placement of Phasor Measurement Units for State Estimation," http://www.pserc.wisc.edu/ecow/get/generalinf/presentati/psercsemin1/2psercsemin/abur_pmu_pserc_teleseminar_nov2005_slides.pdf

[15] A. G. Phadke, J. S. Thorp, and K. J. Karimi, "State Estimlation with Phasor Measurements,"

Power Systems, IEEE Transactions on, vol. 1, pp. 233-238, 1986.

[16] F. P. Sioshansi and W. Pfaffenberger, *electricity market reform in international perspective*, 2006.

[17] D. Kirschen and G. Strbac, "Why investments do not prevent blackouts," http://www.ksg.harvard.edu/hepg/Standard_Mkt_dsgn/Blackout_Kirschen_Strbac_082703.pdf

[18] M. Zhou, V. A. Centeno, J. S. Thorp, and A. G. Phadke, "An Alternative for Including Phasor Measurements in State Estimators," *Power Systems, IEEE Transactions on,* vol. 21, pp. 1930-1937, 2006.

[19] D. Xu, R. He, P. Wang, and T. Xu, "Comparison of several PMU placement algorithms for state estimation," in *Developments in Power System Protection, 2004. Eighth IEE International Conference on*, 2004, pp. 32-35 Vol.1.

[20] R. F. Nuqui and A. G. Phadke, "Phasor measurement unit placement techniques for complete and incomplete observability," *Power Delivery, IEEE Transactions on,* vol. 20, pp. 2381-2388, 2005.

[21] B. Xu and A. Abur, "Observability analysis and measurement placement for systems with PMUs," in *Power Systems Conference and Exposition, 2004. IEEE PES*, 2004, pp. 943-946 vol.2.

[22] G. Huang and H. Zhang, "Transaction Based Power Flow Analysis For Transmission Utilization Allocation," http://www.pserc.wisc.edu/ecow/get/publicatio/2001public/transactionbasedflow.pdf

[23] R. R. J. Cheriyan, "Application algorithms for network problems," 1998.

[24] "Lagrangian Relaxation," http://mat.gsia.cmu.edu/mstc/relax/node9.html

[25] E. W. Fred Glover, "converting the 0-1 polynomial programming problem to a 0-1 linear program," *Operations Research,* vol. 22, pp. 180-182, 1974.

[26] D. Dua, S. Dambhare, R. K. Gajbhiye, and S. A. Soman, "Optimal Multistage Scheduling of PMU Placement: An ILP Approach," in *Power Delivery, IEEE Transactions on : Accepted for future publication*, 2003.

[27] "Adjacency matrix," http://en.wikipedia.org/wiki/Adjacency_matrix

[28] T. W. Cease and B. Feldhaus, "Real-time monitoring of the TVA power system," *Computer Applications in Power, IEEE,* vol. 7, pp. 47-51, 1994.

[29] J. S. Thorp, A. G. Phadke, and K. J. Karimi, "Real Time Voltage-Phasor Measurement For Static State Estimation," *IEEE Transactions on Power Apparatus and Systems,* vol. PAS-104, pp. 3098-3106, 1985.

[30] R. Zivanovic and C. Cairns, "Implementation of PMU technology in state estimation: an overview," in *AFRICON, 1996., IEEE AFRICON 4th*, 1996, pp. 1006-1011 vol.2.

[31] I. W. Slutsker, S. Mokhtari, L. A. Jaques, J. M. G. Provost, M. B. Perez, J. B. Sierra, F. G. Gonzalez, and J. M. M. Figueroa, "Implementation of phasor measurements in state estimator at Sevillana de Electricidad," in *Power Industry Computer Application Conference, 1995. Conference Proceedings., 1995 IEEE*, 1995, pp. 392-398.

[32] A. Abur and A. G. Exposito, *Power System State Estimation Theory and Implementation*. New York: Marcel Dekker, 2004.

[33] J. Zhu and A. Abur, "Effect of Phasor Measurements on the Choice of Reference Bus for State Estimation," in *Power Engineering Society General Meeting, 2007. IEEE*, 2007, pp. 1-5.

[34] U. o. Washington, "Study system data files," http://www.ee.washington.edu/research/pstca/

[35] J. F. Dopazo, S. T. Ehrmann, O. A. Klitin, A. M. A. Sasson, and L. S. A. Van Slyck,

"Implementation of the AEP real-time monitoring system," *Power Apparatus and Systems, IEEE Transactions on,* vol. 95, pp. 1618-1629, 1976.

[36] B. Hague, *Instrument Transformers*: Pitman Publishing Corporation, 1936.

[37] J. H. Harlow, *electric power transformer engineering*: CRC Press, 2004.

[38] "IEEE Standard Requirements for Instrument Transformers," *IEEE Std C57.13-1993(R2003) (Revision of IEEE Std C57.13-1978),* pp. i-73, 2003.

[39] A. P. S. Meliopoulos, F. Zhang, S. Zelingher, G. Stillman, G. J. Cokkinides, L. Coffeen, R. Burnett, and J. McBride, "Transmission level instrument transformers and transient event recorders characterization for harmonic measurements," *Power Delivery, IEEE Transactions on,* vol. 8, pp. 1507-1517, 1993.

[40] A. P. Sakis Meliopoulos, G. J. Cokkinides, F. Galvan, and B. A. Fardanesh, "GPS-Synchronized Data Acquisition: Technology Assessment and Research Issues," in *System Sciences, 2006. HICSS '06. Proceedings of the 39th Annual Hawaii International Conference on*, 2006, pp. 244c-244c.

[41] IEC, "Instrument transformers-Part1: Current transformer," 1996.

[42] IEC, "Instrument transformers- Part 2: Inductive voltage transformers," 2003.

[43] "Accurate CT Calibration for the Model 1133A " http://www.arbiter.com/catalog/power/1133a/additional_docs/ct_calibration_1133a.php

[44] M. M. Adibi and D. K. Thorne, "Remote Measurement Calibration," *Power Systems, IEEE Transactions on,* vol. 1, pp. 194-199, 1986.

[45] M. M. Adibi and R. J. Kafka, "Minimization of uncertainties in analog measurements for use in state estimation," *Power Systems, IEEE Transactions on,* vol. 5, pp. 902-910, 1990.

[46] M. M. Adibi, K. A. Clements, R. J. Kafka, and J. P. A. S. J. P. Stovall, "Integration of remote measurement calibration with state estimation-a feasibility study," *Power Systems, IEEE Transactions on,* vol. 7, pp. 1164-1172, 1992.

[47] M. M. Adibi, K. A. Clements, R. J. Kafka, and J. P. Stovall, "Remote measurement calibration," *Computer Applications in Power, IEEE,* vol. 3, pp. 37-42, 1990.

[48] Z. Shan and A. Abur, "Combined state estimation and measurement calibration," *Power Systems, IEEE Transactions on,* vol. 20, pp. 458-465, 2005.

[49] A. P. S. Meliopoulos, G. J. Cokkinides, F. Galvan, B. A. Fardeanesh, and P. A. Myrda, "Delivering accurate and timely data to all," *Power and Energy Magazine, IEEE,* vol. 5, pp. 74-86, 2007.

[50] A. P. S. Meliopoulos, G. J. Cokkinides, F. Galvan, B. A. F. B. Fardanesh, and P. A. M. P. Myrda, "Advances in the SuperCalibrator Concept - Practical Implementations," in *System Sciences, 2007. HICSS 2007. 40th Annual Hawaii International Conference on*, 2007, pp. 118-118.

[51] W. Hubbi, "Computational method for remote meter calibration in power systems," *Generation, Transmission and Distribution, IEE Proceedings-,* vol. 143, pp. 393-398, 1996.

[52] K. A. Clements and P. W. Davis, "Multiple Bad Data Detectability and Identifiability: A Geometric Approach," *Power Delivery, IEEE Transactions on,* vol. 1, pp. 355-360, 1986.

[53] A. G. Phadke, "Aspects of Phasor Measurement Processes."

Appendix A. Test Systems

IEEE 14 Bus System

```
baseMVA =          100.0;

                bus      type        Pd        Qd        Gs        Bs
bus       =       [
                  1         3         0         0         0         0
                  2         2      21.7      12.7         0         0
                  3         2      94.2        19         0         0
                  4         1      47.8      -3.9         0         0
                  5         1       7.6       1.6         0         0
                  6         2      11.2       7.5         0         0
                  7         1         0         0         0         0
                  8         2         0         0         0         0
                  9         1      29.5      16.6         0        19
                 10         1         9       5.8         0         0
                 11         1       3.5       1.8         0         0
                 12         1       6.1       1.6         0         0
                 13         1      13.5       5.8         0         0
                 14         1      14.9         5         0         0
];

                bus        Pg        Qg      Qmax      Qmin       Vsp      Pmax      Pmin
gen       =       [
                  1     232.4     -16.9        10         0      1.06     332.4         0
                  2        40      42.4        50       -40     1.045       140         0
                  3         0      23.4        40         0      1.01       100         0
                  6         0      12.2        24        -6      1.07       100         0
                  8         0      17.4        24        -6      1.09       100         0
];

               fbus      tbus         r         x         b
branch    =       [
```

```
    1     2  0.01938  0.05917  0.0528
    1     5  0.05403  0.22304  0.0492
    2     3  0.04699  0.19797  0.0438
    2     4  0.05811  0.17632  0.0374
    2     5  0.05695  0.17388   0.034
    3     4  0.06701  0.17103  0.0346
    4     5  0.01335  0.04211  0.0128
    4     7        0  0.20912       0
    4     9        0  0.55618       0
    5     6        0  0.25202       0
    6    11  0.09498   0.1989       0
    6    12  0.12291  0.25581       0
    6    13  0.06615  0.13027       0
    7     8        0  0.17615       0
    7     9        0  0.11001       0
    9    10  0.03181   0.0845       0
    9    14  0.12711  0.27038       0
   10    11  0.08205  0.19207       0
   12    13  0.22092  0.19988       0
   13    14  0.17093  0.34802       0
];
```

IEEE 30 Bus System

baseMVA = 100.0000;

bus	type	Pd	Qd	Gs	Bs
bus = [					
1	3	0	0	0	0
2	2	21.7	12.7	0	0
3	1	2.4	1.2	0	0
4	1	7.6	1.6	0	0
5	1	0	0	0	0.19
6	1	0	0	0	0
7	1	22.8	10.9	0	0
8	1	30	30	0	0
9	1	0	0	0	0
10	1	5.8	2	0	0
11	1	0	0	0	0
12	1	11.2	7.5	0	0
13	2	0	0	0	0
14	1	6.2	1.6	0	0
15	1	8.2	2.5	0	0
16	1	3.5	1.8	0	0
17	1	9	5.8	0	0
18	1	3.2	0.9	0	0
19	1	9.5	3.4	0	0
20	1	2.2	0.7	0	0
21	1	17.5	11.2	0	0
22	2	0	0	0	0
23	2	3.2	1.6	0	0
24	1	8.7	6.7	0	0.04
25	1	0	0	0	0
26	1	3.5	2.3	0	0
27	2	0	0	0	0
28	1	0	0	0	0
29	1	2.4	0.9	0	0
30	1	10.6	1.9	0	0
];					

```
                bus        Pg        Qg      Qmax      Qmin       Vsp      Pmax      Pmin
gen     =         [
                  1     23.54         0       150       -20         1        80    0.0000;
                  2     60.97         0        60       -20         1        80    0.0000;
                 22     21.59         0      62.5       -15         1        50    0.0000;
                 27     26.91         0      48.7       -15         1        55    0.0000;
                 23      19.2         0        40       -10         1        30    0.0000;
                 13        37         0      44.7       -15         1        40    0.0000;
];

                fbus      tbus         r         x         b
branch  =         [
                  1         2      0.02      0.06      0.03
                  1         3      0.05      0.19      0.02
                  2         4      0.06      0.17      0.02
                  3         4      0.01      0.04         0
                  2         5      0.05       0.2      0.02
                  2         6      0.06      0.18      0.02
                  4         6      0.01      0.04         0
                  5         7      0.05      0.12      0.01
                  6         7      0.03      0.08      0.01
                  6         8      0.01      0.04         0
                  6         9         0      0.21         0
                  6        10         0      0.56         0
                  9        11         0      0.21         0
                  9        10         0      0.11         0
                  4        12         0      0.26         0
                 12        13         0      0.14         0
                 12        14      0.12      0.26         0
                 12        15      0.07      0.13         0
                 12        16      0.09       0.2         0
                 14        15      0.22       0.2         0
                 16        17      0.08      0.19         0
                 15        18      0.11      0.22         0
                 18        19      0.06      0.13         0
                 19        20      0.03      0.07         0
                 10        20      0.09      0.21         0
```

```
    10    17    0.03    0.08    0
    10    21    0.03    0.07    0
    10    22    0.07    0.15    0
    21    22    0.01    0.02    0
    15    23     0.1     0.2    0
    22    24    0.12    0.18    0
    23    24    0.13    0.27    0
    24    25    0.19    0.33    0
    25    26    0.25    0.38    0
    25    27    0.11    0.21    0
    28    27       0     0.4    0
    27    29    0.22    0.42    0
    27    30    0.32     0.6    0
    29    30    0.24    0.45    0
     8    28    0.06     0.2 0.02
     6    28    0.02    0.06 0.01
];
```

IEEE 57 Bus System

baseMVA = 100.0;

bus	type	Pd	Qd	Gs	Bs
bus = [					
1	3	55	17	0	0
2	2	3	88	0	0
3	2	41	21	0	0
4	1	0	0	0	0
5	1	13	4	0	0
6	2	75	2	0	0
7	1	0	0	0	0
8	2	150	22	0	0
9	2	121	26	0	0
10	1	5	2	0	0
11	1	0	0	0	0
12	2	377	24	0	0
13	1	18	2.3	0	0
14	1	10.5	5.3	0	0
15	1	22	5	0	0
16	1	43	3	0	0
17	1	42	8	0	0
18	1	27.2	9.8	0	10
19	1	3.3	0.6	0	0
20	1	2.3	1	0	0
21	1	0	0	0	0
22	1	0	0	0	0
23	1	6.3	2.1	0	0
24	1	0	0	0	0
25	1	6.3	3.2	0	5.9
26	1	0	0	0	0
27	1	9.3	0.5	0	0
28	1	4.6	2.3	0	0
29	1	17	2.6	0	0
30	1	3.6	1.8	0	0
31	1	5.8	2.9	0	0

```
    32    1    1.6    0.8    0    0
    33    1    3.8    1.9    0    0
    34    1    0      0      0    0
    35    1    6      3      0    0
    36    1    0      0      0    0
    37    1    0      0      0    0
    38    1    14     7      0    0
    39    1    0      0      0    0
    40    1    0      0      0    0
    41    1    6.3    3      0    0
    42    1    7.1    4.4    0    0
    43    1    2      1      0    0
    44    1    12     1.8    0    0
    45    1    0      0      0    0
    46    1    0      0      0    0
    47    1    29.7   11.6   0    0
    48    1    0      0      0    0
    49    1    18     8.5    0    0
    50    1    21     10.5   0    0
    51    1    18     5.3    0    0
    52    1    4.9    2.2    0    0
    53    1    20     10     0    6.3
    54    1    4.1    1.4    0    0
    55    1    6.8    3.4    0    0
    56    1    7.6    2.2    0    0
    57    1    6.7    2      0    0
];

%    bus    Pg      Qg     Qmax   Qmin   Vsp    Pmax    Pmin
gen = [
    1    478.9   -16.1   300    -200   1.04   575.88   0
    2    0       -0.8    50     -17    1.01   100      0
    3    40      -1      60     -10    0.985  140      0
    6    0       0.8     25     -8     0.98   100      0
    8    450     62.1    200    -140   1.005  550      0
    9    0       2.2     9      -3     0.98   100      0
    12   310     128.5   155    -150   1.015  410      0
```

];

	fbus	tbus	r	x	b
branch = [					
	1	2	0.0083	0.028	0.129
	2	3	0.0298	0.085	0.0818
	3	4	0.0112	0.0366	0.038
	4	5	0.0625	0.132	0.0258
	4	6	0.043	0.148	0.0348
	6	7	0.02	0.102	0.0276
	6	8	0.0339	0.173	0.047
	8	9	0.0099	0.0505	0.0548
	9	10	0.0369	0.1679	0.044
	9	11	0.0258	0.0848	0.0218
	9	12	0.0648	0.295	0.0772
	9	13	0.0481	0.158	0.0406
	13	14	0.0132	0.0434	0.011
	13	15	0.0269	0.0869	0.023
	1	15	0.0178	0.091	0.0988
	1	16	0.0454	0.206	0.0546
	1	17	0.0238	0.108	0.0286
	3	15	0.0162	0.053	0.0544
	4	18	0	0.555	0
	4	18	0	0.43	0
	5	6	0.0302	0.0641	0.0124
	7	8	0.0139	0.0712	0.0194
	10	12	0.0277	0.1262	0.0328
	11	13	0.0223	0.0732	0.0188
	12	13	0.0178	0.058	0.0604
	12	16	0.018	0.0813	0.0216
	12	17	0.0397	0.179	0.0476
	14	15	0.0171	0.0547	0.0148
	18	19	0.461	0.685	0
	19	20	0.283	0.434	0
	21	20	0	0.7767	0
	21	22	0.0736	0.117	0
	22	23	0.0099	0.0152	0
	23	24	0.166	0.256	0.0084

24	25	0	1.182	0
24	25	0	1.23	0
24	26	0	0.0473	0
26	27	0.165	0.254	0
27	28	0.0618	0.0954	0
28	29	0.0418	0.0587	0
7	29	0	0.0648	0
25	30	0.135	0.202	0
30	31	0.326	0.497	0
31	32	0.507	0.755	0
32	33	0.0392	0.036	0
34	32	0	0.953	0
34	35	0.052	0.078	0.0032
35	36	0.043	0.0537	0.0016
36	37	0.029	0.0366	0
37	38	0.0651	0.1009	0.002
37	39	0.0239	0.0379	0
36	40	0.03	0.0466	0
22	38	0.0192	0.0295	0
11	41	0	0.749	0
41	42	0.207	0.352	0
41	43	0	0.412	0
38	44	0.0289	0.0585	0.002
15	45	0	0.1042	0
14	46	0	0.0735	0
46	47	0.023	0.068	0.0032
47	48	0.0182	0.0233	0
48	49	0.0834	0.129	0.0048
49	50	0.0801	0.128	0
50	51	0.1386	0.22	0
10	51	0	0.0712	0
13	49	0	0.191	0
29	52	0.1442	0.187	0
52	53	0.0762	0.0984	0
53	54	0.1878	0.232	0
54	55	0.1732	0.2265	0
11	43	0	0.153	0
44	45	0.0624	0.1242	0.004

```
    40    56     0     1.195    0
    56    41     0.553 0.549    0
    56    42     0.2125 0.354    0
    39    57     0     1.355    0
    57    56     0.174 0.26     0
    38    49     0.115 0.177    0.006
    38    48     0.0312 0.0482   0
     9    55     0     0.1205   0
];
```

IEEE 118 Bus System

baseMVA = 100.0;

	bus	type	Pd	Qd	Gs	Bs
bus = [						
	1	2	51	27	0	0
	2	1	20	9	0	0
	3	1	39	10	0	0
	4	2	39	12	0	0
	5	1	0	0	0	-40
	6	2	52	22	0	0
	7	1	19	2	0	0
	8	2	28	0	0	0
	9	1	0	0	0	0
	10	2	0	0	0	0
	11	1	70	23	0	0
	12	2	47	10	0	0
	13	1	34	16	0	0
	14	1	14	1	0	0
	15	2	90	30	0	0
	16	1	25	10	0	0
	17	1	11	3	0	0
	18	2	60	34	0	0
	19	2	45	25	0	0
	20	1	18	3	0	0
	21	1	14	8	0	0
	22	1	10	5	0	0
	23	1	7	3	0	0
	24	2	13	0	0	0
	25	2	0	0	0	0
	26	2	0	0	0	0
	27	2	71	13	0	0
	28	1	17	7	0	0
	29	1	24	4	0	0
	30	1	0	0	0	0
	31	2	43	27	0	0

32	2	59	23	0	0
33	1	23	9	0	0
34	2	59	26	0	14
35	1	33	9	0	0
36	2	31	17	0	0
37	1	0	0	0	-25
38	1	0	0	0	0
39	1	27	11	0	0
40	2	66	23	0	0
41	1	37	10	0	0
42	2	96	23	0	0
43	1	18	7	0	0
44	1	16	8	0	10
45	1	53	22	0	10
46	2	28	10	0	10
47	1	34	0	0	0
48	1	20	11	0	15
49	2	87	30	0	0
50	1	17	4	0	0
51	1	17	8	0	0
52	1	18	5	0	0
53	1	23	11	0	0
54	2	113	32	0	0
55	2	63	22	0	0
56	2	84	18	0	0
57	1	12	3	0	0
58	1	12	3	0	0
59	2	277	113	0	0
60	1	78	3	0	0
61	2	0	0	0	0
62	2	77	14	0	0
63	1	0	0	0	0
64	1	0	0	0	0
65	2	0	0	0	0
66	2	39	18	0	0
67	1	28	7	0	0
68	1	0	0	0	0
69	3	0	0	0	0

70	2	66	20	0	0
71	1	0	0	0	0
72	2	12	0	0	0
73	2	6	0	0	0
74	2	68	27	0	12
75	1	47	11	0	0
76	2	68	36	0	0
77	2	61	28	0	0
78	1	71	26	0	0
79	1	39	32	0	20
80	2	130	26	0	0
81	1	0	0	0	0
82	1	54	27	0	20
83	1	20	10	0	10
84	1	11	7	0	0
85	2	24	15	0	0
86	1	21	10	0	0
87	2	0	0	0	0
88	1	48	10	0	0
89	2	0	0	0	0
90	2	163	42	0	0
91	2	10	0	0	0
92	2	65	10	0	0
93	1	12	7	0	0
94	1	30	16	0	0
95	1	42	31	0	0
96	1	38	15	0	0
97	1	15	9	0	0
98	1	34	8	0	0
99	2	42	0	0	0
100	2	37	18	0	0
101	1	22	15	0	0
102	1	5	3	0	0
103	2	23	16	0	0
104	2	38	25	0	0
105	2	31	26	0	20
106	1	43	16	0	0
107	2	50	12	0	6

108	1	2	1	0	0
109	1	8	3	0	0
110	2	39	30	0	6
111	2	0	0	0	0
112	2	68	13	0	0
113	2	6	0	0	0
114	1	8	3	0	0
115	1	22	7	0	0
116	2	184	0	0	0
117	1	20	8	0	0
118	1	33	15	0	0

];

gen = [

bus	Pg	Qg	Qmax	Qmin	Vsp	Pmax	Pmin
1	0	0	15	-5	0.955	100	0
4	0	0	300	-300	0.998	100	0
6	0	0	50	-13	0.99	100	0
8	0	0	300	-300	1.015	100	0
10	450	0	200	-147	1.05	550	0
12	85	0	120	-35	0.99	185	0
15	0	0	30	-10	0.97	100	0
18	0	0	50	-16	0.973	100	0
19	0	0	24	-8	0.962	100	0
24	0	0	300	-300	0.992	100	0
25	220	0	140	-47	1.05	320	0
26	314	0	1000	-1000	1.015	414	0
27	0	0	300	-300	0.968	100	0
31	7	0	300	-300	0.967	107	0
32	0	0	42	-14	0.963	100	0
34	0	0	24	-8	0.984	100	0
36	0	0	24	-8	0.98	100	0
40	0	0	300	-300	0.97	100	0
42	0	0	300	-300	0.985	100	0
46	19	0	100	-100	1.005	119	0
49	204	0	210	-85	1.025	304	0
54	48	0	300	-300	0.955	148	0

```
    55     0     0    23    -8   0.952   100     0
    56     0     0    15    -8   0.954   100     0
    59   155     0   180   -60   0.985   255     0
    61   160     0   300  -100   0.995   260     0
    62     0     0    20   -20   0.998   100     0
    65   391     0   200   -67   1.005   491     0
    66   392     0   200   -67    1.05   492     0
    69 516.4     0   300  -300   1.035 805.2     0
    70     0     0    32   -10   0.984   100     0
    72     0     0   100  -100    0.98   100     0
    73     0     0   100  -100   0.991   100     0
    74     0     0     9    -6   0.958   100     0
    76     0     0    23    -8   0.943   100     0
    77     0     0    70   -20   1.006   100     0
    80   477     0   280  -165    1.04   577     0
    85     0     0    23    -8   0.985   100     0
    87     4     0  1000  -100   1.015   104     0
    89   607     0   300  -210   1.005   707     0
    90     0     0   300  -300   0.985   100     0
    91     0     0   100  -100    0.98   100     0
    92     0     0     9    -3    0.99   100     0
    99     0     0   100  -100    1.01   100     0
   100   252     0   155   -50   1.017   352     0
   103    40     0    40   -15    1.01   140     0
   104     0     0    23    -8   0.971   100     0
   105     0     0    23    -8   0.965   100     0
   107     0     0   200  -200   0.952   100     0
   110     0     0    23    -8   0.973   100     0
   111    36     0  1000  -100    0.98   136     0
   112     0     0  1000  -100   0.975   100     0
   113     0     0   200  -100   0.993   100     0
   116     0     0  1000 -1000   1.005   100     0
];


%    fbus    tbus       r          x          b
branch = [
     1       2     0.0303     0.0999     0.0254
```

1	3	0.0129	0.0424	0.01082
4	5	0.00176	0.00798	0.0021
3	5	0.0241	0.108	0.0284
5	6	0.0119	0.054	0.01426
6	7	0.00459	0.0208	0.0055
8	9	0.00244	0.0305	1.162
8	5	0	0.0267	0
9	10	0.00258	0.0322	1.23
4	11	0.0209	0.0688	0.01748
5	11	0.0203	0.0682	0.01738
11	12	0.00595	0.0196	0.00502
2	12	0.0187	0.0616	0.01572
3	12	0.0484	0.16	0.0406
7	12	0.00862	0.034	0.00874
11	13	0.02225	0.0731	0.01876
12	14	0.0215	0.0707	0.01816
13	15	0.0744	0.2444	0.06268
14	15	0.0595	0.195	0.0502
12	16	0.0212	0.0834	0.0214
15	17	0.0132	0.0437	0.0444
16	17	0.0454	0.1801	0.0466
17	18	0.0123	0.0505	0.01298
18	19	0.01119	0.0493	0.01142
19	20	0.0252	0.117	0.0298
15	19	0.012	0.0394	0.0101
20	21	0.0183	0.0849	0.0216
21	22	0.0209	0.097	0.0246
22	23	0.0342	0.159	0.0404
23	24	0.0135	0.0492	0.0498
23	25	0.0156	0.08	0.0864
26	25	0	0.0382	0
25	27	0.0318	0.163	0.1764
27	28	0.01913	0.0855	0.0216
28	29	0.0237	0.0943	0.0238
30	17	0	0.0388	0
8	30	0.00431	0.0504	0.514
26	30	0.00799	0.086	0.908
17	31	0.0474	0.1563	0.0399

29	31	0.0108	0.0331	0.0083
23	32	0.0317	0.1153	0.1173
31	32	0.0298	0.0985	0.0251
27	32	0.0229	0.0755	0.01926
15	33	0.038	0.1244	0.03194
19	34	0.0752	0.247	0.0632
35	36	0.00224	0.0102	0.00268
35	37	0.011	0.0497	0.01318
33	37	0.0415	0.142	0.0366
34	36	0.00871	0.0268	0.00568
34	37	0.00256	0.0094	0.00984
38	37	0	0.0375	0
37	39	0.0321	0.106	0.027
37	40	0.0593	0.168	0.042
30	38	0.00464	0.054	0.422
39	40	0.0184	0.0605	0.01552
40	41	0.0145	0.0487	0.01222
40	42	0.0555	0.183	0.0466
41	42	0.041	0.135	0.0344
43	44	0.0608	0.2454	0.06068
34	43	0.0413	0.1681	0.04226
44	45	0.0224	0.0901	0.0224
45	46	0.04	0.1356	0.0332
46	47	0.038	0.127	0.0316
46	48	0.0601	0.189	0.0472
47	49	0.0191	0.0625	0.01604
42	49	0.0715	0.323	0.086
42	49	0.0715	0.323	0.086
45	49	0.0684	0.186	0.0444
48	49	0.0179	0.0505	0.01258
49	50	0.0267	0.0752	0.01874
49	51	0.0486	0.137	0.0342
51	52	0.0203	0.0588	0.01396
52	53	0.0405	0.1635	0.04058
53	54	0.0263	0.122	0.031
49	54	0.073	0.289	0.0738
49	54	0.0869	0.291	0.073
54	55	0.0169	0.0707	0.0202

54	56	0.00275	0.00955	0.00732
55	56	0.00488	0.0151	0.00374
56	57	0.0343	0.0966	0.0242
50	57	0.0474	0.134	0.0332
56	58	0.0343	0.0966	0.0242
51	58	0.0255	0.0719	0.01788
54	59	0.0503	0.2293	0.0598
56	59	0.0825	0.251	0.0569
56	59	0.0803	0.239	0.0536
55	59	0.04739	0.2158	0.05646
59	60	0.0317	0.145	0.0376
59	61	0.0328	0.15	0.0388
60	61	0.00264	0.0135	0.01456
60	62	0.0123	0.0561	0.01468
61	62	0.00824	0.0376	0.0098
63	59	0	0.0386	0
63	64	0.00172	0.02	0.216
64	61	0	0.0268	0
38	65	0.00901	0.0986	1.046
64	65	0.00269	0.0302	0.38
49	66	0.018	0.0919	0.0248
49	66	0.018	0.0919	0.0248
62	66	0.0482	0.218	0.0578
62	67	0.0258	0.117	0.031
65	66	0	0.037	0
66	67	0.0224	0.1015	0.02682
65	68	0.00138	0.016	0.638
47	69	0.0844	0.2778	0.07092
49	69	0.0985	0.324	0.0828
68	69	0	0.037	0
69	70	0.03	0.127	0.122
24	70	0.00221	0.4115	0.10198
70	71	0.00882	0.0355	0.00878
24	72	0.0488	0.196	0.0488
71	72	0.0446	0.18	0.04444
71	73	0.00866	0.0454	0.01178
70	74	0.0401	0.1323	0.03368
70	75	0.0428	0.141	0.036

69	75	0.0405	0.122	0.124
74	75	0.0123	0.0406	0.01034
76	77	0.0444	0.148	0.0368
69	77	0.0309	0.101	0.1038
75	77	0.0601	0.1999	0.04978
77	78	0.00376	0.0124	0.01264
78	79	0.00546	0.0244	0.00648
77	80	0.017	0.0485	0.0472
77	80	0.0294	0.105	0.0228
79	80	0.0156	0.0704	0.0187
68	81	0.00175	0.0202	0.808
81	80	0	0.037	0
77	82	0.0298	0.0853	0.08174
82	83	0.0112	0.03665	0.03796
83	84	0.0625	0.132	0.0258
83	85	0.043	0.148	0.0348
84	85	0.0302	0.0641	0.01234
85	86	0.035	0.123	0.0276
86	87	0.02828	0.2074	0.0445
85	88	0.02	0.102	0.0276
85	89	0.0239	0.173	0.047
88	89	0.0139	0.0712	0.01934
89	90	0.0518	0.188	0.0528
89	90	0.0238	0.0997	0.106
90	91	0.0254	0.0836	0.0214
89	92	0.0099	0.0505	0.0548
89	92	0.0393	0.1581	0.0414
91	92	0.0387	0.1272	0.03268
92	93	0.0258	0.0848	0.0218
92	94	0.0481	0.158	0.0406
93	94	0.0223	0.0732	0.01876
94	95	0.0132	0.0434	0.0111
80	96	0.0356	0.182	0.0494
82	96	0.0162	0.053	0.0544
94	96	0.0269	0.0869	0.023
80	97	0.0183	0.0934	0.0254
80	98	0.0238	0.108	0.0286
80	99	0.0454	0.206	0.0546

```
    92    100   0.0648     0.295  0.0472
    94    100   0.0178     0.058  0.0604
    95     96   0.0171    0.0547 0.01474
    96     97   0.0173    0.0885   0.024
    98    100   0.0397     0.179  0.0476
    99    100    0.018    0.0813  0.0216
   100    101   0.0277    0.1262  0.0328
    92    102   0.0123    0.0559 0.01464
   101    102   0.0246     0.112  0.0294
   100    103    0.016    0.0525  0.0536
   100    104   0.0451     0.204  0.0541
   103    104   0.0466    0.1584  0.0407
   103    105   0.0535    0.1625  0.0408
   100    106   0.0605     0.229   0.062
   104    105  0.00994    0.0378 0.00986
   105    106    0.014    0.0547 0.01434
   105    107    0.053     0.183  0.0472
   105    108   0.0261    0.0703 0.01844
   106    107    0.053     0.183  0.0472
   108    109   0.0105    0.0288  0.0076
   103    110  0.03906    0.1813  0.0461
   109    110   0.0278    0.0762  0.0202
   110    111    0.022    0.0755    0.02
   110    112   0.0247     0.064   0.062
    17    113  0.00913    0.0301 0.00768
    32    113   0.0615     0.203  0.0518
    32    114   0.0135    0.0612 0.01628
    27    115   0.0164    0.0741 0.01972
   114    115   0.0023    0.0104 0.00276
    68    116  0.00034   0.00405   0.164
    12    117   0.0329      0.14  0.0358
    75    118   0.0145    0.0481 0.01198
    76    118   0.0164    0.0544 0.01356
];
```

IEEE 300 Bus System

baseMVA = 100.0;

bus	type	Pd	Qd	Gs	Bs
bus = [					
1	1	90	49	0	0
2	1	56	15	0	0
3	1	20	0	0	0
4	1	0	0	0	0
5	1	353	130	0	0
6	1	120	41	0	0
7	1	0	0	0	0
8	2	63	14	0	0
9	1	96	43	0	0
10	2	153	33	0	0
11	1	83	21	0	0
12	1	0	0	0	0
13	1	58	10	0	0
14	1	160	60	0	0
15	1	126.7	23	0	0
16	1	0	0	0	0
17	1	561	220	0	0
19	1	0	0	0	0
20	2	605	120	0	0
21	1	77	1	0	0
22	1	81	23	0	0
23	1	21	7	0	0
24	1	0	0	0	0
25	1	45	12	0	0
26	1	28	9	0	0
27	1	69	13	0	0
33	1	55	6	0	0
34	1	0	0	0	0
35	1	0	0	0	0
36	1	0	0	0	0
37	1	85	32	0	0
38	1	155	18	0	0
39	1	0	0	0	0
40	1	46	-21	0	0

41	1	86	0	0	0
42	1	0	0	0	0
43	1	39	9	0	0
44	1	195	29	0	0
45	1	0	0	0	0
46	1	0	0	0	0
47	1	58	11.8	0	0
48	1	41	19	0	0
49	1	92	26	0	0
51	1	-5	5	0	0
52	1	61	28	0	0
53	1	69	3	0	0
54	1	10	1	0	0
55	1	22	10	0	0
57	1	98	20	0	0
58	1	14	1	0	0
59	1	218	106	0	0
60	1	0	0	0	0
61	1	227	110	0	0
62	1	0	0	0	0
63	2	70	30	0	0
64	1	0	0	0	0
69	1	0	0	0	0
70	1	56	20	0	0
71	1	116	38	0	0
72	1	57	19	0	0
73	1	224	71	0	0
74	1	0	0	0	0
76	2	208	107	0	0
77	1	74	28	0	0
78	1	0	0	0	0
79	1	48	14	0	0
80	1	28	7	0	0
81	1	0	0	0	0
84	2	37	13	0	0
85	1	0	0	0	0
86	1	0	0	0	0
87	1	0	0	0	0
88	1	0	0	0	0
89	1	44.2	0	0	0

90	1	66	0	0	0
91	2	17.4	0	0	0
92	2	15.8	0	0	0
94	1	60.3	0	0	0
97	1	39.9	0	0	0
98	2	66.7	0	0	0
99	1	83.5	0	0	0
100	1	0	0	0	0
102	1	77.8	0	0	0
103	1	32	0	0	0
104	1	8.6	0	0	0
105	1	49.6	0	0	0
107	1	4.6	0	0	0
108	2	112.1	0	0	0
109	1	30.7	0	0	0
110	1	63	0	0	0
112	1	19.6	0	0	0
113	1	26.2	0	0	0
114	1	18.2	0	0	0
115	1	0	0	0	0
116	1	0	0	0	0
117	1	0	0	0	325
118	1	14.1	650	0	0
119	2	0	0	0	0
120	1	777	215	0	55
121	1	535	55	0	0
122	1	229.1	11.8	0	0
123	1	78	1.4	0	0
124	2	276.4	59.3	0	0
125	2	514.8	82.7	0	0
126	1	57.9	5.1	0	0
127	1	380.8	37	0	0
128	1	0	0	0	0
129	1	0	0	0	0
130	1	0	0	0	0
131	1	0	0	0	0
132	1	0	0	0	0
133	1	0	0	0	0
134	1	0	0	0	0

135	1	169.2	41.6	0	0
136	1	55.2	18.2	0	0
137	1	273.6	99.8	0	0
138	2	1019.2	135.2	0	0
139	1	595	83.3	0	0
140	1	387.7	114.7	0	0
141	2	145	58	0	0
142	1	56.5	24.5	0	0
143	2	89.5	35.5	0	0
144	1	0	0	0	0
145	1	24	14	0	0
146	2	0	0	0	0
147	2	0	0	0	0
148	1	63	25	0	0
149	2	0	0	0	0
150	1	0	0	0	0
151	1	0	0	0	0
152	2	17	9	0	0
153	2	0	0	0	0
154	1	70	5	0	34.5
155	1	200	50	0	0
156	2	75	50	0	0
157	1	123.5	-24.3	0	0
158	1	0	0	0	0
159	1	33	16.5	0	0
160	1	0	0	0	0
161	1	35	15	0	0
162	1	85	24	0	0
163	1	0	0.4	0	0
164	1	0	0	0	-212
165	1	0	0	0	0
166	1	0	0	0	-103
167	1	299.9	95.7	0	0
168	1	0	0	0	0
169	1	0	0	0	0
170	2	481.8	205	0	0
171	2	763.6	291.1	0	0
172	1	26.5	0	0	0

173	1	163.5	43	0	53
174	1	0	0	0	0
175	1	176	83	0	0
176	2	5	4	0	0
177	2	28	12	0	0
178	1	427.4	173.6	0	0
179	1	74	29	0	45
180	1	69.5	49.3	0	0
181	1	73.4	0	0	0
182	1	240.7	89	0	0
183	1	40	4	0	0
184	1	136.8	16.6	0	0
185	2	0	0	0	0
186	2	59.8	24.3	0	0
187	2	59.8	24.3	0	0
188	1	182.6	43.6	0	0
189	1	7	2	0	0
190	2	0	0	0	-150
191	2	489	53	0	0
192	1	800	72	0	0
193	1	0	0	0	0
194	1	0	0	0	0
195	1	0	0	0	0
196	1	10	3	0	0
197	1	43	14	0	0
198	2	64	21	0	0
199	1	35	12	0	0
200	1	27	12	0	0
201	1	41	14	0	0
202	1	38	13	0	0
203	1	42	14	0	0
204	1	72	24	0	0
205	1	0	-5	0	0
206	1	12	2	0	0
207	1	-21	-14.2	0	0
208	1	7	2	0	0
209	1	38	13	0	0
210	1	0	0	0	0

211	1	96	7	0	0
212	1	0	0	0	0
213	2	0	0	0	0
214	1	22	16	0	0
215	1	47	26	0	0
216	1	176	105	0	0
217	1	100	75	0	0
218	1	131	96	0	0
219	1	0	0	0	0
220	2	285	100	0	0
221	2	171	70	0	0
222	2	328	188	0	0
223	1	428	232	0	0
224	1	173	99	0	0
225	1	410	40	0	0
226	1	0	0	0	0
227	2	538	369	0	0
228	1	223	148	0	0
229	1	96	46	0	0
230	2	0	0	0	0
231	1	159	107	0	-300
232	1	448	143	0	0
233	2	404	212	0	0
234	1	572	244	0	0
235	1	269	157	0	0
236	2	0	0	0	0
237	1	0	0	0	0
238	2	255	149	0	-150
239	2	0	0	0	0
240	1	0	0	0	-140
241	2	0	0	0	0
242	2	0	0	0	0
243	2	8	3	0	0
244	1	0	0	0	0
245	1	61	30	0	0
246	1	77	33	0	0
247	1	61	30	0	0
248	1	29	14	0	45.6

249	1	29	14	0	0
250	1	-23	-17	0	0
281	1	-33.1	-29.4	0	0
319	1	115.8	-24	0	0
320	1	2.4	-12.6	0	0
322	1	2.4	-3.9	0	0
323	1	-14.9	26.5	0	0
324	1	24.7	-1.2	0	0
526	1	145.3	-34.9	0	0
528	1	28.1	-20.5	0	0
531	1	14	2.5	0	0
552	1	-11.1	-1.4	0	0
562	1	50.5	17.4	0	0
609	1	29.6	0.6	0	0
664	1	-113.7	76.7	0	0
1190	1	100.31	29.17	0	0
1200	1	-100	34.17	0	0
1201	1	0	0	0	0
2040	1	0	0	0	0
7001	2	0	0	0	0
7002	2	0	0	0	0
7003	2	0	0	0	0
7011	2	0	0	0	0
7012	2	0	0	0	0
7017	2	0	0	0	0
7023	2	0	0	0	0
7024	2	0	0	0	0
7039	2	0	0	0	0
7044	2	0	0	0	0
7049	3	0	0	0	0
7055	2	0	0	0	0
7057	2	0	0	0	0
7061	2	0	0	0	0
7062	2	0	0	0	0
7071	2	0	0	0	0
7130	2	0	0	0	0
7139	2	0	0	0	0
7166	2	0	0	0	0

```
    9001    1       0       0       0       0
    9002    2       4.2     0       0       0
    9003    1       2.71    0.94    0.001   2.4
    9004    1       0.86    0.28    0       0
    9005    1       0       0       0       0
    9006    1       0       0       0       0
    9007    1       0       0       0       0
    9012    1       0       0       0       0
    9021    1       4.75    1.56    0       0
    9022    1       1.53    0.53    0.001   0
    9023    1       0       0       0       0
    9024    1       1.35    0.47    0.001   0
    9025    1       0.45    0.16    0       0
    9026    1       0.45    0.16    0       0
    9031    1       1.84    0.64    0.001   0
    9032    1       1.39    0.48    0.001   0
    9033    1       1.89    0.65    0.001   0
    9034    1       1.55    0.54    0.001   1.72
    9035    1       1.66    0.58    0.001   0
    9036    1       3.03    1       0       0
    9037    1       1.86    0.64    0.001   0
    9038    1       2.58    0.89    0.001   0
    9041    1       1.01    0.35    0.001   0
    9042    1       0.81    0.28    0       0
    9043    1       1.6     0.52    0       0
    9044    1       0       0       0       0
    9051    2       35.81   0       0       0
    9052    1       30      23      0       0
    9053    2       26.48   0       0       0
    9054    2       0       0       0       0
    9055    2       0       0       0       0
    9071    1       1.02    0.35    0.001   0
    9072    1       1.02    0.35    0.001   0
    9121    1       3.8     1.25    0       0
    9533    1       1.19    0.41    0.001   0
];
```

	bus	Pg	Qg	Qmax	Qmin	Vsp	Pmax	Pmin
gen =	[							
	8	0	0	10	-10	1.0153	100	0
	10	0	0	20	-20	1.0205	100	0
	20	0	0	20	-20	1.001	100	0
	63	0	0	25	-25	0.9583	100	0
	76	0	0	35	12	0.9632	100	0
	84	375	0	240	-240	1.025	475	0
	91	155	0	96	-11	1.052	255	0
	92	290	0	153	-153	1.052	390	0
	98	68	0	56	-30	1	168	0
	108	117	0	77	-24	0.99	217	0
	119	1930	0	1500	-500	1.0435	2030	0
	124	240	0	120	-60	1.0233	340	0
	125	0	0	200	-25	1.0103	100	0
	138	0	0	350	-125	1.055	100	0
	141	281	0	75	-50	1.051	381	0
	143	696	0	300	-100	1.0435	796	0
	146	84	0	35	-15	1.0528	184	0
	147	217	0	100	-50	1.0528	317	0
	149	103	0	50	-25	1.0735	203	0
	152	372	0	175	-50	1.0535	472	0
	153	216	0	90	-50	1.0435	316	0
	156	0	0	15	-10	0.963	100	0
	170	205	0	90	-40	0.929	305	0
	171	0	0	150	-50	0.9829	100	0
	176	228	0	90	-45	1.0522	328	0
	177	84	0	35	-15	1.0077	184	0
	185	200	0	80	-50	1.0522	300	0
	186	1200	0	400	-100	1.065	1300	0
	187	1200	0	400	-100	1.065	1300	0
	190	475	0	300	-300	1.0551	575	0
	191	1973	0	1000	-1000	1.0435	2073	0
	198	424	0	260	-260	1.015	524	0
	213	272	0	150	-150	1.01	372	0
	220	100	0	60	-60	1.008	200	0
	221	450	0	320	-320	1	550	0
	222	250	0	300	-300	1.05	350	0
	227	303	0	300	-300	1	403	0
	230	345	0	250	-250	1.04	445	0

```
    233   300    0   500   -500     1   400   0
    236   600    0   300   -300  1.0165   700   0
    238   250    0   200   -200  1.01     350   0
    239   550    0   400   -400     1   650   0
    241   575.43 0   600   -600  1.05   675.43  0
    242   170    0   100    40   0.993   270   0
    243    84    0    80    40   1.01    184   0
   7001   467    0   210   -210  1.0507  567   0
   7002   623    0   280   -280  1.0507  723   0
   7003  1210    0   420   -420  1.0323 1310   0
   7011   234    0   100   -100  1.0145  334   0
   7012   372    0   224   -224  1.0507  472   0
   7017   330    0   350      0  1.0507  430   0
   7023   185    0   120      0  1.0507  285   0
   7024   410    0   224   -224  1.029   510   0
   7039   500    0   200   -200  1.05    600   0
   7044    37    0    42      0  1.0145  137   0
   7049     0    0    10      0  1.0507 2399.01 0
   7055    45    0    25      0  0.9967  145   0
   7057   165    0    90    -90  1.0212  265   0
   7061   400    0   150   -150  1.0145  500   0
   7062   400    0   150      0  1.0017  500   0
   7071   116    0    87      0  0.9893  216   0
   7130  1292    0   600   -100  1.0507 1392   0
   7139   700    0   325   -125  1.0507  800   0
   7166   553    0   300   -200  1.0145  653   0
   9002     0    0     2     -2  0.9945  100   0
   9051     0    0 17.35 -17.35     1    100   0
   9053     0    0 12.83  -12.8     1    100   0
   9054    50    0    38    -38     1    150   0
   9055     8    0     6     -6     1    108   0
];


    fbus   tbus      r       x       b
branch = [
     37   9001  0.00006 0.00046       0
   9001   9005   0.0008 0.00348       0
   9001   9006  0.02439 0.43682       0
   9001   9012  0.03624 0.64898       0
```

9005	9051	0.01578	0.37486	0
9005	9052	0.01578	0.37486	0
9005	9053	0.01602	0.38046	0
9005	9054	0	0.152	0
9005	9055	0	0.8	0
9006	9007	0.05558	0.24666	0
9006	9003	0.11118	0.49332	0
9006	9003	0.11118	0.49332	0
9012	9002	0.07622	0.43286	0
9012	9002	0.07622	0.43286	0
9002	9021	0.0537	0.07026	0
9021	9023	1.1068	0.95278	0
9021	9022	0.44364	2.8152	0
9002	9024	0.50748	3.2202	0
9023	9025	0.66688	3.944	0
9023	9026	0.6113	3.6152	0
9007	9071	0.4412	2.9668	0
9007	9072	0.30792	2.057	0
9007	9003	0.0558	0.24666	0
9003	9031	0.73633	4.6724	0
9003	9032	0.76978	4.8846	0
9003	9033	0.75732	4.8056	0
9003	9044	0.07378	0.06352	0
9044	9004	0.03832	0.02894	0
9004	9041	0.36614	2.456	0
9004	9042	1.0593	5.4536	0
9004	9043	0.1567	1.6994	0
9003	9034	0.13006	1.3912	0
9003	9035	0.54484	3.4572	0
9003	9036	0.15426	1.6729	0
9003	9037	0.3849	2.5712	0
9003	9038	0.4412	2.9668	0
9012	9121	0.23552	0.99036	0
9053	9533	0	0.75	0
1	5	0.001	0.006	0
2	6	0.001	0.009	0
2	8	0.006	0.027	0.054
3	7	0	0.003	0
3	19	0.008	0.069	0.139
3	150	0.001	0.007	0

4	16	0.002	0.019	1.127
5	9	0.006	0.029	0.018
7	12	0.001	0.009	0.07
7	131	0.001	0.007	0.014
8	11	0.013	0.0595	0.033
8	14	0.013	0.042	0.081
9	11	0.006	0.027	0.013
11	13	0.008	0.034	0.018
12	21	0.002	0.015	0.118
13	20	0.006	0.034	0.016
14	15	0.014	0.042	0.097
15	37	0.065	0.248	0.121
15	89	0.099	0.248	0.035
15	90	0.096	0.363	0.048
16	42	0.002	0.022	1.28
19	21	0.002	0.018	0.036
19	87	0.013	0.08	0.151
20	22	0.016	0.033	0.015
20	27	0.069	0.186	0.098
21	24	0.004	0.034	0.28
22	23	0.052	0.111	0.05
23	25	0.019	0.039	0.018
24	319	0.007	0.068	0.134
25	26	0.036	0.071	0.034
26	27	0.045	0.12	0.065
26	320	0.043	0.13	0.014
33	34	0	0.063	0
33	38	0.0025	0.012	0.013
33	40	0.006	0.029	0.02
33	41	0.007	0.043	0.026
34	42	0.001	0.008	0.042
35	72	0.012	0.06	0.008
35	76	0.006	0.014	0.002
35	77	0.01	0.029	0.003
36	88	0.004	0.027	0.043
37	38	0.008	0.047	0.008
37	40	0.022	0.064	0.007
37	41	0.01	0.036	0.02
37	49	0.017	0.081	0.048
37	89	0.102	0.254	0.033

37	90	0.047	0.127	0.016
38	41	0.008	0.037	0.02
38	43	0.032	0.087	0.04
39	42	0.0006	0.0064	0.404
40	48	0.026	0.154	0.022
41	42	0	0.029	0
41	49	0.065	0.191	0.02
41	51	0.031	0.089	0.036
42	46	0.002	0.014	0.806
43	44	0.026	0.072	0.035
43	48	0.095	0.262	0.032
43	53	0.013	0.039	0.016
44	47	0.027	0.084	0.039
44	54	0.028	0.084	0.037
45	60	0.007	0.041	0.312
45	74	0.009	0.054	0.411
46	81	0.005	0.042	0.69
47	73	0.052	0.145	0.073
47	113	0.043	0.118	0.013
48	107	0.025	0.062	0.007
49	51	0.031	0.094	0.043
51	52	0.037	0.109	0.049
52	55	0.027	0.08	0.036
53	54	0.025	0.073	0.035
54	55	0.035	0.103	0.047
55	57	0.065	0.169	0.082
57	58	0.046	0.08	0.036
57	63	0.159	0.537	0.071
58	59	0.009	0.026	0.005
59	61	0.002	0.013	0.015
60	62	0.009	0.065	0.485
62	64	0.016	0.105	0.203
62	144	0.001	0.007	0.013
63	526	0.0265	0.172	0.026
69	211	0.051	0.232	0.028
69	79	0.051	0.157	0.023
70	71	0.032	0.1	0.062
70	528	0.02	0.1234	0.028
71	72	0.036	0.131	0.068
71	73	0.034	0.099	0.047

72	77	0.018	0.087	0.011
72	531	0.0256	0.193	0
73	76	0.021	0.057	0.03
73	79	0.018	0.052	0.018
74	88	0.004	0.027	0.05
74	562	0.0286	0.2013	0.379
76	77	0.016	0.043	0.004
77	78	0.001	0.006	0.007
77	80	0.014	0.07	0.038
77	552	0.0891	0.2676	0.029
77	609	0.0782	0.2127	0.022
78	79	0.006	0.022	0.011
78	84	0	0.036	0
79	211	0.099	0.375	0.051
80	211	0.022	0.107	0.058
81	194	0.0035	0.033	0.53
81	195	0.0035	0.033	0.53
85	86	0.008	0.064	0.128
86	87	0.012	0.093	0.183
86	323	0.006	0.048	0.092
89	91	0.047	0.119	0.014
90	92	0.032	0.174	0.024
91	94	0.1	0.253	0.031
91	97	0.022	0.077	0.039
92	103	0.019	0.144	0.017
92	105	0.017	0.092	0.012
94	97	0.278	0.427	0.043
97	100	0.022	0.053	0.007
97	102	0.038	0.092	0.012
97	103	0.048	0.122	0.015
98	100	0.024	0.064	0.007
98	102	0.034	0.121	0.015
99	107	0.053	0.135	0.017
99	108	0.002	0.004	0.002
99	109	0.045	0.354	0.044
99	110	0.05	0.174	0.022
100	102	0.016	0.038	0.004
102	104	0.043	0.064	0.027
103	105	0.019	0.062	0.008
104	108	0.076	0.13	0.044

104	322	0.044	0.124	0.015
105	107	0.012	0.088	0.011
105	110	0.157	0.4	0.047
108	324	0.074	0.208	0.026
109	110	0.07	0.184	0.021
109	113	0.1	0.274	0.031
109	114	0.109	0.393	0.036
110	112	0.142	0.404	0.05
112	114	0.017	0.042	0.006
115	122	0.0036	0.0199	0.004
116	120	0.002	0.1049	0.001
117	118	0.0001	0.0018	0.017
118	119	0	0.0271	0
118	1201	0	0.6163	0
1201	120	0	-0.3697	0
118	121	0.0022	0.2915	0
119	120	0	0.0339	0
119	121	0	0.0582	0
122	123	0.0808	0.2344	0.029
122	125	0.0965	0.3669	0.054
123	124	0.036	0.1076	0.117
123	125	0.0476	0.1414	0.149
125	126	0.0006	0.0197	0
126	127	0.0059	0.0405	0.25
126	129	0.0115	0.1106	0.185
126	132	0.0198	0.1688	0.321
126	157	0.005	0.05	0.33
126	158	0.0077	0.0538	0.335
126	169	0.0165	0.1157	0.171
127	128	0.0059	0.0577	0.095
127	134	0.0049	0.0336	0.208
127	168	0.0059	0.0577	0.095
128	130	0.0078	0.0773	0.126
128	133	0.0026	0.0193	0.03
129	130	0.0076	0.0752	0.122
129	133	0.0021	0.0186	0.03
130	132	0.0016	0.0164	0.026
130	151	0.0017	0.0165	0.026
130	167	0.0079	0.0793	0.127
130	168	0.0078	0.0784	0.125

133	137	0.0017	0.0117	0.289
133	168	0.0026	0.0193	0.03
133	169	0.0021	0.0186	0.03
133	171	0.0002	0.0101	0
134	135	0.0043	0.0293	0.18
134	184	0.0039	0.0381	0.258
135	136	0.0091	0.0623	0.385
136	137	0.0125	0.089	0.54
136	152	0.0056	0.039	0.953
137	140	0.0015	0.0114	0.284
137	181	0.0005	0.0034	0.021
137	186	0.0007	0.0151	0.126
137	188	0.0005	0.0034	0.021
139	172	0.0562	0.2248	0.081
140	141	0.012	0.0836	0.123
140	142	0.0152	0.1132	0.684
140	145	0.0468	0.3369	0.519
140	146	0.043	0.3031	0.463
140	147	0.0489	0.3492	0.538
140	182	0.0013	0.0089	0.119
141	146	0.0291	0.2267	0.342
142	143	0.006	0.057	0.767
143	145	0.0075	0.0773	0.119
143	149	0.0127	0.0909	0.135
145	146	0.0085	0.0588	0.087
145	149	0.0218	0.1511	0.223
146	147	0.0073	0.0504	0.074
148	178	0.0523	0.1526	0.074
148	179	0.1371	0.3919	0.076
152	153	0.0137	0.0957	0.141
153	161	0.0055	0.0288	0.19
154	156	0.1746	0.3161	0.04
154	183	0.0804	0.3054	0.045
155	161	0.011	0.0568	0.388
157	159	0.0008	0.0098	0.069
158	159	0.0029	0.0285	0.19
158	160	0.0066	0.0448	0.277
162	164	0.0024	0.0326	0.236
162	165	0.0018	0.0245	1.662
163	164	0.0044	0.0514	3.597

165	166	0.0002	0.0123	0
167	169	0.0018	0.0178	0.029
172	173	0.0669	0.4843	0.063
172	174	0.0558	0.221	0.031
173	174	0.0807	0.3331	0.049
173	175	0.0739	0.3071	0.043
173	176	0.1799	0.5017	0.069
175	176	0.0904	0.3626	0.048
175	179	0.077	0.3092	0.054
176	177	0.0251	0.0829	0.047
177	178	0.0222	0.0847	0.05
178	179	0.0498	0.1855	0.029
178	180	0.0061	0.029	0.084
181	138	0.0004	0.0202	0
181	187	0.0004	0.0083	0.115
184	185	0.0025	0.0245	0.164
186	188	0.0007	0.0086	0.115
187	188	0.0007	0.0086	0.115
188	138	0.0004	0.0202	0
189	208	0.033	0.095	0
189	209	0.046	0.069	0
190	231	0.0004	0.0022	6.2
190	240	0	0.0275	0
191	192	0.003	0.048	0
192	225	0.002	0.009	0
193	205	0.045	0.063	0
193	208	0.048	0.127	0
194	219	0.0031	0.0286	0.5
194	664	0.0024	0.0355	0.36
195	219	0.0031	0.0286	0.5
196	197	0.014	0.04	0.004
196	210	0.03	0.081	0.01
197	198	0.01	0.06	0.009
197	211	0.015	0.04	0.006
198	202	0.332	0.688	0
198	203	0.009	0.046	0.025
198	210	0.02	0.073	0.008
198	211	0.034	0.109	0.032
199	200	0.076	0.135	0.009
199	210	0.04	0.102	0.005

200	210	0.081	0.128	0.014
201	204	0.124	0.183	0
203	211	0.01	0.059	0.008
204	205	0.046	0.068	0
205	206	0.302	0.446	0
206	207	0.073	0.093	0
206	208	0.24	0.421	0
212	215	0.0139	0.0778	0.086
213	214	0.0025	0.038	0
214	215	0.0017	0.0185	0.02
214	242	0.0015	0.0108	0.002
215	216	0.0045	0.0249	0.026
216	217	0.004	0.0497	0.018
217	218	0	0.0456	0
217	219	0.0005	0.0177	0.02
217	220	0.0027	0.0395	0.832
219	237	0.0003	0.0018	5.2
220	218	0.0037	0.0484	0.43
220	221	0.001	0.0295	0.503
220	238	0.0016	0.0046	0.402
221	223	0.0003	0.0013	1
222	237	0.0014	0.0514	0.33
224	225	0.01	0.064	0.48
224	226	0.0019	0.0081	0.86
225	191	0.001	0.061	0
226	231	0.0005	0.0212	0
227	231	0.0009	0.0472	0.186
228	229	0.0019	0.0087	1.28
228	231	0.0026	0.0917	0
228	234	0.0013	0.0288	0.81
229	190	0	0.0626	0
231	232	0.0002	0.0069	1.364
231	237	0.0001	0.0006	3.57
232	233	0.0017	0.0485	0
234	235	0.0002	0.0259	0.144
234	237	0.0006	0.0272	0
235	238	0.0002	0.0006	0.8
241	237	0.0005	0.0154	0
240	281	0.0003	0.0043	0.009
242	245	0.0082	0.0851	0

242	247	0.0112	0.0723	0
243	244	0.0127	0.0355	0
243	245	0.0326	0.1804	0
244	246	0.0195	0.0551	0
245	246	0.0157	0.0732	0
245	247	0.036	0.2119	0
246	247	0.0268	0.1285	0
247	248	0.0428	0.1215	0
248	249	0.0351	0.1004	0
249	250	0.0616	0.1857	0
3	1	0	0.052	0
3	2	0	0.052	0
3	4	0	0.005	0
7	5	0	0.039	0
7	6	0	0.039	0
10	11	0	0.089	0
12	10	0	0.053	0
15	17	0.0194	0.0311	0
16	15	0.001	0.038	0
21	20	0	0.014	0
24	23	0	0.064	0
36	35	0	0.047	0
45	44	0	0.02	0
45	46	0	0.021	0
62	61	0	0.059	0
63	64	0	0.038	0
73	74	0	0.0244	0
81	88	0	0.02	0
85	99	0	0.048	0
86	102	0	0.048	0
87	94	0	0.046	0
114	207	0	0.149	0
116	124	0.0052	0.0174	0
121	115	0	0.028	0
122	157	0.0005	0.0195	0
130	131	0	0.018	0
130	150	0	0.014	0
132	170	0.001	0.0402	0
141	174	0.0024	0.0603	0
142	175	0.0024	0.0498	-0.087

143	144	0	0.0833	0
143	148	0.0013	0.0371	0
145	180	0.0005	0.0182	0
151	170	0.001	0.0392	0
153	183	0.0027	0.0639	0
155	156	0.0008	0.0256	0
159	117	0	0.016	0
160	124	0.0012	0.0396	0
163	137	0.0013	0.0384	-0.057
164	155	0.0009	0.0231	-0.033
182	139	0.0003	0.0131	0
189	210	0	0.252	0
193	196	0	0.237	0
195	212	0.0008	0.0366	0
200	248	0	0.22	0
201	69	0	0.098	0
202	211	0	0.128	0
204	2040	0.02	0.204	-0.012
209	198	0.026	0.211	0
211	212	0.003	0.0122	0
218	219	0.001	0.0354	-0.01
223	224	0.0012	0.0195	-0.364
229	230	0.001	0.0332	0
234	236	0.0005	0.016	0
238	239	0.0005	0.016	0
196	2040	0.0001	0.02	0
119	1190	0.001	0.023	0
120	1200	0	0.023	0
7002	2	0.001	0.0146	0
7003	3	0	0.01054	0
7061	61	0	0.0238	0
7062	62	0	0.03214	0
7166	166	0	0.0154	0
7024	24	0	0.0289	0
7001	1	0	0.01953	0
7130	130	0	0.0193	0
7011	11	0	0.01923	0
7023	23	0	0.023	0
7049	49	0	0.0124	0
7139	139	0	0.0167	0

```
    7012    12    0    0.0312    0
    7017    17    0    0.01654   0
    7039    39    0    0.03159   0
    7057    57    0    0.05347   0
    7044    44    0    0.18181   0
    7055    55    0    0.19607   0
    7071    71    0    0.06896   0
];
```